

**2021 PUBLICATION
CRITERIA 3
3.3.1**

ALGAL DIVERSITY IN MIDSTREAM OF THE ACHANKOVIL RIVER DURING MONSOON AND POST MONSOON SEASON

Meera Krishnan*, Praveen Dhar Thulasidas**, Sreejai Raghavan**, Sreeja Thankappan***

* University of Kerala, Mahatma Gandhi College, Thiruvananthapuram, Kerala, India

** University of Kerala, St. Stephen's College, Pathanapuram, Kollam, Kerala, India

*** University of Kerala, Nair Service Society College, Nilamel, Kollam, Kerala, India

corresponding author: Praveen Dhar Thulasidas, e-mail: dharpaveent@gmail.com



This work is licensed under a
[Creative Commons Attribution 4.0
International License](https://creativecommons.org/licenses/by/4.0/)

Professional paper
Received: April 6th, 2020
Accepted: May 4th, 2020
HAE-1949

<https://doi.org/10.33765/thate.11.1.3>

ABSTRACT

Algae are simple organisms whose size ranges from microscopic to macroscopic large seaweeds over thirty meters long. The study examined the algal diversity in the midstream of the Achankovil River. Pandalm is located in the central point of the Achankovil River. Water samples were collected during the monsoon and post monsoon seasons. Samples were collected in the early morning; phytoplanktonic forms were gathered by plankton net. The exploration identified the presence of 41 algal genera pertaining to the classes of Chlorophyceae, Bacillariophyceae, Cyanophyceae and Euglenophyceae. The pollution-indicating species increased in post monsoon season in comparison to monsoon season of the river and larger numbers of algal species are reported during monsoon season.

Keywords: *algal diversity, Achankovil River, pre and post monsoon season*

INTRODUCTION

Algae belong to the kingdom of Protista and their size varies from the microscopic to macroscopic. Algae are diverse life forms, found almost everywhere on the planet. They take a central position in many ecosystems and play a pivotal role in balancing the biotic and abiotic components. Algae are the primary producers in aquatic ecosystem and form essential components of the food web; they may have an important role in maintaining the equilibrium between living and non-living factors [1]. Algae capture more amount of the

solar energy and release more oxygen than green plants. The algal diversity in an ecosystem is determined by the level of richness of species and their functional importance in ecosystem, depending upon the seasons the algae appear and disappear [2]. Algal diversity researches are useful for the assessment of the water body type and quality [3]. The Achankovil River is an important fresh water resource in Kerala, located in the southern tip of the peninsula and originating from Western Ghats and it enriches Pathanamthitta District of the Kerala state. The river is 128 km long and bounded with



Synthesis, spectral characterization and biological evaluations with DFT analysis on molecular geometry and NLO of 1,4,7,10-tetraazacyclotetradecane-11,14-dione

J.P. Remiya^a, T.S. Sikha^a  , B. Shyni^a, L. Anitha^a, C.S. Nair Lakshmi^a, E.G. Jayasree^b

[Show more](#) 

 Share  Cite

<https://doi.org/10.1016/j.jics.2021.100132> 

[Get rights and content](#) 

Highlights

- Synthesis and spectral characterization of diamide macrocyclic ligand.
- Simulated IR and Raman frequencies data correlated well with the experimental spectral results.
- TD-DFT calculation explains the excitation properties of the compound.
- MESP and NBO analysis were performed.
- NLO activity of the compound was determined experimentally.

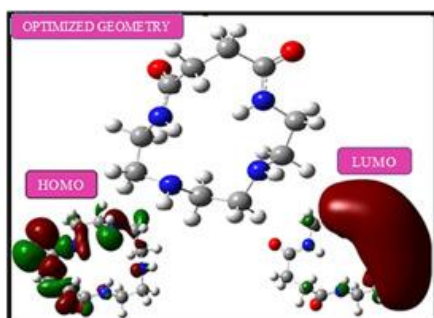
Abstract

A novel 14-membered tetradentate N₄ macrocyclic ligand, STETA (1,4,7,10-tetraazacyclotetradecane-11,14-dione) was synthesized by [1+1] cyclic condensation of succinic acid with triethylenetetramine through reflux method in ethanolic solvent. The synthesized macrocyclic ligand was experimentally characterized by C H N analysis, FT-IR, FT-Raman, electronic, ¹H NMR, ¹³C NMR and ESI MS. Optimization of molecular geometry and spectral (FT-IR, FT-Raman, ¹H/¹³C NMR) analysis of STETA were performed by employing DFT with B3LYP/6-311+G(d) basis set and computational results were correlated with experimental (NMR, IR, Raman) spectral values. Electronic absorption properties of STETA were monitored using TD-DFT approach and also theoretical UV-vis results were experimentally compared. EMO analysis, MEP plot, global reactivity descriptors, first-order hyperpolarizability and NBO analysis were rationalized on the

ground of DFT computation. NLO activity of title molecule was confirmed by both molecular hyperpolarizability calculations and SHG measurements. *In vitro* antibacterial activity and DPPH radical scavenging effects of STETA were screened.

Graphical abstract

Tetraaza macrocyclic compound was synthesized and characterized by spectral techniques. Molecular geometry optimization was performed by employing DFT/B3LYP/6-311+G(d) method. Computational results were comparable with experimental spectral values.



[Download : Download high-res image \(159KB\)](#)

[Download : Download full-size image](#)

Introduction

Macrocycles is a fascinating area of research in the development of supramolecular chemistry [1]. They have a great impact on multidisciplinary research fields due to their selective substrate recognition, transport capabilities, stable complex formation, catalysis, designing of molecular magnets and fluorogenic chemosensors [[2], [3], [4], [5]]. They can be readily accessed by the cyclic condensation reactions of dicarbonyl compounds with primary diamines and exhibit a broad spectrum of biological activities [6]. Macrocyclic compounds have become of monumental importance due to their diverse applications as luminescent sensors [7], therapeutic agents [8] and control enzymes for cleaving DNA and RNA [9]. The impetus for research of macrocyclic compounds has been accentuated by the recognition of the fact that the basic structural units of bio-macrocyclic systems such as haemoglobin, chlorophyll and vitamin B₁₂ are essential for creative evolution and continuation of life process [10].

The synthesis of tetraazamacrocyclic compounds received much attention of coordination chemists [11] due to their potential applications ranging from the elimination of toxic metals from unwanted streams, radiotherapy to MRI contrast agents [[12], [13], [14]]. Shiekh R A et al. carried out large quantum of research work on tetraazamacrocyclic compounds [[15], [16], [17]]. They reported biologically active tetraazamacrocyclic divalent complexes of cobalt, nickel and copper derived from the condensation of aliphatic dicarboxylic acids with ethylenediamine.

Macrocyclic compounds having carbonyl groups (free C = O) have been much less focused during the past few decades [18]. But, a considerable number of macrocycles have been reported and reviewed [19,20] where the carbonyl group lies adjacent to the secondary amine of the cyclic framework giving rise to amide functionalized system. The amide macrocyclic complexes deserve special attention in view of the presence of nitrogen and oxygen donor atoms which may be involved in coordination [21].

There is an urgent need for exploration and the development of NLO materials to meet the present demand due to their extensive opportunities within the field of photonics and optoelectronics [22] including optical data storage, high-



Synthesis and crystal structure of a heterobimetallic cadmium–sodium complex of 1,3,5-triazine-2,4,6-trione, [CdNa₂(C₃H₂N₃O₃)₄(H₂O)₈]

R. Divya,^a B. R. Bijini,^a V. S. Dhanya,^a K. Rajendra Babu^a and M. Sithambaresan^{b*}



^aPG Department and Research Centre in Physics, M.G. College, University of Kerala, Thiruvananthapuram 695004, India, and ^bDepartment of Chemistry, Faculty of Science, Eastern University, Sri Lanka, Chenkalady, Sri Lanka

*Correspondence e-mail: msithambaresan@gmail.com

Edited by J. Reibenspies, Texas A & M University, USA (Received 5 July 2021; accepted 8 August 2021; online 17 August 2021)

Heterobimetallic crystals of a cadmium–sodium complex of 1,3,5-triazine-2,4,6-trione, namely, μ -aqua-1:2 κ^2 O:O-heptaaqua-1 κ^3 O,2 κ^2 O,3 κ^2 O-bis(μ -4,6-dioxo-1,4,5,6-tetrahydro-1,3,5-triazin-2-olato)-1:2 κ^2 O²:N¹;2:3 κ^2 N¹:O²-bis(4,6-dioxo-1,4,5,6-tetrahydro-1,3,5-triazin-2-olato)-1 κ O²,3 κ O²-2-cadmium-1,3-disodium, [CdNa₂(C₃H₂N₃O₃)₄(H₂O)₈], were grown by the single gel diffusion technique. The asymmetric unit of the title compound comprises four 1,3,5-triazine-2,4,6-trione ligands, two sodium atoms and one cadmium atom. Of the four ligands, two are monodentately coordinated to two Na atoms. The third ligand is coordinated bidentately to one Na and the Cd atom and the fourth is also coordinated bidentately to the Cd atom and the other Na atom. All the metal atoms are six-coordinate with a distorted octahedral geometry. The water molecules bridge the Na atoms, constructing coordination polymer chains along the *a* axis and hence are linked by two Cd and one Na coordinations through the cyanuric acid ligands present in the coordination polymer chains, generating a two-dimensional coordination polymer in the (110) plane. The polymer formation is further assisted by means of many intermolecular and intramolecular N–H \cdots O, O–H \cdots O and O–H \cdots N hydrogen bonds between the water molecules and the ligands.

Keywords: crystal structure; heterobimetallic cadmium–sodium complex; gel growth; 1,3,5-triazine-2,4,6-trione; two-dimensional coordination polymer.

CCDC reference: 1576691

[Similar articles](#)

[Reuse permissions](#)

[PowerPoint slides](#)

1. Chemical context

Chelation is considered as the preferred method for the reduction of toxic effects of heavy metals, in which the metals are removed in the form of stable complex chelates. Cadmium, one of the most toxic heavy metals, can accumulate in the human body, leading to renal dysfunction, lung cancer, etc. In

addition, chelation reactions are utilized in the determination of cadmium toxicity (Flora & Pachauri, 2010) with 1,3,5-triazine-2,4,6-trione, also known as cyanuric acid, being the preferred ligand used for the chelation as it has multiple hydrogen-bond donor centres (Mistri *et al.*, 2014). 1,3,5-Triazine-2,4,6-trione exists in either the keto or enol form but the most stable isomer is the keto form (Reva, 2015). In this work, we report the crystal structure of a heterobimetallic cadmium and sodium complex of 1,3,5-triazine-2,4,6-trione.

2. Structural commentary

The title complex crystallizes in the triclinic space group $P\bar{1}$. Fig. 1 shows the asymmetric unit of the crystal, which consists of four cyanuric acid ligands, two sodium atoms (Na1 and Na2) and one cadmium atom. Of the four ligands, two are monodentately coordinated to Na1 and Na2 atoms each. The third ligand is coordinated bidentately to Na1 and Cd1 atoms and the fourth one also coordinated bidentately to Na2 and Cd1 atoms. The sodium atom Na2 is coordinated to oxygen atoms of two cyanuric acid ligands [O5—Na2—O14 = 94.52 (6)°]. The Na1 atom is also coordinated to oxygen atoms of two cyanuric acid ligands [O10—Na1—O13 = 173.39 (7)°]. The Cd1 atom is coordinated to nitrogen atoms of two cyanuric acid ligands [N1—Cd1—N4 = 174.58 (6)°]. In addition to the ligand coordination, atoms Na1, Na2 and Cd1 are also coordinated by two, three and four water molecules, respectively.

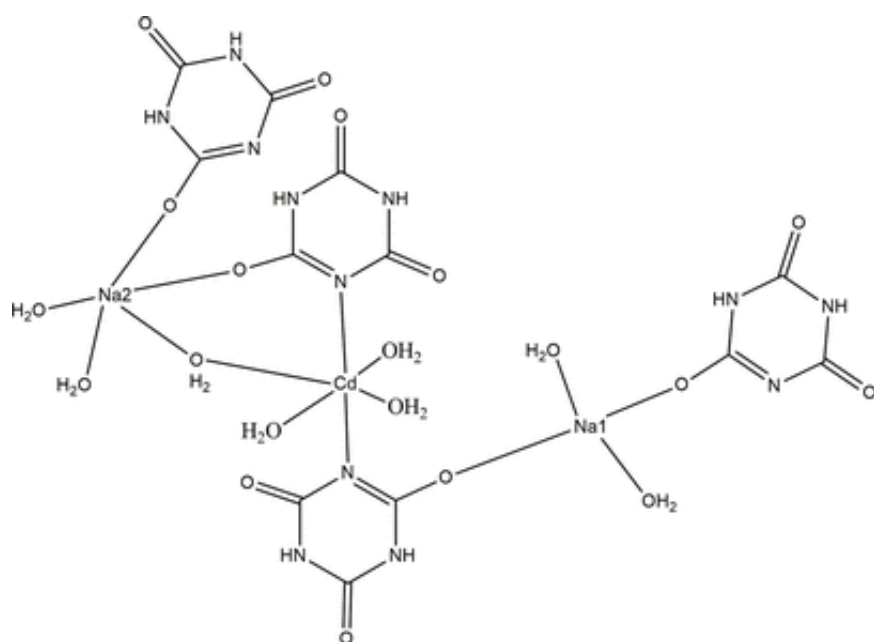


Figure 1

The asymmetric unit of the title compound with displacement ellipsoids drawn at the 50% probability level.

The title compound forms a two dimensional coordination polymer. In the coordination environment of the polymer, the Na1 atom is six-coordinate with the coordination angle varying from 90° [78.82 (6)–90.60 (6)°], forming a distorted octahedral geometry. Atom Na2 also exhibits a distorted octahedral geometry, with the coordination angles ranging from 77.17 (6) to 91.77 (6)°. The cadmium atom also shows a distorted octahedral geometry with coordination angles in the range 87.94 (5) to 95.46 (6)°. A similar geometry is observed for the Cd atom in the heterobimetallic compound tetraaquabis-



Log in



Register



Cart

Home ▶ All Journals ▶ Polycyclic Aromatic Compounds ▶ List of Issues ▶ Volume 42, Issue 9
▶ Insilico Insight into the Association be ...



Enter keywords, author

This Journal



Advanced search

Polycyclic Aromatic Compounds >

Volume 42, 2022 - Issue 9

[Submit an article](#)[Journal homepage](#)

161

Views

2

CrossRef
citations to date

0

Altmetric

Research Articles

Insilico Insight into the Association between Polycyclic Aromatic Hydrocarbons and Human Toll like Receptor in Progression of Esophageal Carcinogenesis

Sreeja T. G.  & Resmi Raghunandan 

Pages 5975-5990 | Received 10 Jan 2021, Accepted 28 Jul 2021, Published online: 27 Aug 2021

 Cite this article <https://doi.org/10.1080/10406638.2021.1964990> Full Article Figures & data References Supplemental Citations Metrics

Related

[Reprints & Permissions](#)[Read this article](#)Research People
also
readRecommended
articles

Abstract

Cancer creates enormous burden and is a leading cause of death in most of the countries. Esophageal cancer (EC) is one of the most common cancers in the world and has the worst survival of all cancers. Esophageal Squamous Cell Carcinoma (ESCC) and adenocarcinoma are the two main types of esophageal cancer. Exposure of polycyclic aromatic hydrocarbons (PAHs) can be cited as one of the reasons for development of Esophageal Squamous Cell Carcinoma. Toll Like Receptors (TLRs) present in human esophageal epithelial cells may pose a major role in pathogen recognition, activation of innate immunity and cancer. The study attempts to predict the role of carcinogenic PAHs in TLR4 signaling pathway and how it can ultimately result in immuno suppression and development of esophageal cancer by insilico docking evaluation. For the study we retrieved the structure of sixteen PAHs from the PubChem database and the protein model of TLR4 (PDB ID: 4G8A) from protein data bank (PDB). The binding affinity of PAHs to the TLR4 receptor was calculated using molecular docking software Auto Dock1.5. The results showed that Benzo[a]pyrene showed strong interaction toward TLR4 receptor with the

Photocatalytic and antimicrobial activities of pure and Mn doped ZnO nanoparticles synthesised by *Annona Muricata* leaf extract [➤](#)

Vindhya P S et al.
International Journal
of Environmental
Analytical Chemistry
Published online: 13
Sep 2022

Functionalised Graphene Quantum Dots for Cholesterol Detection in Human Blood Serum

Original Article Published: 24 March 2021

Volume 31, pages 847–852, (2021) Cite this article



Journal of Fluorescence

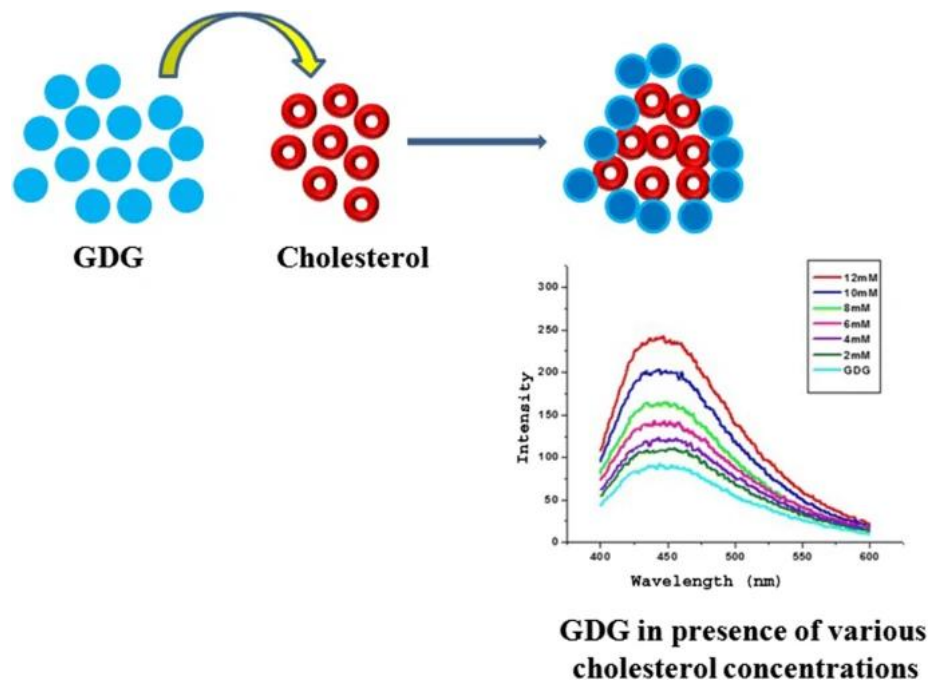
[Aims and scope](#)[Submit manuscript](#)[Shanti Krishna Ayilliath](#) , [Sreekanth Radhakrishnan Nair](#), [Gopu Chandrasekharan Lakshmi](#) & [Sreenivasan Kunnatheery](#) 528 Accesses  3 Citations [Explore all metrics](#) →

Abstract

The varied applications of nanotechnology have paved way for several breakthroughs in the realm of biomedical technology. In this challenging era when illness multiplies, timely and accurate disease diagnosis is very important. Thus, well founded novel approaches matter very much in areas like disease diagnosis and monitoring. Nanomedicine has tremendous implications in the given context. An elevated cholesterol concentration in blood is risky and is associated with cardiovascular diseases (CVD). CVD remains the No. 1 global cause of death and hence there is an urge to understand cholesterol level and take preventive measures. Highly fluorescent graphene quantum dots (GQs) are well known for their biocompatibility, non toxicity and aqueous solubility. Here in we report an easy and sensitive non enzymatic based cholesterol detection using digitonin conjugated graphene quantum dots (GDG). Selectivity studies and the cholesterol detection in human blood serum suggests the probe to be reliable and selective for blood cholesterol monitoring.

Graphical abstract

Digitonin conjugated fluorescent graphene quantumdots, an efficient probe for cholesterol sensing



 This is a preview of subscription content, [log in via an institution](#) to check access.

Access this article

[Log in via an institution](#)

[Buy article PDF 39,95 €](#)

Price includes VAT (India)

Instant access to the full article PDF.

Rent this article via [DeepDyve](#)

[Institutional subscriptions](#) →

Similar content being viewed by others

[Nitrogen-doped graphene quantum dot-based sensing platform for metabolite detection](#)

Article | 31 August 2020

[Functionalized N-doped graphene quantum dots for electrochemical determination of cholesterol through host-guest inclusion](#)

Article | 30 October 2018

[Highly sensitive and selective detection of free bilirubin using blue emitting graphene quantum dots \(GQDs\)](#)

Article | 12 August 2022

Data Availability

Development of MOF Based Corrosion Inhibitors

K.S. Beena Kumari ^{*1}, Sudha Devi R. ², O. Lekshmy ²

^{*1}Department of Chemistry, All Saints' College, Thiruvananthapuram, University of Kerala, India

²Post graduate and Research centre, Mahatma Gandhi College, Thiruvananthapuram, University of Kerala, India

Abstract:- A variety of corrosion inhibitors including inorganic salts and organic molecules with heteroatoms as well as π – electron clouds were applied as corrosion inhibitors of metals in different corrosive environments. Nanomaterials found numerous applications in the field of corrosion inhibition due to their greater surface area. Nano cages and hollow spheres present in metal organic framework increase their applications in the field of electrochemistry. A short review on the study of MOF as corrosion inhibitors was discussed in this article. Many features of MOF based corrosion inhibitors as well as their current trends and future scope were also discussed.

Keywords:- Corrosion, Inhibitor, MOF, Nanomaterials, Electrochemistry.

I. INTRODUCTION

Metals have properties like good electrical and thermal conductivity, high melting and boiling point, ductility, and malleability. Most of the metals react with humidity, gases and salts present in the environment and form stable compounds of their oxides, hydroxides, or sulphides as the corrosion products [1, 2]. Different techniques are applied to reduce the corrosion of the metals. These methods include painting, cathodic and anodic protection, use of corrosion inhibitors etc. [3, 4]. Nanomaterials found numerous applications in the field of corrosion inhibition due to their greater surface area [5, 6]. Nanomaterials prevent the corrosion by covering the active sites on the metal surface and thus increase their strength and durability [7]. MOF (metal-organic-framework) derived nanostructures have higher specific surface area, good morphology such as nano cages and hollow spheres, compared to other nanostructures.

1.1. MOF as corrosion inhibitors

A few studies are available in literature showing the application of MOF as good corrosion inhibitor. A 3D network of silver based MOF was reported [8] and was found to be suitable for preventing corrosion of carbon steel in 1M HCl solution. The above study reported that, this MOF is a mixed type inhibitor and adsorbed on the metal surface obeying Freundlich adsorption isotherm. Another similar study showed the metal organic framework based on both silver and nitrogen donors were good corrosion inhibitor for copper in HCl solution [9]. MOF containing organic ligand with substituted aryl, heteroaryl or heterocyclic compounds having an exocyclic sulphur group for corrosion inhibitor of metals and its alloys [10] was also reported. A new MOF was reported in literature from

Cadmium sulphate and 6- methylequinoline in presence of KSCN [11]. The authors of the above study used IR, H-NMR, UV- VISIBLE, TGA and XRD for characterization of MOF and reported that the MOF synthesized in their study consist of cyclic building blocks of (CdSCN)_n.

Influence of three metals based MOFs for the corrosion protection of mild steel was reported in 2017 [12]. The metals employed in MOF were Co, Ni and Cu. The prepared MOFs were characterised by XRD, FT-IR and TG analysis. Above study revealed that, both Ni and Cu MOFs were of one dimensional nanorods having foam like morphology whereas that of Co was large chunky particles with etched edges having uniform size and shape [12]. Development in the studies of MOFs leads to use of hydrophobic MOF like ZIF-8 in anticorrosion industry [13]. The conversion of ZnAl-CO₃ layered double hydroxide precursor buffer layers to well inter grown ZIF-8 coatings [13] was employed in that study. The MOF coatings showed a corrosive current which was four orders of magnitude lesser than bare Al substrate [13]. The difficulty in controlling the arrangement of inhibitor molecules in MOF pores leads to the application of Cetyltrimethyl ammonium bromide (CTAB) which contains hydrophobic and hydrophilic tails in classic HKUST-1 thin film for bronze conservation [14].

Literature showed the enhancement of anticorrosive properties of epoxy coating with MOF [15]. The BTA-Cu-MOF coating was analysed using FTIR, TG, XRD and SEM and it revealed that MOF was well dispersed in epoxy resin [15]. A recent study prepared an anticorrosive film from Samarium (III) nitrate and [bis(phosphonomethyl)amino] methylphosphonic acid (ATMP) for the protection of mild steel in saline solutions [16]. This thin film forms a uniform coating over steel surface. A novel MOF named as Zeolite imidazolate framework nano structure was reported as corrosion inhibitor for carbon steel in HCl medium [17] and using the ANOVA analysis the authors of the above study reported that temperature was not very significant in inhibition efficiency of the inhibitor. The very good inhibition property of MOF on metal surface was due to chemisorption of MOF on metal surface as revealed by thermodynamic study [17].

1.2. Futuristic Approach

Many of the synthetic organic corrosion inhibitors are known to have been restraining environmental protocols due to their perilous effects. Lot of research works are going on for the development of low cost, eco friendly and high inhibition efficiency inhibitors. The MOF is seems to be a

promising inhibitor due to the presence of a metal ion and organic frame work. The more electropositive metals like zinc and magnesium can protect the iron articles. The presence of more electropositive metal in organic frame work enhances the inhibition efficiency by sacrificial action. On the other hand, the organic frame work forms a protective layer over metal surface which reduces the corrosion rate. In view of this, green inhibitors such as plant extracts, can further improve the corrosion inhibition efficiency while using along with MOF. These green inhibitors are adsorbed on cathodic / anodic sites on the metal surface preventing the electrochemical reaction. The green corrosion inhibitors can be added along with MOF or can be incorporated in MOF during their synthesis. Another promising aspect in this direction is development of a MOF with a metal ion and organic frame work derived from a plant or other natural substance. Such types of inhibitors are eco friendly in nature and also low cost.

II. CONCLUSIONS

MOF (metal-organic-framework) derived nanostructures were found to be good corrosion inhibitors due to their higher specific surface area and good morphology compared to other nanostructures. MOF forms a mixed type inhibitor and adsorbed on the metal surface obeying Freundlich adsorption isotherm. The chemisorption of the MOF on the metal surface was also reported. The MOF can be used for protecting a variety of metals and its alloys which are exposed to different corrosive environments. The future will be of using a MOF prepared by combining a metal with green substrate as corrosion inhibitor.

REFERENCES

- [1]. Yaroslav G, Oleksandr B and Abdessamad F., The effect of humidity, impurities, initial state on the corrosion of carbon and stainless steel in molten hitecXL salt for CSP application, *Sol. Energy Mater. Sol. Cells*, 2018; 174: 34-41.
- [2]. Yan L, Wenguang Y, Guoyong W, Yaming W, Ana S M, Zhiwu H, and Luquan R, Reversibly switchable wettability on aluminium alloy substrate corresponding to different pH droplet and its corrosion resistance, *Chem. Eng.*, 2016; 303: 565-574.
- [3]. Behzad F, Navid N, and Amir D A., On coating techniques for surface protection : A Review, *J. Manufact. Mat. Proc.* 2019; 3(1): 28.
- [4]. Beenakumari K.S., Inhibitory effects of *Murraya koenigii* (curry leaf) leaf extract on the corrosion of mild steel in 1 M HCl, ***Green Chem. Lett. Rev.***, 2011; 4(2):117-120.
- [5]. Mosavat S. H., Shariat M. H., and Bahrololoom M. E., Study of corrosion performance of electrodeposited nanocrystalline Zn-Ni alloy coating, *Corros. Sci.*, 2012; 59: 81-87.
- [6]. Kunyao C, Zongxue Y, Din Y, Legang C, Yong J, and Lijuan Z., Fabrication of BTA-MOF-TEOS-GO nanocomposite coating systems with active inhibition and durable anticorrosion performances, *Prog. Org. Coat.*, 2020; 143: 105629.
- [7]. Muhammed A P and Anuradha R, Corrosion resistance of BIS 2062-grade steel coated with nano-metal oxide mixtures of iron, cerium, and titanium in the marine environment, *Appl. Nanosci.*, 2018; 8: 41-51.
- [8]. Safaa E H E, Abd E, Fouda S, Structure, Characterization and Anti-Corrosion Activity of the New Metal-Organic Framework [Ag(qox)(4-ab)], *J. Inorg. Organomet. Pol. Mat.*, 2011; 21: 327- 335.
- [9]. Abd E, Fouda S, Safaa E, Etaiw H., MOFs based on silver(I) and N-donors as new corrosion inhibitors for Cu in HCl solutions, *J. Mol. Liq.*, 2016;213: 228-234.
- [10]. Mardel J I, COLE I S, Markley T A, Harvey T G, Osborne J and Sapper E., Polymeric Agents And Compositions For Inhibiting Corrosion, Patent Number: WO2017152240 (WIPO).
- [11]. Safaa E H, Etaiw M, Elbendary M, Manal M and Maher A., A new metal-organic framework based on cadmium thiocyanate and 6-methylequinoline as corrosion inhibitor for copper in 1 M HCl solution, *Prot. Met. Phys. Chem. Surf.*, 2017; 53: 937-949.
- [12]. Kumaraguru S, Pavulraj R and Mohan S., Influence of Co, Ni, Cu-based MOFs on the corrosion protection of mild steel, *Int. J. Surf. Eng. Coat.*, 2017; 95(3)
- [13]. Mu Z, Liang M, Liangliang W, Yanwei S and Yi L, Insights into the Use of Metal-Organic Framework As High-Performance Anticorrosion Coatings, *Appl. Mat. Interfaces.*, 2018; 10: 2259-2263.
- [14]. Weijin L, Baohui R, Yanning C, Xusheng W and Rong C., Excellent efficiency of MOF films for bronze art work conservation : The key role of HKUST-1 film nano containers in selectively positioning and protecting inhibitors, *Appl. Mat. Interfaces*, 2018; 10 (43): 37529-37534.
- [15]. Di Y, Zongxue Y, Legang C and Kunyao C., Enhancement of the Anti-Corrosion Performance of Composite Epoxy Coatings in Presence of BTA-loaded Copper-Based Metal-Organic Frameworks, *Int. J. Electrochem. Sci.*, 2019; 14: 4240-4253.
- [16]. Ali D, Fatemeh P, Ghasem B and Bahram R., Fabrication of metal-organic based complex film based on three-valent samarium ions-[bis (phosphonomethyl) amino] methylphosphonic acid (ATMP) for effective corrosion inhibition of mild steel in simulated seawater, *Constr. Build. Mater.*, 2020; 239: 117812.
- [17]. Sakinch Z, Mahdi N S and Mahboube G., New MOF-based corrosion inhibitor for carbon steel in acidic media, *Met. Mater.*, Int. 2020; 26: 25-38.

On the General Position Number of Complementary Prisms

Article type: Research Article

Authors: [Neethu, P. K.](https://content.iospress.com:443/search?q=author%3A%28%22Neethu, P. K.%22%29) (https://content.iospress.com:443/search?q=author%3A%28%22Neethu, P. K.%22%29)^a | [Chandran, S.V. Ullas](https://content.iospress.com:443/search?q=author%3A%28%22Chandran, S.V. Ullas%22%29) (https://content.iospress.com:443/search?q=author%3A%28%22Chandran, S.V. Ullas%22%29)^a | [Changat, Manoj](https://content.iospress.com:443/search?q=author%3A%28%22Changat, Manoj%22%29) (https://content.iospress.com:443/search?q=author%3A%28%22Changat, Manoj%22%29)^b | [Klavžar, Sandi](https://content.iospress.com:443/search?q=author%3A%28%22Klavžar, Sandi%22%29) (https://content.iospress.com:443/search?q=author%3A%28%22Klavžar, Sandi%22%29)^c; *

Affiliations: [a] Department of Mathematics, Mahatma Gandhi College, University of Kerala, Thiruvananthapuram-695004, Kerala, India. p.kneethu.pk@gmail.com (mailto:p.kneethu.pk@gmail.com), svuc.math@gmail.com (mailto:svuc.math@gmail.com) | [b] Department of Futures Studies, University of Kerala, Thiruvananthapuram-695581, Kerala, India. mchangat@keralauniversity.ac.in (mailto:mchangat@keralauniversity.ac.in) | [c] Faculty of Mathematics and Physics, University of Ljubljana, Slovenia. sandi.klavzar@fmf.uni-lj.si (mailto:sandi.klavzar@fmf.uni-lj.si)

Correspondence: [*] Address for correspondence: Faculty of Mathematics and Physics, University of Ljubljana, Slovenia. Also affiliated at: Faculty of Natural Sciences and Mathematics, University of Maribor, Slovenia and Institute of Mathematics, Physics and Mechanics, Ljubljana, Slovenia.

Abstract: The general position number $gp(G)$ of a graph G is the cardinality of a largest set of vertices S such that no element of S lies on a geodesic between two other elements of S . The complementary prism GG^- of G is the graph formed from the disjoint union of G and its complement G^- by adding the edges of a perfect matching between them. It is proved that $gp(GG^-) \leq n(G) + 1$ if G is connected and $gp(GG^-) \leq n(G)$ if G is disconnected. Graphs G for which $gp(GG^-) = n(G) + 1$ holds, provided that both G and G^- are connected, are characterized. A sharp lower bound on $gp(GG^-)$ is proved. If G is a connected bipartite graph or a split graph then $gp(GG^-) \in \{n(G), n(G)+1\}$. Connected bipartite graphs and block graphs for which $gp(GG^-) = n(G) + 1$ holds are characterized. A family of block graphs is constructed in which the gp -number of their complementary prisms is arbitrary smaller than their order.

Keywords: general position set, complementary prism, bipartite graph, split graph, block graph

DOI: 10.3233/FI-2021-2006

Journal: [Fundamenta Informaticae](https://content.iospress.com:443/journals/fundamenta-informaticae) (https://content.iospress.com:443/journals/fundamenta-informaticae), vol. 178, no. 3, pp. 267-281, 2021

Received January 2020 | October 2020 | **Published:** 15 January 2021

Price: EUR 27.50



REVISTAS CIENTÍFICAS
de la Universidad Católica del Norte.
revistas@ucn.cl



doi 10.22199/issn.0717-6279-2021-02-0023

PROYECCIONES
Journal of Mathematics

ISSN 0717-6279 (On line)

On independent position sets in graphs

Elias John Thomas¹  orcid.org/0000-0003-0598-4726
Ullas Chandran S. V.²  orcid.org/0000-0002-2081-9094

¹Mar Ivanios College, University of Kerala, Dept. of Mathematics, Thiruvananthapuram, KL, India.

✉ eliasjohnkalarickal@gmail.com

²Mahatma Gandhi College, University of Kerala, Dept. of Mathematics, Thiruvananthapuram, KL, India.

✉ svuc.math@gmail.com

Received: April 2020 | Accepted: October 2020

Abstract:

An independent set S of vertices in a graph G is an independent position set if no three vertices of S lie on a common geodesic. An independent position set of maximum size is an ip-set of G . The cardinality of an ip-set is the independent position number, denoted by $ip(G)$. In this paper, we introduce and study the independent position number of a graph. Certain general properties of these concepts are discussed. Graphs of order n having the independent position number 1 or $n - 1$ are characterized. Bounds for the independent position number of Cartesian and Lexicographic product graphs are determined and the exact value for Corona product graphs are obtained. Finally, some realization results are proved to show that there is no general relationship between independent position sets and other related graph invariants.

Keywords: General position set; Independent set; Independent number; Independent position number.

MSC (2020): 05C12, 05C69.

Cite this article as (IEEE citation style):

E. J. Thomas and U. Chandran S. V., "On independent position sets in graphs", *Proyecciones (Antofagasta, On line)*, vol. 40, no. 2, pp. 385-398, 2021, doi: 10.22199/issn.0717-6279-2021-02-0023



Article copyright: © 2021 Elias John Thomas and Ullas Chandran S. V. This is an open access article distributed under the terms of the Creative Commons License, which permits unrestricted use and distribution provided the original author and source are credited.



1. Introduction

The general position problem in a graph G is to find the maximum size of a set S of vertices in G such that no three vertices of S lie on a common shortest path. The general position problem in graph theory was introduced and studied in [1] after getting inspiration from the century old Dudeney's no-three-in-line problem [2] and by the general position subset selection problem [3,4] from discrete geometry. But the same concept has already been studied two years earlier in [5] under the name *geodetic irredundant sets*. Refer [6,7,8,9,10,11] to understand the recent developments on general position number.

Graphs in this paper are finite, undirected and simple. The *distance* between two vertices u and v in a connected graph G is the length of a shortest u, v -path in G , denoted as $d(u, v)$. A u, v -*geodesic* is a u, v -path of length $d(u, v)$. Obviously the distance is a metric on the vertex set V . The maximum distance between all pairs of vertices of G is the diameter, $diam(G)$ of G . The *interval* $I_G[u, v]$ between vertices u and v of a graph G is the set of vertices x such that there exists a u, v -geodesic which contains x . For a positive integer n , let $[n] = 1, \dots, n$.

A set of vertices $S \subseteq V(G)$ is a *general position set* of G if no three vertices of S lie on a common geodesic. A gp-set is thus a largest general position set. The *general position number* (*gp-number* for short) of G is the cardinality of a gp-set of G . An independent set or a stable set S , is a set of vertices in a graph such that no two vertices of S are adjacent. The vertex independence number of a graph (or simply, independence number) is the cardinality of the largest independent vertex set. The independence number is most commonly denoted by $\alpha(G)$.

In this paper, we investigate the properties of a graph invariant named independent position number which admits both the properties of general position set and independence set. In the following section definitions and preliminary observations are listed. In Section 3, we prove some bounds for independent position number on Cartesian product, lexicographic product and an exact value for corona product of graphs. In section 4, we prove some realization results which shows that the independent position number is different from other related invariants.

In this paper, we make use of the following results.

Theorem 1.1. [5] *For a connected graph G of order n and diameter d , $gp(G) \leq n - d + 1$.*

Theorem 1.2. [5] For a connected graph G , $gp(G) = 2$ if and only if $G = P_n$ or $G = C_4$.

Theorem 1.3. [5] For any tree T with k end vertices, $gp(T) = k$.

2. Independent general position sets in graphs

A set S of vertices in a graph G is considered to be an independent position set if S is both an independent set and a general position set in G . An independent position set of maximum size is called an *ip*-set of G . The cardinality of an *ip*-set is called the independent position number, denoted by $ip(G)$. It is clear that every independent position set is a general position set and so we have the following observation.

Observation 2.1. For any connected graph G of order n , $1 \leq ip(G) \leq gp(G) \leq n$.

Example 2.2. For the graph G in Figure 1, the set $S = \{v_1, v_2, v_3, v_4\}$ is a maximum general position set of G . Then $gp(G) = 4$. On the other hand, any independent position set of G contains at most one vertex from the set $\{v_1, v_2, v_3, v_4\}$ and so $ip(G) \leq 3$. Now, since the set $T = \{v_5, v_1, v_6\}$ is an independent position set, it follows that $ip(G) = 3$.

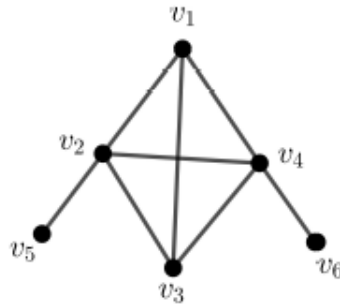


Figure 1

Proposition 2.3. For a connected graph G of order n and diameter d , $ip(G) \leq n - d + 1$.

Proof. This follows from Theorem 1.1 and Observation 2.1. ■

Proposition 2.4. . For any connected graph G of order n , $1 \leq ip(G) \leq \alpha(G)$.

Proof. The left inequality is trivial and the right inequality follows from the fact that every independent position set is an independent set. The independent position number can be significantly small while compared to the independent number. To certain instant, consider the path $P_n (n \geq 5)$. Then it is clear from Theorem 1.2 and Observation 2.1 that $ip(G) = 2$, where as $\alpha(G) = \lceil \frac{n}{2} \rceil$. ■

Theorem 2.5. Let G be a connected graph with diameter atleast 3. Then $ip(G) = \alpha(G)$.

Proof. By Proposition 2.4, it remains to prove that $ip(G) \geq \alpha(G)$. For, let S be a maximum independent set of G . Assume the contrary that there exists three vertices x, y and z in S such that $y \in I_G[x, z]$. Let $P : x = x_0, x_1, \dots, x_i = y, x_{i+1}, \dots, x_n = z$ be an x, z - geodesic in G containing the vertex y . Now, since S is an independent set, it follows that $2 \leq i \leq n - 2$. This shows that $d_G(x, z) \geq 4$, a contradiction to the fact that $diam(G) \leq 3$. Hence S must be a general position set of G and so $ip(G) \geq |S| = \alpha(G)$. ■

The converse need not be true. Consider the graph in Figure 2. Then $diam(G) = 4$ whereas, the set $\{v_2, v_3, v_5, v_6\}$ is a maximum independent set which is also a general position set. Hence $ip(G) = 4 = \alpha(G)$.

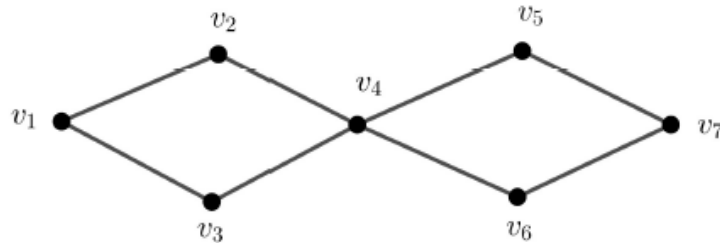


Figure 2

In view of Theorem 2.5, we have the following open problem.

Problem 2.6. Characterize the classes of graphs in which $ip(G) = \alpha(G)$.

Theorem 2.7. For any tree T with k end vertices, $ip(T) = k$.

Proof. Since the set of all end vertices of T is an independent position set, it follows that $ip(T) \geq k$. Now, it follows from Theorem 1.3 and Observation 2.1 that $ip(T) \leq gp(T) = k$. ■

Theorem 2.8. Let G be a connected graph of order n . Then

1. $ip(G) = 1$ if and only if $G \cong K_n$.
2. $ip(G) = n - 1$ if and only if $G \cong K_{1,n-1}$.

Proof.

1. If $G \cong K_n$, then it is obvious that $ip(G) = 1$. On the other hand, let $ip(G) = 1$. If G is non-complete, then there exists vertices u and v in G such that $u, v \notin E(G)$. Then $\{u, v\}$ is an independent position set and so $ip(G) \geq 2$, impossible. Hence $G \cong K_n$.
2. First, suppose that $ip(G) = n - 1$. Then it follows from Proposition 2.3 that $diam(G) \leq 2$. Since, the complete graph K_n has independent position number 1, it follows that $diam(G) = 2$. Let $S = \{v_1, v_2, \dots, v_{n-1}\}$ be an independent set of size $n - 1$ and $v \in V(G)$ such that $v \notin S$. Now, since S is an independent set and G is connected, we have that v must be adjacent to all the vertices of S . Then $G \cong K_{1,n-1}$. On the other hand, if $G \cong K_{1,n-1}$ then it is evident that $ip(G) = n - 1$. ■

Theorem 2.9. If G is a bipartite graph, then $ip(G) = gp(G)$.

Proof. If $G = P_n$ or $G = C_4$, then one can easily verify that $ip(G) = gp(G) = 2$. So in the following we may assume that G is neither a path nor a C_4 , so that $gp(G) \geq 3$. Now, let S be a maximum general position set of G . Let S_1, S_2, \dots, S_k ($k \geq 1$) be the components of the induced subgraph of S in G . Since G is bipartite and each S_i ($1 \leq i \leq k$) induces a clique, it follows that $|S_i| \leq 2$ for all $i \in [k]$. This shows that $k \geq 2$. In the following, we claim that $|S_i| = 1$ for all $i \in [k]$. Assume the contrary that S_1 contains two vertices, say u and v . Since S_1 induces a clique in G , we have that u and v are adjacent in G . Let w be any vertex in S_2 . Since S is a general position

set, it follows that $d(u, w) = d(v, w)$. Now, let $P : w = x_1, x_2, \dots, x_r = u$ be a w, u -geodesic in G and let $Q : w = y_1, y_2, \dots, y_r = v$ be a w, v -geodesic in G . Let t be the largest suffix such that $x_t \in V(Q)$. Since $d(u, w) = d(v, w)$, it follows that $x_t = y_t$ and hence the x_t, u -subpath of P and y_t, v -subpath of Q together with the edge uv forms an odd cycle in G . This is impossible in a bipartite graph. This shows that $|S_i| = 1$ for all $i \in [k]$. Hence S is an independent general position set in G and so $ip(G) \geq |S| = gp(G)$. Now, Observation 2.1 implies that $ip(G) = gp(G)$. ■

The converse of the above theorem need not be true. For, consider the non-bipartite graph shown in the Figure 3. Then the set $S = \{u_2, u_3, u_5, u_6\}$ is an independent position set in G . On the other hand, any general position set of G contains at most two vertices from each component of $G \setminus u_4$. This shows that S is a maximum independent position set as well as a maximum general position set of G . Thus $gp(G) = ip(G)$.

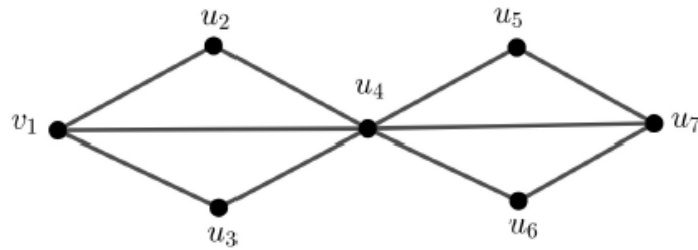


Figure 3

3. Independent position number on some graph operations

In the following section, we determine some bounds of independent position number on cartesian product, lexicographic product and an exact value for corona product of graphs. For more on the product graphs see [12].

3.1. Cartesian products

The Cartesian product $G \square H$ of graphs G and H has the vertex set $V(G) \times V(H)$ and the edge set $E(G \square H) = \{(g, h)(g', h') : gg' \in E(G) \text{ and } h = h', \text{ or, } g = g' \text{ and } hh' \in E(H)\}$. If $(g, h) \in V(G \square H)$, then the G -layer G^h through the vertex (g, h) is the subgraph of $G \square H$ induced by the vertices $(g', h) : g' \in V(G)$. Similarly, the H -layer H^g through (g, h) is the subgraph of $G \square H$ induced by the vertices $(g, h') : h' \in V(H)$. It is well-known that for given vertices $u = (g_1, h_1)$ and $v = (g_2, h_2)$ of $G \square H$ we have $d_{G \square H}(u, v) = d_G(g_1, g_2) + d_H(h_1, h_2)$.

The announced lower bound reads as follows.

Theorem 3.1. *For any connected graphs G and H , $ip(G \square H) \geq ip(G) + ip(H) - 2$.*

Proof. Let S and T be the maximum independent position sets of G and H respectively. Let $g \in S$ and $h \in T$ and $S_1 = \{(x, h) | x \in S\}$ and $T_1 = \{(g, y) | y \in T\}$. We claim that $W = (S_1 \cup T_1) \setminus \{(g, h)\}$ is an independent position set in $G \square H$. First, we prove that W is an independent set in $G \square H$. Since S and T are independent set in G and H respectively, it follows that both S_1 and T_1 are independent sets in $G \square H$. Let $(x, h) \in S_1$ and $(g, y) \in T_1$. Then it is clear that $x \neq g$ and $y \neq h$ and so by definition it follows that (x, h) is not adjacent to (g, y) . Thus there is no adjacency between the vertices of S_1 and T_1 in $G \square H$. This shows that W is an independent set in $G \square H$. Next, we claim that W is a general position set in $G \square H$. Since layers are convex sets in $G \square H$, it follows that both S_1 and T_1 are general position sets in $G \square H$. Now, suppose there exist vertices $(x, h), (u, v), (g, y) \in W$ such that $(u, v) \in I_{G \square H}[(x, h), (g, y)]$. Without loss of generality, we may assume that $(u, v) \in S_1$. Then $(u, v) \neq (g, h)$ and $v = h$. Let $P : (x, h) = (x_1, y_1), (x_2, y_2), \dots, (x_i, y_i) = (u, h), (x_{i+1}, y_{i+1}), \dots, (x_n, y_n) = (g, y)$ geodesic in $G \square H$ containing the vertex (u, v) . Since G -layer G^h is a convex set in $G \square H$, it follows that $y_1 = y_2 = \dots = y_i = h$. Thus $x_j \neq g$ for all $j = [i]$. Let k be the largest suffix such that $y_k = h$. Thus $x_{k+1} = x_{k+2} \dots = x_n = g$. This shows that $x = x_1, x_2, \dots, x_i = u, \dots, x_n = g$ is a x, g -geodesic in G containing the vertex u with $x, u, g \in S$. This is a contradiction to the fact that S is a general position set, Thus W must be a general position set in $G \square H$ and $ip(G \square H) \geq |W| = ip(G) + ip(H) - 2$. ■

3.2. Lexicographic products

The lexicographic product $G[H]$ of two graphs G and H has vertex set $V(G) \times V(H)$ and two vertices (u_1, v_1) and (u_2, v_2) are adjacent whenever $u_1u_2 \in E(G)$, or $u_1 = u_2$ and $v_1v_2 \in E(H)$. To prove the bound on Lexicographic products, we may make use of the following Lemma.

Lemma 3.2. [13] *Let G and H be graphs. Then*

1. *The graph $G[H]$ is connected if and only if G is connected.*
2. *The lexicographic product is associative but not commutative.*
3. *If G is connected, then $d_{G[H]}((g, h), (g', h')) = d_G(g, g')$ if $g \neq g'$
 $d_{G[H]}((g, h), (g, h')) = 2$ if $hh' \notin E(H)$
 $d_{G[H]}((g, h), (g, h')) = 1$ if $hh' \in E(H)$*

Theorem 3.3. *For any connected graphs G and H , $ip(G[H]) \geq ip(G)ip(H)$.*

Proof. Let S be an ip -set of G and T be an ip -set of H . We first show that $S \times T$ is an independent position set in $G[H]$. For, suppose that the vertices (g_1, h_1) and (g_2, h_2) in $S \times T$ are adjacent in $G[H]$, then we have either $g_1g_2 \in E(G)$ or $h_1h_2 \in E(H)$. This is impossible. Thus $S \times T$ is an independent set in $G[H]$. Next, we claim that $S \times T$ is a general position set in $G[H]$. Assume on contrary that there exist $(g_1, h_1), (g_2, h_2), (g_3, h_3) \in S \times T$ such that $(g_2, h_2) \subseteq I_{G[H]}[(g_1, h_1), (g_3, h_3)]$. First, suppose that $(g_1, h_1), (g_3, h_3)$ belongs to the same H -layer H^g . Thus $g_1 = g_3 = g$ and $d_{G[H]}[(g, h_1), (g, h_3)] = 2$. In this case (g_2, h_2) is adjacent with both (g_1, h_1) and (g_3, h_3) , a contradiction to the fact that $S \times T$ is an independent set. Hence $g_1 \neq g_3$. Let $(g_1, h_1) = (x_1, y_1), (x_2, y_2), \dots, (x_i, y_i) = (g_2, h_2), \dots, (x_n, y_n) = (g_3, h_3)$ be a $(g_1, h_1), (g_3, h_3)$ -geodesic contains the vertex (g_2, h_2) . Then by Lemma 3.2 $d_G(g_1, g_3) = d_{G[H]}[(g_1, h_1), (g_3, h_3)]$ and so $g_1 = x_1, x_2, \dots, x_i = g_2, \dots, x_n = g_3$ is a g_1, g_3 -geodesic in G containing the vertex g_2 . This is a contradiction. Hence $S \times T$ is an independent position set in $G[H]$. So $ip(G[H]) \geq |S \times T| = ip(G)ip(H)$. ■

The bound is sharp. Consider the graph $C_4[K_2]$ shown in the Figure 4.

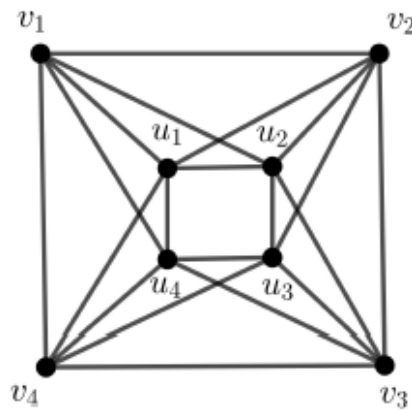


Figure 4

Clearly from the Figure 4, we can choose atmost two vertices v_1, v_3 or v_2, v_4 or u_1, u_3 or u_2, u_4 from the every layer. If we choose only one vertex from first layer say, v_1 then the possible choice of vertex from the second layer is u_3 only, since v_1 is adjacent to v_2, v_4, u_1, u_2, u_4 . Therefore, $ip(C_4[K_2]) = |S \times T| = 2 = |S| \times |T| = ip(C_4)ip(K_2)$.

3.3. Corona of graphs

Let G and H be graphs where $V(G) = \{v_1, \dots, v_{n(G)}\}$. The corona $G \circ H$ of graphs G and H is obtained from the disjoint union of G and $n(G)$ disjoint copies of H , say $H_1, \dots, H_{n(G)}$, where for all $i \in [n(G)]$, the vertex $v_i \in V(G)$ is adjacent to each vertex of H_i .

Theorem 3.4. For any graphs G and H , $ip(G \circ H) = n(G)\alpha(H)$.

Proof. Let $V(G) = \{v_1, v_2, \dots, v_n\}$ and let H_1, H_2, \dots, H_n be the corresponding copies of H in $G \circ H$. For each $i \in [n]$, let S_i denote the maximum independent set in H . Then the set $S = S_1 \cup S_2 \dots \cup S_n$ is an independent position set in $G \circ H$. Hence $ip(G \circ H) \geq |S| = n(G)\alpha(H)$. On the other hand, let T be the maximum general position set in $G \circ H$. Then $|T| \geq n(G)\alpha(H)$.

Claim: $T \subseteq \bigcup_{i=1}^n H_i$.

Suppose that there exists a vertex $v_i \in T$ for some i with $1 \leq i \leq n$. Then since T is an independent set, we have that $V(H_i) \cap T = \emptyset$. Moreover, the set $(T \setminus \{v_i\}) \cup S_i$ is an independent position set of size atleast the size of T . Hence without loss of generality, we may assume that $T \subseteq \bigcup_{i=1}^n H_i$. Moreover, since T is an independent set, we have that $T \cap H_i$ is also an independent subset of H_i . Then $|T \cap H_i| \leq \alpha(H)$. Hence $|T| = \sum_{i=1}^n |H_i| \leq n(G)\alpha(H)$. This shows that $ip(G \circ H) = n(G)\alpha(H)$. ■

4. Some Realization Results

Here, we prove some realization results which shows that the independent position number is different from other related invariants.

Theorem 4.1. *For integers k and n with $1 \leq k < n$, there is a connected graph G of order n such that $ip(G) = k$.*

Proof. If $k = 1$ or $k = n - 1$, obviously the graphs K_n and $K_{1,n-1}$ respectively having the desired properties. If $k = n - 2$, then it follows from Theorem 2.7 that $ip(T) = n - 2$ for any tree T with diameter 3. So, assume that $2 \leq k \leq n - 3$. Let G be the graph obtained from the cycle $C_{(n-k+2)} : v_1, v_2, \dots, v_{(n-k+2)}, v_1$ by adding $k - 2$ new vertices $u_1, u_2, \dots, u_{(k-2)}$ and joining each u_i to both v_1 and $v_{(n-k+2)}$. The graph G is shown in the Figure 5.

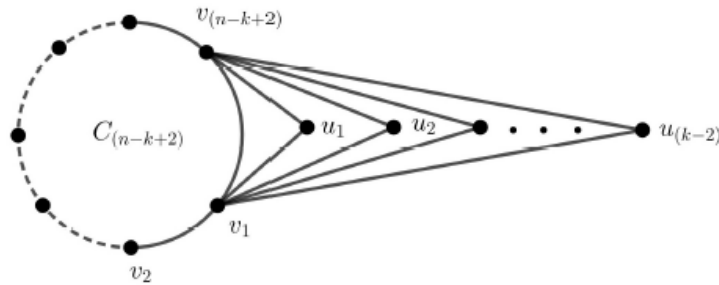


Figure 5

From the graph G in Figure 5, it is clear that $|G| = n - k + 2 + k - 2 = n$. We claim that $ip(G) = k$, it is clear that any independent position set contains at most two vertices from the cycle. Thus $ip(G) \leq n - (n - k + 2) + 2 = k$. Now, on the other hand, the set $M = \{u_1, u_2, \dots, u_{(k-2)}, v_i, v_m\}$ with $i, m \in \{1, n - k + 2\}$ is an ip -set in G , we have that $ip(G) = k$. ■

Theorem 4.2. For every pair of positive integers a, b with $2 \leq a \leq b < n$, there exists a connected graph G with $ip(G) = a$ and $gp(G) = b$.

Proof. We consider the following two cases.

Case 1. $a = b$. In this case, the graph G of order n with desired properties is constructed as follows. Let G be the graph obtained from the path $P : v_1, v_2, \dots, v_{(n-a+2)}$ by adding $(a - 2)$ new vertices $\{u_1, u_2, \dots, u_{(a-2)}\}$ and joining each u_i to the vertex v_3 . The graph G is shown in the Figure 6. Then, from Theorem 2.7 and Theorem 1.3 we get that $ip(G) = gp(G) = a$.

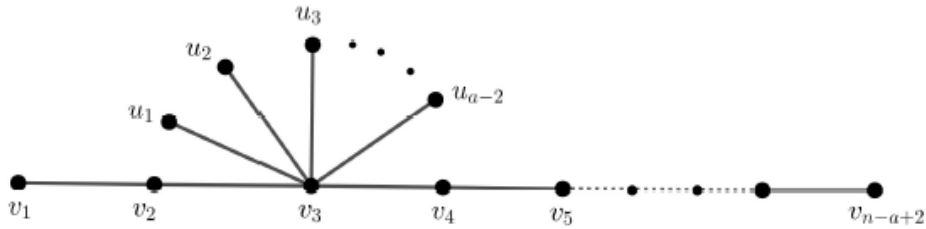


Figure 6

Case 2. $2 < a < b < n$

Let H be the graph obtained from the complete graph $K_{(b-a+2)} : w_1, w_2, \dots, w_{(b-a+2)}$ and a vertex disjoint path $P : u_0, u_1, u_2, \dots, u_{(n-b-1)}$ by identifying the vertices w_1 and u_0 . Let G the graph obtained from the graph H by adding $a - 1$ new vertices $v_1, v_2, \dots, v_{(a-1)}$ and join each v_i to the vertex $u_{(n-b-1)}$. The graph G of order n is shown in the Figure 7.

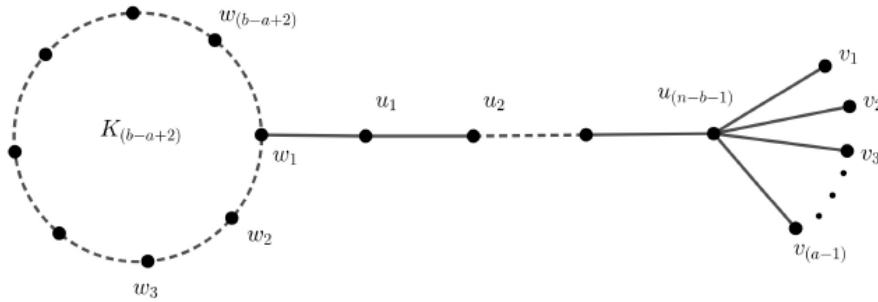


Figure 7

Let S be a maximum general position set of G . Then S contains at most two vertices from the set $\{w_1, u_1, u_2, \dots, u_{(n-b-1)}, v_1\}$. This shows that $|S| \leq b$. Now, on the other hand, since the set $\{w_2, w_3, \dots, w_{(b-a+2)}, v_1, v_2, \dots, v_{(a-1)}\}$ is a maximum general position set in G , it follows that $gp(G) = |S| = a - 1 + (b - a + 1) = b$.

Next, we prove that $ip(G) = a$. Let T be any independent position set. Then T contains at most one vertex from the the set $\{w_1, w_2, \dots, w_{(b-a+2)}\}$. Also, T contains at most two vertices from the set $\{w_1, u_1, u_2, \dots, u_{(n-b-1)}, v_1\}$. Hence $|S| \leq a$. Now, since the set $\{w_1, v_1, v_2, \dots, v_{(a-1)}\}$ is an independent position set, we have that $ip(G) = a$. ■

Theorem 4.3. For every pair of positive integers a, b with $2 \leq a \leq b$, there exists a connected graph G with $ip(G) = a$ and $\alpha(G) = b$.

Proof. We consider the following two cases.

Case 1. $a = b$. Then the the complete bipartite graph $K_{a,a}$ has the required properties.

Case 2. $2 < a < b$.

Let G be the graph obtained from the cycle $C_{2(b-a+2)} : v_1, v_2, \dots, v_{2(b-a+2)}$ by adding $a - 2$ new vertices $u_1, u_2, \dots, u_{(a-2)}$ and joining each u_i to the vertex v_1 . The graph G thus obtained is shown in the Figure 8.

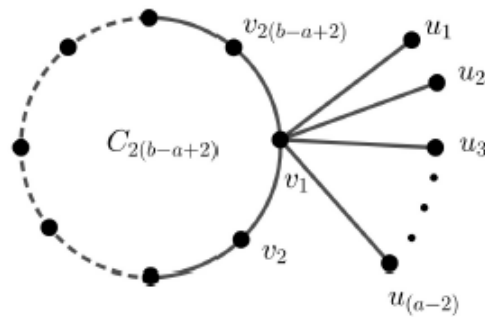


Figure 8

Let I be a maximum independent set in G . Then I contains at most $b-a+2$ vertices from the cycle $C_{2(b-a+2)}$. If $v_1 \in I$, then $|I| = b-a+2 \leq b$. So assume that $v_1 \notin I$. Then $|I| \leq b$. On the other hand, since the set $\{v_2, v_4, \dots, v_{2(b-a+2)}, u_1, u_2, \dots, u_{(a-2)}\}$ is an independent set of size b , we have that $|I| = \alpha(G) = b-a+2+a-2 = b$.

Next, we prove that $ip(G) = a$. Note that any independent position set S contains at most two vertices from the cycle $C_{2(b-a+2)}$. This shows that $ip(G) \leq a$. Now, since the set $\{v_{2(b-a+2)}, v_2, u_1, u_2, \dots, u_{(a-2)}\}$ is an independent position set of size a , we have that $ip(G) = |S| = 2+a-2 = a$. ■

References

- [1] P. Manuel and S. Klavžar, "A general position problem in graph theory", *Bulletin of the Australian Mathematical Society*, vol. 98, no. 2, pp. 177-187, 2018, doi: 10.1017/S0004972718000473
- [2] H. E. Dudeney, *Amusements in mathematics*. New York, NY: Dover, 1958.
- [3] V. Froese, I. Kanj, A. Nichterlein, and R. Niedermeier, "Finding points in general position", *International journal of computational geometry & applications*, vol. 27, no. 4, pp. 277-296, 2017, doi: 10.1142/S021819591750008X

- [4] M. S. Payne and D. R. Wood, "On the general position subset selection problem", *SIAM journal on discrete mathematics*, vol. 27, no. 4, pp. 1727-1733, 2013, doi: 10.1137/120897493
- [5] S. Ullas Chandran and G. J. Parthasarathy, "The geodesic irredundant sets in graphs", *International journal of mathematical combinatorics*, vol. 4, 2016. [On line]. Available: <https://bit.ly/3aWmKN3>
- [6] B. S. Anand, S. Ullas Chandran, M. Changat, S. Klavžar, and E. J. Thomas, "Characterization of general position sets and its applications to cographs and bipartite graphs", *Applied mathematics and computation*, vol. 359, pp. 84-89, 2019, doi: 10.1016/j.amc.2019.04.064
- [7] M. Ghorbani, S. Klavžar, H. R. Maimani, M. Momeni, F. Rahimi Mahid, and G. Rus, "The general position problem on kneser graphs and on some graph operations", Mar. 2019. *arXiv*: 1903.04286.
- [8] B. Patkós, "On the general position problem on kneser graphs", Mar. 2019. *arXiv*:1903.08056.
- [9] P. Neethu, S. Ullas Chandran, M. Changat, and S. Klavžar, "On the general position number of complementary prisms", Jan. 2020. *arXiv*:2001.02189.
- [10] G. M. Thankachy, E. J. Thomas, and S. Ullas Chandran, "On the vertex position number of a graph", unpublished.
- [11] E. J. Thomas and S. Ullas Chandran, "Characterization of classes of graphs with large general position number", *AKCE international journal of graphs and combinatorics*, vol. 17, no. 3, 2020, doi: 10.1016/j.akcej.2019.08.008
- [12] R. Hammack, W. Imrich, and S. Klavžar, *Handbook of product graphs*, 2nd ed. Boca Raton: CRC Press, 2011, doi: 10.1201/b10959
- [13] B. S. Anand, M. Changat, U. Chandran, and P. P. Goswami, "The edge geodetic number of product graphs," in *Algorithms and discrete applied mathematics*, B. S. Panda, Ed. Cham: Springer, 2018, pp. 143-154, doi: 10.1007/978-3-319-74180-2_12

Emotional autonomy and impulsivity among adolescents

Gopika S S¹ and Dr Aneesh V Appu²

¹BSc Psychology Student, Department of Psychology, Mahatma Gandhi College, Trivandrum, Kerala

²Assistant Professor, Department of Psychology, Mahatma Gandhi College, Trivandrum, Kerala

Abstract--Adolescence, an extraordinary phase in development, marks the journey from a careless child to a self-reliant adult. The current research focused on adolescent emotional autonomy and impulsivity. The goal of the study was to see if these factors differed between males and females. The study also aimed to study the correlation of each of the variables. The participants in the current study were 70 adolescents. The Emotional Autonomy Scale (Steinberg & Silverberg, 1986) and Barratt's Impulsiveness Scale (Patton, Stanford, & Barrat, 1995) were utilized in the study, and data was through online questionnaires. On analysis of the data using t-test and Pearson correlation, it was discovered that dimensions of emotional autonomy and impulsivity vary significantly among males and females. Emotional autonomy and impulsivity were also found to be adversely associated. According to the findings, adolescent's should be taught to be emotionally self-sufficient with the support of their parents. The study also suggests that adolescent's impulsivity can be curbed to a certain extent by providing emotional support to them.

Keywords-- adolescence, emotional autonomy, impulsivity, gender

1. INTRODUCTION

Adolescence is an extraordinary phase in a human's life where individuals are often confused about the role between their responsibilities as growing adults and their desires as children. It marks the progression from childhood to adulthood phase. Any person between the ages of 10 and 19 is classified as an adolescent by the World Health Organization (WHO, 2019). Adolescence was characterized by fleeting physical, cognitive, emotional, social and behavioral changes. Many studies described the biological and psychological changes that occur during adolescence, as well as the parental, peer and cultural influences that have a significant impact on teenagers' lives (Marshall & Tanner, 1970; Hofmann & Greydanus, 1997). Growth spurt and sexual maturation marks the beginning of puberty. The growth surge, which is characterized by fast skeletal growth, normally starts around the ages of 10-12 for girls and 12-14 for boys and ends around the ages of 17-19 for girls and 20 for boys (Hofmann & Greydanus, 1997). For the majority of adolescents, sexual maturity entails establishing fertility as well as physical changes that aid fertility. The onset of puberty involves breast budding and menstruation in females and enlargement of testes and first ejaculation in males. The secondary sexual characteristic involves development of body hairs and change in voice, which occurs later in puberty (Marshall & Tanner, 1970).

The cognitive development in adolescence is marked by the ability to think in more abstract ways. It lays the foundation for moral thinking, honesty and prosocial conduct like helping others, volunteering or caring for others. The formation of a genuine and coherent sense of self in the context of relating to others as well as learning to cope with stress and control emotions, are all part of adolescent emotional development (Santrouk, 2001). The context in which adolescents' social development happens is the most important constraint. Some contexts include interactions with family, peers and at school as well as at work and in the community. The physical, cognitive, emotional and social ways of development prepare adolescents to experiment with new behaviors. Adolescents compose their identities, get experience with new decision-making abilities and create realistic appraisals of themselves, others and the environment by taking risks (Ponton, 1997).

Being autonomous is a significant task during adolescence which involves distancing from one's parents and taking responsibility for oneself. Autonomy is defined as the ability of a person to think, feel and make judgments and act independently (Russell & Bakken, 2002). Emotional, behavioral and value autonomy are the three sorts of autonomy (Russell & Bakken, 2002). The term *emotional autonomy* coined by Steinberg and Silverberg (1986) describes the adolescent's affective detachment from his or her

Social Connectedness and Psychological Distress of Elders During Covid-19

Tripta Nair and Aneesh V Appu

Department of Psychology Mahatma Gandhi College,
Trivandrum,(Kerala)

ABSTRACT

The study aimed to investigate the relationship between social connectedness and psychological distress in elderly people during Covid-19. A total lack of social connections with people around during the pandemic may lead to psychological distress in people, especially the elderly. The sample of the present study consisted of 40 elderly people, aged 60 years and above. A purposive sampling technique was used to collect data from the sample. Data was collected using Google forms and the tools used to collect data included the Social Connectedness Scale-Revised (SCS-R) which was used to assess social connectedness and Kessler Psychological distress scale (K10) was used to measure psychological distress. Regression analysis was used to find out the relationship between social connectedness and psychological distress. The results indicate that there lies a significant negative relationship between social connectedness and psychological distress of elderly people indicating that psychological distress increases as social connectedness of elderly people decreases. Therefore, it is important to keep a check on the social connections of elderly people and take the required steps to improve their psychological well-being.

Keywords: Covid-19, Social connectedness, Psychological distress, Elderly.

Re-intensifying the Social Exclusion: A Study on Elderly Abuse

Subalekshmi G S

Abstract

The speed of ageing population worldwide has created fear that abuse of older persons may increase in its incidence, prevalence and complexity. Nationally, the number of elderly maltreatments is projected to increase due to resource constraints. There is no such clear statistics available, which makes it difficult to have a good understanding of the dimensions of the problem and to monitor the trends. Violence and related forms of abuse against elders is a global public health and human rights problem, with far-reaching consequences, resulting in death, disability, and exploitation with collateral effects on the victim's wellbeing. Kerala, being in an advanced stage of demographic transition, called the "greying state of India" achieved below replacement level fertility, much ahead of other Indian States. It holds the highest proportion of elderly population. According to 2011 statistics, people above 60 constitute 12.6% of the State's total population compared to the National figure of 8.2%. It will be expected to cross 20% by 2026. Family, the primary care giving support system, has crumbled away due to the disintegration of the joint families. The absence of a Government Support System leaves the elderly further marginalized, abused and

Assistant Professor, Department of Sociology, Mahatma Gandhi College,
Thiruvananthapuram | lekshmisivam@gmail.com

Research Article

A study on ectoparasites in Indian Mackerel, *Rastrelliger kanagurta* (Cuvier, 1817) of Thiruvananthapuram coast, South India

Amrutha Shyla Suresh

Postgraduate Department of Zoology and Research Centre, Mahatma Gandhi College, Thiruvananthapuram-695004 (Kerala), India

Balamurali Raghavan Pillai Sreekumaran Nair*

Postgraduate Department of Zoology and Research Centre, Mahatma Gandhi College, Thiruvananthapuram-695004 (Kerala), India

Arya Unni

Postgraduate Department of Zoology and Research Centre, Mahatma Gandhi College, Thiruvananthapuram-695004 (Kerala), India

Binumon Thankachan Mangalathettu

Department of Zoology, University of Kerala, Karyavattom, Thiruvananthapuram-695034 (Kerala), India

*Corresponding author. E-mail: drbala@mgcollegetvm.ac.in

Article Info

<https://doi.org/10.31018/jans.v13i3.2833>

Received: July 7, 2021

Revised: August 28, 2021

Accepted: September 1, 2021

How to Cite

Suresh, A. S. *et al.* (2021). A study on ectoparasites in Indian Mackerel, *Rastrelliger kanagurta* (Cuvier, 1817) of Thiruvananthapuram coast, South India. *Journal of Applied and Natural Science*, 13(3), 993 - 1002. <https://doi.org/10.31018/jans.v13i3.2833>

Abstract

Parasitic infestation in marine fish requires urgent attention, especially those that infect economically important fishes, which affect their aesthetic quality and palatability. Ectoparasites in Indian Mackerel, *Rastrelliger kanagurta* (Cuvier, 1817), have not been studied well. Morphological and seasonal study of ectoparasites in *R. kanagurta* from the Thiruvananthapuram coast was conducted during March-August 2018. The study investigated three parasitic groups: Trichodinids, Digenean cysts (*Centrocestus* Looss, 1899), and Cymothoids (*Norileca indica* Milne Edwards, 1840 and *Nerocila phaiopleura* Bleeker, 1857) from *R. kanagurta* during the present study. Of the 240 fishes examined, the Trichodinids and digeneans showed 100% prevalence on the gill samples. Seasons had no significant effect on trichodinids and digeneans prevalence. However, parasitic Cymothoids fluctuated significantly according to the season. They showed greater prevalence during the pre-monsoon (45%) and least in monsoon (25%) due to environmental parameters like rainfall, salinity, and temperature. Trichodinids parasitized gills of *R. kanagurta* showed increased mucus production, paleness in the gills, and multifocal whitish areas. The Cymothoid infested fish showed lesions with the erosion of the epidermis and underlying dermis at the site of attachment. The noticeable changes were observed in the gill epithelium due to the encystment of digeneans. The Trichodinid ciliates and Heterophyid digenean cysts (*Centrocestus* Looss, 1899) are reported for the first time in *R. kanagurta*.

Keywords: *R. kanagurta*, Trichodinids, Digeneans, *N. indica*, *N. phaiopleura*

INTRODUCTION

Parasitic fish diseases are one of the most serious issues in the fisheries sector (Sethi *et al.*, 2013). The fish parasites were ranging from microscopic protozoans to easily visible crustaceans and annelids. Some of them are parasitic in the external surface of fish, and others are parasitic in the internal organs. The effects of parasites on different host species may differ (Roberts, 2012). Parasites interfere with the nutrition, metabolism, and secretory function of the alimentary canal, damage the nervous system and upset the host's

normal reproduction. Besides direct losses, parasites may have a considerable impact on the behaviour of fish, reduced fecundity, their resistance to other stressing factors, susceptibility to other infections, the potential legislative burdens, and their presence may also reduce the marketability of fish (Paladini *et al.*, 2017). Ectoparasite infestation is one of the most hazardous threats to fish health. It causes low body weight gain, high mortality, and poor marketability due to skin and gill abrasions that promote opportunistic microorganisms invasion (Eissa, 2002).

The Indian mackerel, *Rastrelliger kanagurta*, consti-

tutes an important commercial fisheries species in countries bordered with the Indian Ocean, Indonesia, Pakistan, India, Sri Lanka, Bangladesh, Myanmar, Thailand (Jayabalan *et al.*, 2014). The Indian mackerel constitutes a prominent group in the landings of both the Arabian Sea and the Bay of Bengal (Goutham and Mohanraju, 2015), with a significant increase in the annual landings of Indian mackerel along the Indian coast. An average annual catch in the country was estimated to be 0.16 million tonnes (CMFRI, 2019).

The available information deals with reports of parasite species in *R. kanagurta* belonging to Monogenea, Digenea, and Crustacea (Madhavi and Triveni Lakshmi, 2011; Rameshkumar and Ravichandran, 2010). Madhavi and Triveni Lakshmi (2011) reported the metazoan parasite fauna of the fish from the Visakhapatnam coast, Bay of Bengal and discussed its role as a host different species of metazoan parasites. Later, Madhavi and Triveni Lakshmi (2012) studied the community ecology of the metazoan parasites of the *R. kanagurta*. Recently, seasonal variation in the prevalence of cymothoid isopod, *Norileca indica*, was studied by Jemi *et al.*, (2020). There have been no studies on the distribution and infestation of ectoparasites in *R. kanagurta*.

Accurate identification and changes in the occurrence of ectoparasites in these fishes are important due to their food value, consumer preference and availability in the market. Hence, this study aimed to identify major ectoparasites in Indian mackerel, *R. kanagurta* collected from fish landing centres of Thiruvananthapuram coast, South India.

MATERIALS AND METHODS

Fish species and sampling

Samples of Indian mackerel, *Rastrelliger kanagurta* were collected from major harbours of the Thiruvananthapuram coast –Perumathura (Longitude: E. 76°48'0.03", Latitude: N. 8° 37'30.59") and Vizhinjam (Longitude: E. 76° 59'15", Latitude: N. 8° 22' 30") during the period from October 2017 to September 2018 for parasitological analysis. The fish were collected from commercial fishing harbours caught by local fishermen to investigate parasite infestation. Thus, the animals used in this study (fish/parasites) did not require ethical committee approval for the present work. The collected fishes were transported to the laboratory and were examined immediately. A total of 240 fish with an average total length of 13 to 16 were used for this study.

Seasonal analysis

Monthly collection of 20 fish each was done for each pre-monsoon (February-May), monsoon (June-September), and post-monsoon (October-January) season. Prevalence and mean intensity of infestation of

Trichodinids, Cymothoids and digenea cysts in relation to the month of the collection were calculated (Margolis *et al.*, 1982).

Parasitological examination

Each fish was examined thoroughly and carefully for the presence of parasites after measuring length and weight. The methods suggested by Kennedy (1977) were adopted for parasitological studies. The location of the site of interaction and the number and types of parasites in each site of interaction was noted. Skin scrapings from different regions of the body were examined under the high power of Transmission Light Microscope (TLM) (Optika Microscope; Optikam B5 Digital Camera) for the possible presence of ectoparasites. The buccal cavity was also subjected to thorough microscopical examination. After completing the external examination, the operculum on either side was taken out, and their inner sides were thoroughly examined. Gills from the blind and ocular sides were excised and transferred to separate Petri dishes containing 0.65% saline.

Processing of protozoans

Thin slides were prepared for microscopic ciliate protozoan parasites from the skin and gill scrapings of the fish. The slides were stained according to Klein's dry silver impregnation method (Klein, 1958). The slides were air-dried and covered with a 2% aqueous solution of silver nitrate (AgNO₃) for 8 minutes. After that, rinse the slides thoroughly in distilled water and exposed to direct sunlight for 1-2 hr. The slides were then allowed to dry and mount with DPX mountant.

Processing of digeneans

Gill examinations for the presence of digenean cysts were carried out under Stereo Dissecting Microscope (SDM) (Carl Zeiss Microscopy; GmbH Stemi 508) according to the methods suggested by Madhavi (2006). Encysted digeneans were carefully dissected under TLM to release the contained digenean parasite. After that, they were stained in Gower's Carmine (Roberts, 1978). Stained materials were mounted in D. P. X.

Processing of cymothoids

Cymothoids encountered during the examination were carefully isolated and cleaned off mucus and other debris adhering to their bodies and preserved in 10% neutral buffered formalin. The general morphological features of the parasites were studied by using a hand lens and cleared in 50% lactic acid. Taxonomically important body parts such as pereopods, pleopods, uropod and mouthparts were carefully dissected out under SDM according to the techniques described by Aneesh *et al.* (2019).

Photographs

The photomicrographs of trichodinids and digeneans were taken under TLM. Taxonomic drawings of isopods were made using a drawing tube attached to TLM and the computer programme CorelDraw Version 14. The photographs of isopods were taken using Canon EOS 800D with a 35mm macro lens.

Trichodinids, Digeneans and Cymothoids (*Norileca indica* and *Nerocila phaiopleura*) were identified using the taxonomic keys of Reichenbach-Klinke and Elkan (1965); Chauhan (1953); and Bruce (1987 and 1990), respectively. All the linear measurements are represented in micrometres for protozoan parasites. For metazoan parasites, the measurements are represented in micrometres as well as millimetres.

RESULTS

In the present study, it was observed that the Trichodinid ciliates were present in the scrapings from the body surface, buccal cavity, and gills of *R. kanagurta*. Digenean cysts were observed attached to the gill epithelium. Cymothoids were found to be present on the body surface, mouth, opercular cavity and gills.

Taxonomic description of the ectoparasites in *R. kanagurta*

Trichodinids (Mobilidae: Trichodinidae)

Taxonomic description (8 specimens studied, all measurements are in microns): A flat disc-shaped body having a diameter of 275.76 μ m with rows of cilia at the circular periphery. Boarder membrane 19.37 μ m long. Adhesive disc concave, surrounded by fine striated border membrane. The lightly stained central area of the adhesive disc presents, which helps attach firmly to the fish skin or gills. Adhesive disc 148.80 μ m in diameter. Denticular ring present with denticles. Denticular ring 98.10 μ m in diameter. The denticle spans 31.18 μ m in width. The denticle blade had a length of 11.55 μ m. Central area and ray were visible. The central part was 37.92 μ m wide and Ray 9.49 μ m long (Fig. 1B-D).

Cymothoids (Isopoda: Cymothoidae)

Norileca indica

Taxonomic description of the female (10 specimens studied): Body asymmetrical, oblong, pale creamy, the dorsal surface highly convex, eyes dark and distinct. Body about 2.4-2.5 times wide, twisted to one side; widest at pereonite 4; dorsum moderately convex.

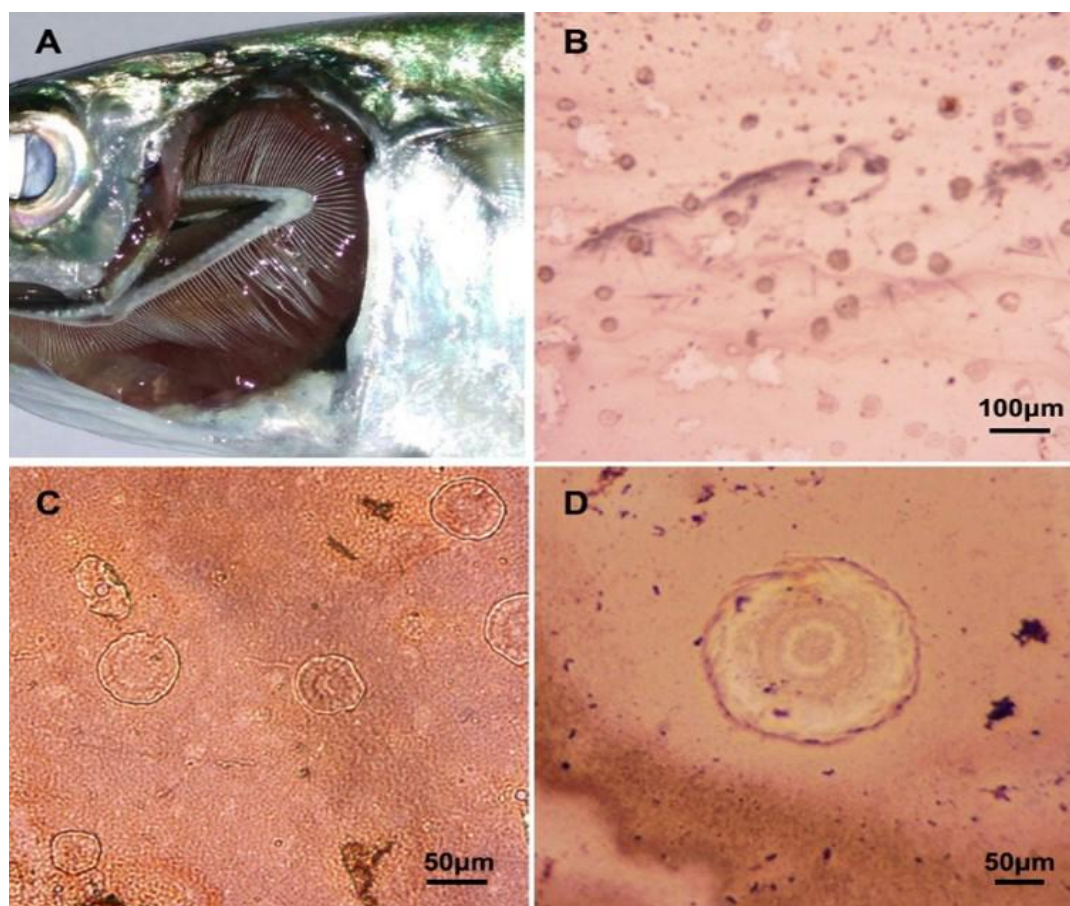


Fig. 1. *R. kanagurta* parasitised by Trichodinid ciliates. A) Gill filaments of the infested fish showing increased mucus production and paleness. B-D) Photomicrographs showingf Klein's silver-impregnated specimens of Trichodinids from the gill smears- Magnification X 100, X 40 and X 10 respectively.

Cephalon not deeply immersed in pereonite 1, interior margin sub truncate; eyes 0.47-0.52 width of the cephalon. Pereonite 1 with posterolateral angles weakly produced. Coxae of pereonite 2 as long as the segment; coxae of pereonites 3-7 all about 0.8 as long as the respective segment. Posterior margin of pereonite 7 weakly concave. Pleon 0.66-0.74 width of pereonite 4, with all segments about as wide as pereonite 7, pleonite 5 as wide as pleonite 1; lateral margins posteriorly directed. Pleotelson triangular, anteromedial surface vaulted. Antennule extends to pereonite 1, bases set wide apart, composed of 8 articles; antenna is slightly longer than antennule, with 9 articles (Fig. 1B).

Mandible with large palp, article 2 flattened, expanded; article 3 0.35 as long as article 2. Maxilliped article 3 with 4 large recurved spines. Pereopod 1 ischium 0.69 lengths of basis; dactylus is curving abruptly at about proximal 0.2 of its length, extending to anterior of the carpus, which has a recess that receives dactylus apex. Pereopods 2 and 3 alike 1 but slightly longer. Pereopods 4-7 similar to each other; pereopod 7 ischium 1.03 length of basis, dactylus extends to posterior of carpus with a recess that receives dactylus apex; propodal palm with 2 small spines. Uropods about 0.55-0.60 length of pleotelson, rami subequal in length, apices rounded; endopod slightly tapered (Figs. 1 D-G).

***N. phaiopleura* Bleeker, 1857**

Taxonomic description of the female: Eyes large, about 0.5 widths of the cephalon. Pleonites 1 and 2 with ventrolateral margins weakly times longer than article 2. Lateral margin with about 22 stout setae. Maxilliped article 3 with 4 recurved spines. Pereopods 1-5 with weak swelling on anteroproximal margin of dactylus; pereopod 7 with 2 spines on posterior margin of propodus. Uropod slender, tapering exopod, 1.7-2.1 times longer than endopod; endopod apex narrowly rounded or obliquely truncate (Figs. 3 C-H).

Digenean cysts (Trematoda: Heterophyidae)

Metacercariae of *Centrocestus* spp. (Looss, 1899)

Metacercariae of *Centrocestus* spp. were released from the cyst attached in the gill epithelium of *R. kanagurta* (Figs. 4 A-C).

Taxonomic description

Body (0.308-0.328 x 0.08-0.12) somewhat elongate, narrower in the extreme anterior end, pitcher shaped and covered with small cuticular spines up to the extreme posterior end. Oral sucker (0.026 x 0.04) large and terminal. Spines on the outer surface surround these suckers. The posterior sucker (0.0187) was small round and situated in the posterior half of the body. Oe-

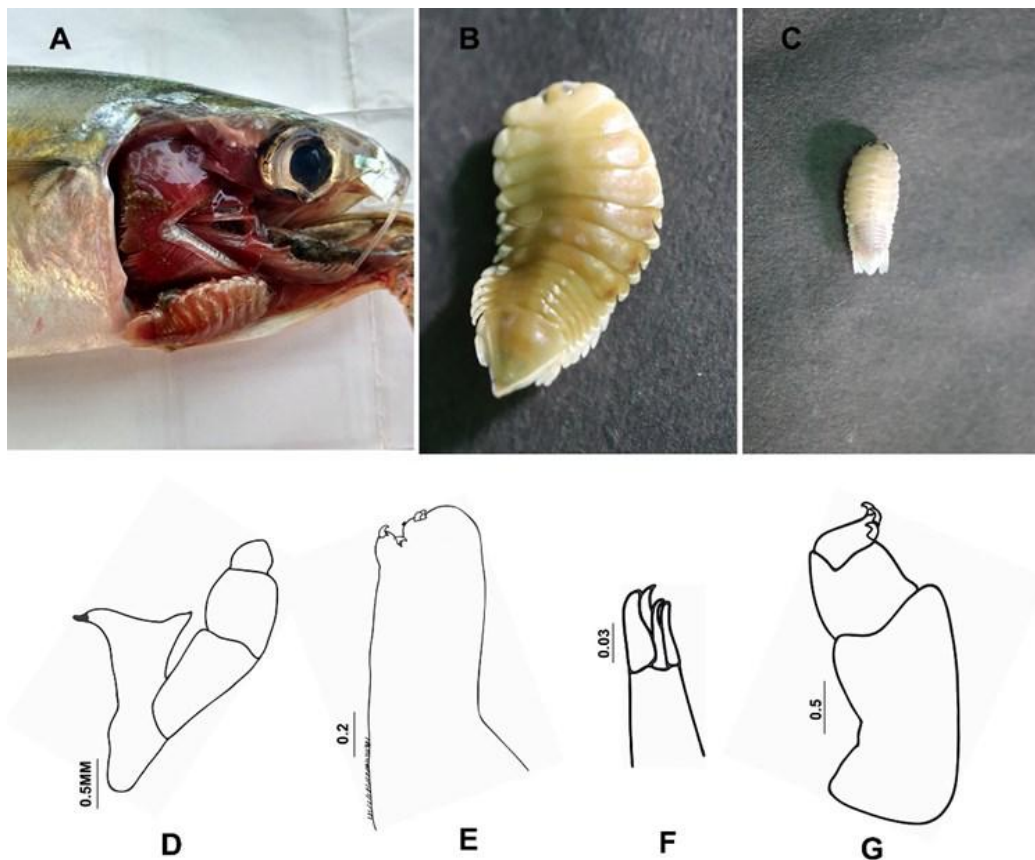


Fig. 2. *N. indica* infestation on *R. kanagurta*. A) Parasite attached on the buccal cavity of the fish. B) *N. indica* Female C) Male, D) Mandible, E) Maxilla, F) Maxillule, G) Maxilliped.

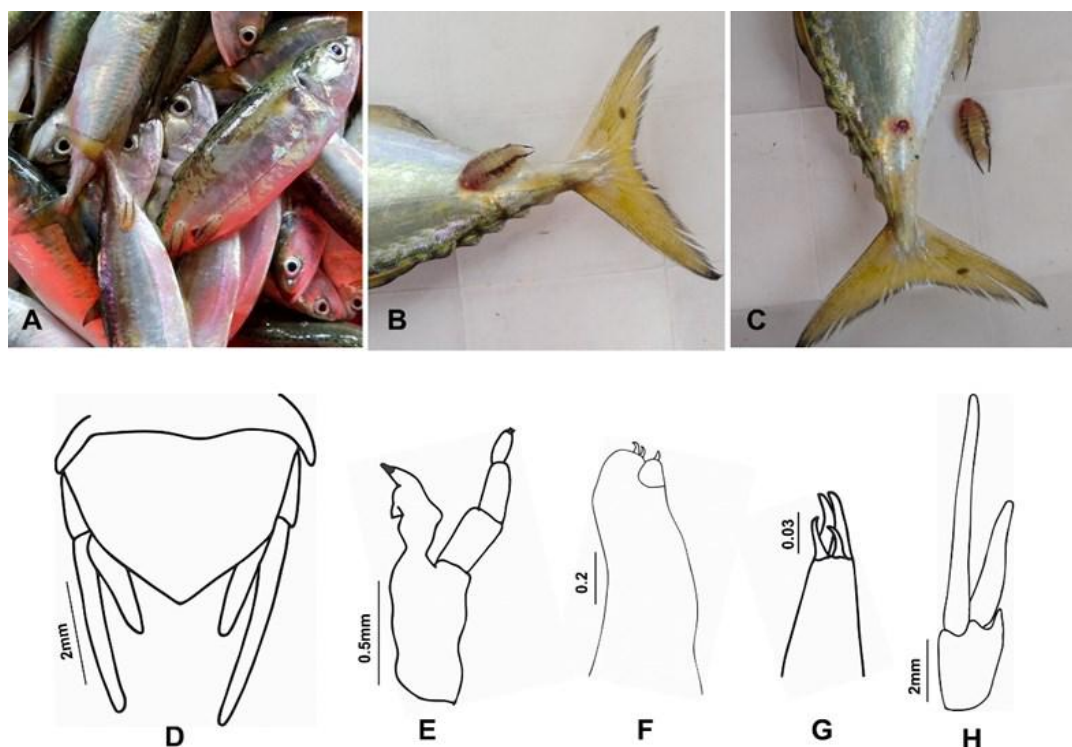


Fig. 3. *N. phaiopleura* infestation on *R. kanagurta*. A&B) Parasite attached on the posterior body surface of the fish. C) Large hemorrhagic wound made by the parasite on the fish. D) Pleotelson, dorsal view. E) Mandible F) Maxilla G) Maxillule H) Uropod.

sophagus (0.051-0.0457) long, slender. Pharynx small, at about $\frac{1}{4}$ distance from anterior end. Bifurcation of ceca at about one-third distance from anterior end. Ceca long (0.194-0.205), extending up to the posterior end of the body. Reproductive organs were rudimentary and situated at the extreme posterior end. Excretory bladder nearly 'X' shaped (Fig. 4D).

Nature of infestation of the ectoparasites in *R. kanagurta*

There was no seasonal variation in the prevalence of Trichodinids and digenean cysts. These parasites showed 100% prevalence in all the seasons. Eighty *R. kanagurta* specimens were examined for each season, and all of them were infested with Trichodinids and digenean cysts. Trichodinid parasitizing the gills of the fish showed increased mucus production, paleness in the gills, and multifocal whitish areas (Fig. 1A). The parasites were in permanent rotation while attached to a host, which irritated the epithelial cells.

Seasonal variations in the rate of infestation of *N. indica* were observed (Table 1). The prevalence of parasitic Cymothoids fluctuated significantly according to the season. Out of 80 specimens of *R. kanagurta* examined, 36 were infested during pre-monsoon, 20 fishes were infested during monsoon, and 26 were infested during post-monsoon. A significant increase was observed in Isopods during pre-monsoon (45%) and

showed a decrease during monsoon (25%). The highest prevalence of the parasite was observed during March (50%) and the least in September (20%).

The mouth and gills (Fig. 2A) were the major sites of attachment for *N. indica*. In the parasitized fish, lesions with the erosion of the epidermis and underlying dermis were observed at the site of parasite attachment. Juveniles; males (Fig. 2C); transitionals; non-brooded ovigerous females; and Brooded ovigerous females carrying marsupiumites (Fig. 2B) of *N. indica* were recovered from the fish. The posterior body surface was the preferred site for *N. phaiopleura* (Fig. 3A and B), and it showed site-specificity in the host. Large haemorrhagic wound/ulceration was observed at the parasite attachment site (Fig. 3C). Out of 80 specimens of *R. kanagurta* examined, 30 were infested by *N. phaiopleura*. Brooded ovigerous females and transitionals of *N. phaiopleura* were recovered during the present study.

DISCUSSION

The study based on the examination of *R. kanagurta* collected as monthly samples from the Thiruvananthapuram coast (Arabian Sea) revealed the fish's protozoan and metazoan parasite fauna was fairly rich, comprising of trichodinids, digeneans, and Isopods.

Trichodinid ciliates are geographically a widely dispersed group of ectoparasites in all the aquatic environ-

Table 1. Seasonal occurrence of Cymothoids (*N. indica*) in *R. kanagurta* during October, 2017-September, 2018.

Season	Post-monsoon			Pre-monsoon			Monsoon					
Month	Oct.	Nov.	Dec.	Jan.	Feb.	Mar.	Apr.	May	Jun.	Jul.	Aug.	Sep.
No. of fish examined	20	20	20	20	20	20	20	20	20	20	20	20
No. of fish infected	6	6	7	7	8	10	9	9	6	5	5	4
Prevalence (%)	30	30	35	35	40	50	45	45	30	25	25	20
Average	33%			45%			25%					

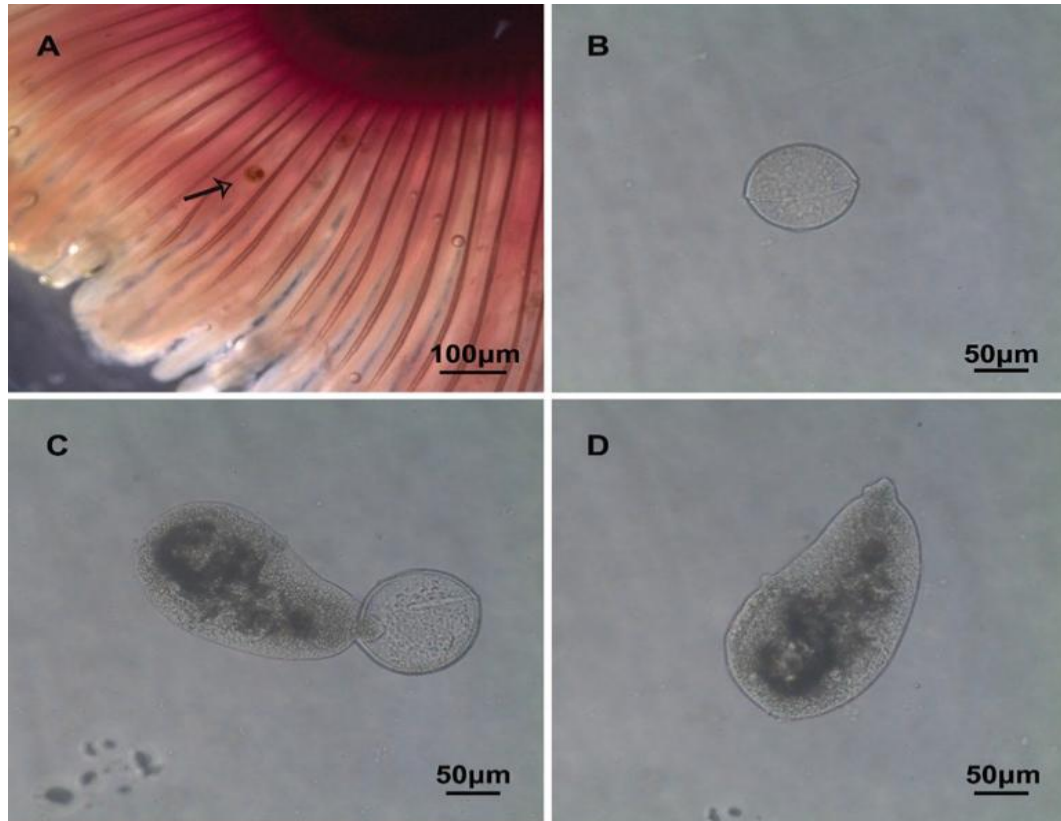


Fig. 4 (A-D). Digenean infestation on *R. kanagurta*. A) Digenean cyst in the gill of the fish (Magnification X 8). B) Digenean cyst (Magnification X 40). C) Metacercaria of *Centrocestus* (Looss, 1899) releasing from the cyst (Magnification X 40). D) Metacercariae of *Centrocestus* (Magnification X 40)

ments- freshwater, marine and euryhaline environments. Trichodinids are probably the most common protozoan parasites found in many other fishes from different parts of the world (Tantry *et al.*, 2016).

Isopods reported from *R. kanagurta* in this study belonged to the family Cymothoidae (Leach, 1814), which represent the largest family of parasitic isopods infesting several fish species of economic importance, as reported by Ravichandran *et al.* (2019). Digeneans are also a common group of fish parasites and are reported from *R. kanagurta* so far from different parts of the world (Al-Zubaidy and Mhaisen, 2014; Madhavi and Triveni Lakshmi, 2011).

In the present study, the seasonal analysis revealed that the trichodinids and digeneans cysts showed a 100% prevalence over other parasites. This higher occurrence of these species may be due to the selection of larger sized fishes for the present study. According

to Ozer and Erdem (1998), the severity of most parasitic infections increases with the age of the host fish, possibly due to the greater accumulation period and the larger space for feeding and breeding of the parasite. In a study of *Trichonia* spp. on the ornamental fishes of West Bengal, Saha and Bandyopadhyay (2017) stated that the biological factors, as well as environmental factors of the host, may play a pivotal role in the outbreak of protozoans. Xu *et al.* (2002) reported that the factors like pollution and stress, which lowered the host's immune response, may also result in the proliferation of the parasite.

In the present study, the seasonality effect on trichodinid infestation and digenean cysts had no significant impact on parasite prevalence, similar to the work of Suliman *et al.* (2021) who reported the higher prevalence of trichodina on *Oreochromis niloticus* in the fish farms of Saudi Arabia in all seasons. Bo-ping and

Xianghua (2000) report that the prevalence, mean intensity and relative density of metacercarial cyst infestation of *Centrocestus formosanus* on the gills of grass carps *Ctenopharyngodon idellus* were not obviously correlated with the seasonal change of water temperature. In a study of metacercarial distribution of *C. formosanus* (Digenea: Heterophyidae) among fish hosts in the Guadalupe River drainage of Texas, Fleming *et al.*, 2011 found that these digenean cysts showed 100% prevalence in the fishes, *Cyprinella lutrensis*, *Dionda nigrotaeniata* and *Ameiurus natalis*.

Season dependent variation was noticed in the intensity and prevalence of parasitic Cymothoids from *R. kanagurta* during the present study period (Table 1). *Norileca indica* showed greater prevalence during the pre-monsoon and least in monsoon season in this study. The prevalence could be dependent on environmental parameters like rainfall, salinity, and temperature. According to Aneesh *et al.* (2013), parasitic cymothoids' prevalence and mean intensity depend on the environment's seasonal variation. Higher prevalence in pre-monsoon during the present investigation may be due to the effect of increased salinity. Our findings support the work of Kottarathil *et al.* (2019), who suggested that higher salinity favours the isopod parasitization of fish which might be favourable for the parasite to infect its host fish. The low prevalence observed during the monsoon period in our study may be due to the weak salinity resulting from the heavy rainfall, inducing an unfavourable environment for the parasitic infestation. In a study on *Nerocila* spp. parasitized marine fishes of the Malabar Coast, India, Aneesh *et al.* (2013) corroborated with our findings. An increase in the infestation of the parasites from post-monsoon to pre-monsoon was observed during the study. The gradual increase in salinity during the post-monsoon season seems to facilitate the more parasitic infestation. Still, the exact mechanism by which the salinity plays a role in the parasitization is unclear, and a detailed and systematic experimental study is needed to confirm this. al. 2005).

In the present study, the skin of trichodinid parasitized fish showed a change in body colouration and excessive production of mucus. The body of the host fish was observed dull with a thin film of mucus. Woo (2006) suggested that the clinical signs of trichodinid infestation most commonly observed were a mottled/grey appearance on the skin (caused by the excessive production of the mucus) in a study of *Trichodina* infestation on the skin of Tilapia. In the present study, Trichodinid parasitizing gills of *R. kanagurta* showed increased mucus production, paleness in the gills along with multifocal whitish areas (Fig. 1A). Valladao *et al.* (2013) found mucous production, paleness and multifocal whitish areas in the severely infested gills of Nile tilapia by

Trichodinid, *Paratrichodina africana*. Complete fusion of the secondary lamellae, proliferation of mucous cells, mononuclear and eosinophilic inflammatory infiltrate, multifocal areas of necrosis, congestion, and desquamated cells may be the reason for these changes observed. These parasites attack the fish and cause massive destruction of the skin and gill epithelium (Sterud *et al.*, 2008). Outbreaks and mass mortality of Atlantic cod (*Gadus morhua*) infested with *Trichodina murmanica* infection was reported in a coastal embayment of Newfoundland (Khan, 2004).

In the present study, digeneans were observed as cysts attached to the gill epithelium, and changes were noticed in the gill epithelium of the host (Fig. 4A). The changes that occurred in the gills could be due to epithelial hyperplasia and fusion of the filaments. Mitchell *et al.* (2000) studied heterophyid trematode infecting the gills of an endangered fish, the Fountain darter, *Etheostoma fonticola*, in two Central Texas spring-fed rivers. They found that digenean cyst infected gill filaments of the fish were shortened, thickened, and often distorted. Ravichandran and Rameshkumar (2012) studied the gill-infecting Didymozoid in fishes of Pazhayar, India and reported that the most common effect of digenean cyst on affected fish are epithelial cells on gill lamellae, damage to gill epithelium and thus respiration is affected. They also suggested that heavily infested digenean parasitized fish were often weak, thin, inactive, and fed poorly. According to Mitchell *et al.* (2005), metacercariae encysted in gills causes pathological alterations related to developmental delay and death, giving rise to economic losses in the fish farming industry.

Cymothoid infested fishes in this study showed damage to gills (Fig. 3A), skin (Fig. 3C), and tongue. During the study, lesions with the erosion of the epidermis and underlying dermis were observed at the site of parasite attachment in the *N. indica* parasitized fish. The result of the present study is corroborated with the study of Rameshkumar *et al.* (2013), who reported localized destruction of the epidermis and an inflammatory response around the site of attachment of Cymothoid, *Catoessa boscii* in *Carangoides malabaricus* from Tamil Nadu, India. In the present study, the gills of *R. kanagurta* were damaged due to the attachment of Cymothoid *N. indica* (Fig. 3A). While studying the effect of the Cymothoid, *Joryma hilsae*, on the branchial area of *Stolephorus commersonii*, Ravichandran and Rameshkumar (2014) suggested that erosion of gill lamellae, damage to gill rakers, and pale gills were the significant gross lesions found as a result of isopod infestation. In our study, large haemorrhagic wound/ulceration was observed on the body surface of *R. kanagurta* infested by *N. phaiopleura* (Fig. 3C). It is also reported that *N. phaiopleura* cause skin damages in a

variety of fish species, including *Dussumieria acuta* (Ravichandran and Rameshkumar, 2014), *Thunnus orientalis* (Nagasawa and Shirakashi, 2017a) and *Sardinops melanostictus* (Nagasawa *et al.*, 2020). In the present investigation, the damages in the body surface, buccal cavity and branchial cavity may be due to the feeding and the pressure exerted by the parasite on the host. The posterior body surface was the preferred site for attachment for the parasite *N. phaiopleura* (Fig. 3B), and it showed site-specificity in the host. In a study on *Nerocila* spp. from Indian marine fishes, Trilles *et al.* (2013) reported that body surface is the preferred attachment site for *N. phaiopleura*.

The Indian mackerel constitutes a prominent group in the landings of both the Arabian Sea and the Bay of Bengal (Goutham and Mohanraju, 2015). Different types of parasites found on the fish *R. kanagurta* during the present study indicate that Indian mackerel from the Thiruvananthapuram coast appear to be a potential host for these parasites. Considering the wide geographical distribution and host range of the trichodinids (Tantry *et al.*, 2016), Heterophyid Digeneans (Gamit *et al.*, 2018) and Cymothoids (Nagasawa and Isozaki, 2017b), these parasites have the potential to become a threat to coastal farming also. The Cymothoid, *N. phaiopleura*, is also reported to facilitate secondary microbial infections in fishes (Ravichandran *et al.*, 2016). Fishborne Heterophyid Digeneans are known to have a zoonotic potential (Chai and Jung, 2017). Thus, adequate management measures, including chemical Indian mackerel prophylaxis, are needed to control the infection of these parasites to some extent in coastal farming.

Conclusion

The present study revealed that the Indian mackerel *R. kanagurta* is a potential host for three major parasitic groups, namely Trichodinids, Digeneans cysts (*Centrocestus* spp.) and Cymothoids (*Norileca indica* and *Nerocila phaiopleura*). The Trichodinids and digeneans showed 100% infestation in all the seasons. In contrast, seasonal fluctuation was observed in the prevalence of parasitic isopods. The Trichodinid infestation resulted in increased mucus production, paleness in the gills, and multifocal whitish areas. The encystment of digeneans in the gills of the fish also resulted in significant changes. In the Cymothoid infested fish, lesions with the erosion of the epidermis and underlying dermis were observed at the site of attachment. The parasites may induce damages to the attachment sites, thus harming the host's physiological status. A heavy infestation can affect the commercial value of fish. The Trichodinid ciliates and heterophyid digenean cysts of *Centrocestus* spp. are reported for

the first time from the gills of *R. kanagurta* from the world.

ACKNOWLEDGEMENTS

The authors acknowledge Dr B Santhosh, Principal Scientist, Central Marine Fisheries Institute, Vizhinjam, Thiruvananthapuram, for supporting research work. We acknowledge Dr Aneesh P T, UGC- DS Kothari Post-Doctoral Fellow, Department of Aquatic Biology & Fisheries, University of Kerala, for the constant support. We thank the University of Kerala for providing Research Grant (AcE VI/117/ZOO/15059/2017).

Conflict of interest

The authors declare that they have no conflict of interest.

REFERENCES

1. Al-Zubaidy, A. & Mhaisen, F. (2014). Four new records of trematodes from the Indian mackerel *Rastrelliger kanagurta* (Cuvier, 1816) from the Yemeni coastal waters of the Red Sea. *American Journal of Biology and Life Sciences*, 2(6), 141–145.
2. Aneesh, P.T., Helna, A.K., Trilles, J.P. & Chandra, K. (2019). A taxonomic review of the genus *Joryma* Bowman and Tareen, 1983 (Crustacea: Isopoda: Cymothoidae) parasitizing the marine fishes from Indian waters, with a description of a new species. *Marine Biodiversity*. 49(1), 1449–1478. doi.org/10.1007/s12526-017-0799-8
3. Aneesh, P.T., Sudha, K., Arshad, K., Anilkumar, G. & Trilles, J.P. (2013). Seasonal fluctuation of the prevalence of cymothoids representing the genus *Nerocila* (Crustacea, Isopoda), parasitizing commercially exploited marine fishes from the Malabar Coast, India. *Acta Parasitologica*, 58(1), 80–90. doi.org/10.2478/s11686-013-0112-3
4. Bo-ping, Z. & Xianghua, L. (2000). Monthly changes of the metacercarial cyst infrapopulation of *Centrocestus formosanus* (Nishigori, 1924) on the gills of grass carps *Ctenopharyngodon idellus*. *Acta Hydrobiologica Sinica*, 24(2), 137–142. Retrieved Aug. 06, 2021. <https://www.cabi.org/isc/abstract/20000807252>
5. Bruce, N.L. (1987). Australian species of *Nerocila* Leach, 1818, and *Creniola* n.gen. (Isopoda: Cymothoidae), crustacean parasites of marine fishes. *Records of the Australian Museum*, 39(6), 355–412. doi.org/10.3853/j.0067-1975.39.1987.174
6. Bruce, N.L. (1990). The genera *Catoessa*, *Elthusia*, *Enispa*, *Ichthyoxenus*, *Idusa*, *Livoneca* and *Norileca* n.gen., (Isopoda, Cymothoidae), crustacean parasites of marine fishes, with descriptions of eastern Australian species. *Records of the Australian Museum*, 42(3), 247–300. doi.org/10.3853/j.0067-1975.42.1990.118
7. Central Marine Fisheries Research Institute (CMFRI). (2019). Estimated marine fish landings in India during 2019. Annual National Data for 2019. Retrieved June 20, 2021, <https://www.cmfri.org.in/2019>
8. Chai, J.Y. & Jung, B.K. (2017). Fishborne zoonotic heterophyid infections: an update. *Food Waterborne Parasitol*, 8

- (9), 33–63. doi.org/10.1016/j.fawpar.2017.09.001
9. Chauhan, B.S. (1953). Studies on the trematode fauna of India. Part III Subclass Digenea (Gasterostomata). *Records of the Indian Museum*, 51(2), 231–287. Retrieved July 8, 2021, <https://www.cabdirect.org/cabdirect/abstract/19530802360>
 10. Eissa, I.A.M. (2002). *Parasitic fish diseases in Egypt*. Dar El-Nahdda El-Arabia publishing.
 11. Fleming, B.P., Huffman, D.G., Bonner, T.H., Brandt, T.M. (2011). Metacercarial distribution of *Centrocestus formosanus* among fish hosts in the Guadalupe River drainage of Texas. *Journal of Aquatic Animal Health*, 23(3), 117–24. doi.org/10.1080/08997659.2011.616840
 12. Gamit, A.B., Nanda, P.K., Bhar, R., Bandyopadhyay, S. & Bandyopadhyay, S. (2018). A Report of *Centrocestus formosanus* (Nishigori, 1924) (Digenea: Heterophyidae) in Intermediate Host (Fish). *International Journal of Current Microbiology and Applied Sciences*, 7(7), 928–936. doi.org/10.20546/ijcmas.2018.707.112
 13. Goutham, J., Mohanraju, R. (2015). Some aspects of mackerel diversity and morphometric studies of *Rastrelliger* genera from Port Blair Andaman waters. *International Journal of Fish and Aquatic Studies*, 3(1), 196–198. Retrieved July 7, 2021. <https://www.fisheriesjournal.com/archives/2015/vol3issue1/PartC/2-6-19.pdf>
 14. Jayabalan, N., Zaki, S., Al-Kiyumi, F. & Al-Kharusi, L. (2014). Age, growth and stock assessment of the Indian mackerel *Rastrelliger kanagurta* (Cuvier, 1817) along the Sohar coast of Oman. *Indian Journal of Fisheries*, 61(1), 1–6. Retrieved January 18, 2021. <http://epubs.icar.org.in/ejournal/index.php/IJF/article/view/26468>
 15. Jemi, J.N., Hatha, A.A.M. & Radhakrishnan, C.K. (2020). Seasonal variation of the prevalence of cymothoid isopod *Norileca indica* (Crustacea, Isopoda), parasitizing on the host fish *Rastrelliger kanagurta* collected from the Southwest coast of India. *Journal of Parasitological Diseases*, 44 (2), 314–318. doi.org/10.1007/s12639-020-012 08-6
 16. Kennedy, C.R. (1979). The distribution and biology of the cestode *Eubotrium parvum* in Capelin, *mallotus villosus*, (Pallas) in the Barents Sea, its use as a biological tag. *Journal of Fish Biology*, 15, 223–236. doi.org/10.1111/j.1095-8649.1979.tb03585.x
 17. Khan, R.A. (2004). Disease outbreaks and mass mortality in cultured Atlantic cod, *Gadus morhua* L., associated with *Trichodina murmanica* (Ciliophora). *Journal of Fish Diseases*, 27(3), 181–184. doi.org/10.1111/j.1365-2761.200 4.00525.x
 18. Klein, B.M. (1958). The dry silver method and its proper use. *Journal of Parasitology*, 5(2), 99–103. doi.org/10.1 111/j.1550-7408.1958.tb02535.x
 19. Kottarathil, H.A., Sahadevan, A.V., Kattamballi, R. & Kap-palli, S. (2019). *Norileca indica* (Crustacea: Isopoda, Cymothoidae) infects *Rastrelliger kanagurta* along the Mala-bar coast of India – Seasonal variation in the prevalence and aspects of host-parasite interactions. *Zoological studies*, 58, e35. doi.org/10.6620/ZS.2019.58-35
 20. Madhavi, R. & Lakshmi, T.T. (2011). Metazoan parasites of the Indian mackerel, *Rastrelliger kanagurta* (Scombridae) of Visakhapatnam coast, Bay of Bengal. *Journal of Parasitological Diseases*, 35(1), 66–74. doi.org/10.1007/s12639-011-0028-5
 21. Madhavi, R. & Triveni Lakshmi, T. (2012). Community ecology of the metazoan parasites of the Indian mackerel *Rastrelliger kanagurta* (Scombridae) from the coast of Visakhapatnam, Bay of Bengal. *Journal of Parasitological Diseases*, 36(2), 165–70. doi.org/10.1007/s12639-012- 0097-0.
 22. Madhavi, R. (2006). Distribution of metacercariae of *Centrocestus formosanus* (Trematoda: Heterophyidae) on the gills of *Aplocheilus panchax*. *Journal of Fish Biology*, 29, 685–690. doi.org/10.1111/j.1095-8649.1986.tb04984.x
 23. Margolis, L.G., Esch, W., Holmes, J.C., Kuris, A.M. & Shad, G.A. (1982). The use of ecological terms in parasitology (report of an ad hoc committee of the American Society of Parasitologists). *Journal of Parasitology*, 68, 131–133. Retrieved June 2, 2021. <http://links.jstor.org/sici?sici=00223395%28198202%2968%3A1%3C131%3ATUOETI%3E2.0.CO%3B2-U>
 24. Mitchell, A.J., Overstreet, R.M., Goodwin, A.E. & Brandt, T.M. (2005). Spread of an exotic fish-gill trematode: a far-reaching and complex problem. *Fisheries*, 30, 11–16. doi.org/10.1577/1548-8446(2005)30[11:SOAEFT] 2.0.CO;2
 25. Mitchell, A.J., Salmon, M.J., Huffman, D.G., Goodwin A. E. & Brandt T. M. (2000). Prevalence and Pathogenicity of a Heterophyid Trematode infecting the gills of an endangered fish, the Fountain Darter, in Two Central Texas Spring-Fed Rivers. *Journal of Aquatic Animal Health*, 12 (4),283–289.<https://www.sciencebase.gov/catalog/item/50576efee4b01ad7e027b246>
 26. Nagasawa, K. & Shirakashi, S. (2017a). *Nerocila phaiopleura*, a cymothoid isopod parasitic on Pacific bluefin tuna, *Thunnus orientalis*, cultured in Japan. *Crustacean Research*, 46, 95–101. doi: 10.18353/crustacea.46.0_95
 27. Nagasawa, K. and S. Isozaki. (2017b). Three new host records for the marine fish ectoparasite, *Nerocila phaiopleura* (Isopoda: Cymothoidae), with a list of its known hosts. *Crustacean Research*, 46, 153–159. doi.org/10.183 53/crustacea.46.0_153
 28. Nagasawa, K., Nitta, M., Otawa, T. & Ishikawa, T. (2020). *Nerocila phaiopleura* (Isopoda: Cymothoidae): a new record from Ibaraki Prefecture, central Japan, with a discussion of its distribution in Japanese waters. *Crustacean Research*, 49, 41–47. doi.org/10.18353/crustacea.49.0_41
 29. Ozer, A. & Erdem, O. (1998). Ectoparasitic protozoa fauna of the common carp (*Cyprinus carpio* L., 1758) caught in the Sinop region of Turkey. *Journal of Natural History*, 32 (3), 441–454. doi.org/10.1080/00222939800770231
 30. Paladini, G., Longshaw, M., Gustinelli, A. & Shinn, A.P. (2017). Parasitic diseases in aquaculture: Their biology, diagnosis and control. In: *Diagnosis and Control of Diseases of Fish and Shellfish* (pp 37–107). John Wiley & Sons Ltd, USA.
 31. Rameshkumar, G. & Ravichandran S. (2010). New host record, *Rastrelliger kanagurta*, for *Nerocila phaeopleura* parasites (Crustacea, Isopoda, Cymothoidae). *Middle-East Journal of Scientific Research*, 5, 54–56. Retrieved June 6, 2021. [https://www.idosi.org/mejsr/mejsr5\(1\)/10.pdf](https://www.idosi.org/mejsr/mejsr5(1)/10.pdf)
 32. Rameshkumar, G. & Ravichandran, S. (2013). Effect of the parasitic isopod, *Catoessa bosicii* (Isopoda, Cymothoidae), a buccal cavity parasite of the marine fish, *Caran-goides malabaricus*. *Asian Pacific Journal of Tropical Bio-*

- medicine*, 3(2), 118–122. doi.org/10.1016/S2221-1691(13)60035-0
33. Ravichandran S. & Rameshkumar G. (2012). Host-Parasite Interaction of a Gill-Infecting Didymozoid in the Pazhayar, Southeast Coast of India. *World Journal of Fish and Marine Sciences*, 4 (1), 60–64. doi.org/10.5829/idosi.wjfm.2012.04.01.6215
 34. Ravichandran S. & Rameshkumar G. (2014). Effect of parasitic Isopods in commercial marine fishes. *Journal of Aquatic Biology and Fisheries*, 2, 574–579. Retrieved July 11, 2021. <http://keralamarinelife.in/Journals/Vol2-2/91.pdf>
 35. Ravichandran, S., Sivasubramanian, K., Parasuraman, P., Karthick Rajan, D. & Ramesh kumar G. Isopod parasite induced secondary microbial infection in marine food fishes. *Fish Pathology*, 29(1), 1–5. doi.org/10.7847/jfp.2016.29.1.001
 36. Ravichandran, S., Vigneshwaran, P. & Rameshkumar, G. (2019). A taxonomic review of the fish parasitic isopod family Cymothoidae Leach, 1818 (Crustacea: Isopoda: Cymothoidea) of India. *Zootaxa*, 4622(1), 1–99. doi.org/10.11646/zootaxa.4622.1.1
 37. Reichenbach-Klinke, H. & Elkan, E. (1965). *The principal diseases of lower vertebrates*, Imprint, USA. Retrieved July 11, 2021. <https://www.elsevier.com/books/the-principal-diseases-of-lower-vertebrates/reichenbach-klinke/978-1-4832-3303-1>
 38. Roberts, R.J. (1978). Therapy of fish diseases. In: *Fish pathology* (pp 268-275). Gateway West (Argyll) Ltd. Ford, Argyll, Scotland, UK.
 39. Roberts, R.J. (2012). *Fish Pathology*. 4th Ed. Blackwell Publishing Ltd, USA. doi.org/10.1002/9781118222942
 40. Saha, M. & Bandyopadhyay, P.K. (2016). Seasonal incidence of protozoan parasitic infestation in ornamental fishes of West Bengal, India. *Journal of Parasitic Diseases*, 41(2), 523–526. doi.org/10.1007/s12639-016-0842-x
 41. Sethi, S., Jithendran, K.P., & Kannappan, S. (2013). Co-infection of Yellowtip Halfbeak Fish (*Hemiramphus marginatus*) with Isopod and Copepod parasites from the Coromandal Coast. *India Fishery Technology*, 50(4), 357–360. Retrieved July 10, 2021. <http://epubs.icar.org.in/ejournal/index.php/FT/article/view/34167>
 42. Sterud, E., Harris, P.H. & Bake, T.A. (2008). The influence of *Gyrodactylus salaris* Malmberg 1957 (Monogenea) on the epidermis of Atlantic salmon, *Salmo salar* L., and brook trout, *Salvelinus fontinalis* (Mitchill): experimental studies. *Journal of Fish Diseases*, 21(4), 257–263. doi.org/10.1046/j.1365-2761.1998.00099.x
 43. Suliman, E.M., Osman, H.A. & Al-Deghayem, W.A. (2021). Histopathological changes induced by ectoparasites on gills and skin of *Oreochromis niloticus* (Burchell 1822) in fish. *Journal of Applied Biology & Biotechnology*, 9(1), 68–74. doi.org/10.7324/JABB.2021.9109.
 44. Tantry, T.A., Nazir, R., Chishti, M.Z., Ahmad, F., Dar, G.H. & Dar, J.S. (2016). A report on the incidence of *Trichodina heterodontata* from fishes of Jammu, J&K India. *Journal of Parasitological Diseases*, 40(2), 524–527. doi.org/10.1007/s12639-014-0538-z
 45. Trilles, J.P., Rameshkumar, G. & Ravichandran, S. (2013). *Nerocila* species (Crustacea, Isopoda, Cymothoidae) from Indian marine fishes. *Parasitology Research*, 112(3), 1273–1286. doi.org/10.1007/s00436-012-3263-5
 46. Valladao, G.M.R., Pádua, S.B., Gallani, S.U., Menezes-Filho, R.N., Dias-Neto, J., Martins, M.L. & Pilarski, F. (2013). *Paratrichodina africana* (Ciliophora): a pathogenic gill parasite in farmed Nile tilapia. *Veterinary Parasitology*, 197(3-4), 705–710. doi.org/10.1016/j.vetpar.2013.04.043
 47. Woo, P.T.K. (2006). *Fish Diseases and Disorders*. Protozoan and Metazoan Infections. 2nd Ed. University of Guelph, Canada. Retrieved July 10, 2021. <https://www.cabi.org/bookshop/book/9780851990156/>
 48. Xu, K., Choi, J.K., Yang, E.J., Lee, K.C. & Lei, Y. (2002). Biomonitoring of coastal pollution status using protozoan communities with a modified PFU method. *Marine Pollution Bulletin*, 44(9), 877–886. doi.org/10.1016/S0025-326X(02)00090-5

STUDY ON THE EFFECT OF DIETARY FIBER FROM CORIANDRUM SATIVUM AND SOLANUM TORVUM ON FECAL BILE ACIDS IN RATS

Bijukumar.B.S^{1*}, Suresh Chandra Kurup.R² and Suja.S.R³

Received: 20/3/2021

Revised: 22/5/2021

Accepted: 23/5/2021

Abstract

The effect of dietary fibers in the form of Neutral Detergent Fiber (NDF) from *Coriandrum sativum* (CS NDF) and *Solanum torvum* (ST NDF) on fecal bile acids in rats was studied. The rats were fed with synthetic diet containing 10% NDF. From the study, it was evident that fibre fed rats showed increased excretion of bile acids including cholic and chenodeoxy cholic acids in the feces. Among the two fibres ,ST NDF fed rats showed higher fecal excretion of bile acids than CS NDF fed ones.

Keywords: *Coriandrum sativum*, *Solanum torvum* , Dietary fiber, Neutral detergent fiber, Bile acids

Introduction

Dietary fibre (DF) is that part of plant material in the diet which is resistant to enzymatic digestion. DF is mainly composed of cellulose, noncellulosic polysaccharides such as hemicellulose, pectic substances, gums, mucilages and a non-carbohydrate component lignin (Devinder Dhingra). Different systems are proposed to classify the components of dietary fibre based on their role in the plant, based on the type of polysaccharide, based on their simulated gastrointestinal solubility etc (Tungland and Meyer) . Anita and Abraham reported that dietary fibre is mainly classified into two categories such as water- insoluble/ less fermented fibres(cellulose, hemicellulose,

lignin) and the water- soluble/well fermented fibres:(pectin, gums and mucilages) . Many studies reported that consumption of DF reduces the chances of occurrences of many diseases like colon cancer, atherosclerosis, diabetes *etc*. Ghada A. Soliman (2019) reported that dietary fiber intake is associated with decreased risk of cardiovascular disease.. Foods rich in insoluble fibers such as whole grains and cereals are consistently associated with a reduced risk of developing Type 2 diabetes in observational studies (Parker *et al.*, 2013). Many reports indicate that dietary fibre reduce the level of lipids (Shufen Han *et al.*, 2019).

1 ,2 Post Graduate Department of Zoology and Research Centre
Mahatma Gandhi College,
Thiruvananthapuram, Kerala, India
email: bijukumarbsd@gmail.com

3. Tropical Botanic Garden and Research Institute, Palode, Thiruvananthapuram, Kerala, India
*Bijukumar.B.S (Corresponding author)

Materials and Methods

For the study, male albino rats of Sprague – Dawley strain weighing 80-120 g bred and maintained in the animal house were used. The rats were divided into 3 groups.

Group I - Isocaloric fiber free diet (FF)

Group II - 10% *Coriandrum sativum* NDF (CSNDF)

Group III - 10% *Solanum torvum* NDF (ST NDF)

The animals were fed with synthetic diet. 10g. of the NDF was added at the expense of CHO (CHO – equal parts of glucose, dextrin, sucrose & corn starch) in fiber diet fed groups. The caloric intake of all the groups was maintained unchanged by adjusting the food intake. The composition of diet is given below.

Composition of diet

Composition of diet	Fiber free (gm/100gm)	NDF (gm/100g m)
*CHO	65.00	55.00
Casein (Vitamin & Fat free)	20.00	20.00
Ground nut oil	10.00	10.00
Fiber	-	10.00
Salt mixture	4.00	4.00
Vitamin mixture	1.00	1.00

*CHO – Equal parts of glucose, dextrin, sucrose & Corn starch.

The experiment has 30 days duration. At the end of 30th day, animals were sacrificed by cervical dislocation.

Analytical methods

Fecal bile acids were determined according to the procedure of Snell and Snell . 24 hours fecal samples collected from individual rats were homogenized with equal weight of water and lyophilised to fine powder. 600mg of the stool sample was extracted with 10ml of 1N NaOH in 90% ethanol at 80^oC for 2 hrs. The mixture was cooled, centrifuged and the residue was again extracted with 10ml of 1N NaOH in 90% ethanol. The alkaline fecal extract was diluted with equal volume of water and was extracted with hexane. The solution left after the extraction with hexane was then acidified to pH 2.0 and

bile acids were extracted with ethyl acetate. The ethyl acetate layer was collected, washed with water and evaporated to dryness. The bile acids were dissolved in a known volume of ethyl acetate and aliquots were taken for the estimation of bile acids. From the aliquots bile acids were determined according to the procedure of Snell & Snell.

Results and Discussion

Table 1. Concentration of fecal bile acids

Groups	Cholic acid (mg/rat/day)	Chenodeoxycholic acid (mg/rat/day)
1. FF	11.70 ± 0.357	4.02 ± 0.120
2. CSNF	17.61 ± 0.616	5.79 ± 0.173
3. STNF	20.70 ± 0.496	6.23 ± 0.199

Values are ± SEM form six rats in each group

Groups with common superscripts are not significantly different at P< 0.05

Groups without superscripts are significantly different at P< 0.05

Results are recorded in table 1. Significantly elevated levels of cholic acid and chenodeoxycholic acid were found in the feces of CS/ST NDF fed rats as compared to fiber free diet fed control group. The increased excretion of bile acids was more in ST NDF fed group than in CS NDF fed ones.

The increased concentration of fecal bile acids in NDF fed groups may indicate increased hepatic degradation of cholesterol. Binding of bile acids by the fibre facilitates increased excretion. The bile acid binding and their consequent removal from the gut resulted in less bile acids reaching the liver by enterohepatic circulation. Thus the feedback inhibition of bile acid synthesis by bile acids is less and more cholesterol is degraded to bile acids. In this connection Marlett et al. reported that oat bran lowers serum cholesterol level in part by altering bile acid metabolism and fecal excretion of bile acids in man. It was also reported that soluble dietary fiber from psyllium inhibits cholesterol stone formation by reducing the biliary cholesterol saturation index in prairie dogs fed on cholesterol supplemented diet (Schwesinger WH, Kurtin WE et al). Kay, R. M et al reported that lignin is the most potent bile acid adsorbent and its binding is apparently influenced by molecular weight, pH, and the presence of methoxyl and carbonyl groups on the lignin molecule. Adsorption was maximum for the less polar, unconjugated dihydroxy bile acids and reduction of environmental pH enhanced binding especially of trihydroxy bile acids. This study suggests that among the two fibres, ST NDF fed rats showed higher fecal excretion of bile acids than CS NDF fed ones. This may be due to the high amount of lignin present in ST NDF.

Summary and Conclusion

The study indicated that feeding of NDF from *Coriandrum sativum* /*Solanum torvum* to rats at 10% level resulted significant elevation of the excretion of bile acids through feces. This may be due to the adsorption of bile acids by NDF. Increased excretion of bile acids results the degradation of more cholesterol from liver and thus lowers the cholesterol level. Among the two fibres, ST NDF fed ones showed more bile acid excretion than CS NDF fed ones.

References

- Anita FP, Abraham P. Clinical dietetics and nutrition. (1997) Calcutta: Delhi Oxford University Press; pp. 73–77
- Devinder Dhingra, Mona Michael, Hradesh Rajput, and R. T. Patil (2012) Dietary fibre in foods: a review J Food Sci Technol. 49(3): 255–266.
- Ghada A. Soliman (2019) Dietary Fiber, Atherosclerosis, and Cardiovascular Disease, Nutrients 2019, P 2 - 11, 1155; doi:10.3390/nu11051155
- Kay, R. M., S. M. Strasberg, C. N. Petrunka, and M. Wayman. 1979. Differential adsorption of bile acids by lignins. In Dietary Fibers: Chemistry and Nutrition. G Inglett and I. Falkehag, editors. Academic Press, New York. 57-66.
- Marlett, J.H., Hosig, K.B., Vollendorf, N.W., Shinnick, F.L., Haeck, V.S and Story, J.A. (1994) Increasing amounts of dietary fiber provided by foods normalizes physiologic response of the large bowel without altering calcium balance or fecal steroid excretion Hepatology, 20 (6): 1450-7.
- Parker E.D., Liu S., Van Horn L., Tinker L.F., Shikany J.M., Eaton C.B., Margolis K.L. (2013) The association of whole grain consumption with incident type 2 diabetes: The women's health initiative observational study. Ann. Epidemiol. 23:321–327.

Schwesinger WH, Kurtin WE, Page CP, Stewart RM, Johnson R(1999) Soluble dietary fiber protects against cholesterol gallstone formation. *Am J Surg* ;177:307–310.

Shufen Han, Wei Zhang, Ru Zhang, etal (2019) Cereal fiber improves blood cholesterol profiles and modulates intestinal cholesterol metabolism in C57BL/6 mice fed a high-fat, high-cholesterol diet. *Food Nutr Res.* 2019; 63: 10.29219/fnr.v63.1591.

Snell, F.D and Snell C.T (1961) Estimations of bile acids In: *Colorimetric methods of analysis vol. 3A: Van Nostrand, New York P.351*

Tunland BC, Meyer D. Nondigestible oligo and polysaccharides (dietary fibre): their physiology and role in human health and food.(2002) *Compr Rev Food Sci Food*;1:73–92.

ISSN: 2348-5906
CODEN: IJMRK2
IJMR 2021; 8(6): 20-23
© 2021 IJMR
www.dipterajournal.com
Received: 25-08-2021
Accepted: 14-10-2021

Lekshmi R
Post Graduate, Department of
Zoology and Research Centre,
Mahatma Gandhi College,
Thiruvananthapuram, Kerala,
India

Adhira M Nayar
Post Graduate, Department of
Zoology and Research Centre,
Mahatma Gandhi College,
Thiruvananthapuram, Kerala,
India

Sumodan PK
Post Graduate and Research,
Department of Zoology,
Government College,
Madappally, Vadakara, Kerala,
India

Corresponding Author:
Sumodan PK
Post Graduate and Research
Department of Zoology,
Government College,
Madappally, Vadakara, Kerala,
India

A rapid entomological reconnaissance during the first Zika outbreak in Thiruvananthapuram city, Kerala, India

Lekshmi R, Adhira M Nayar and Sumodan PK

DOI: <https://doi.org/10.22271/23487941.2021.v8.i6a.567>

Abstract

There was an outbreak of Zika virus in Thiruvananthapuram city of Kerala state, India in July 2021. In order to ascertain the prevalence and breeding pattern of the potential vectors, a study was conducted from 22 July 2021 to 27 July 2021. Breeding habitat surveys were conducted in seven localities in the city from where Zika cases were reported. House to house searches were conducted from mosquito breeding in 35-40 houses in each locality. Fourth instar larvae were identified using larval keys and later confirmed their identities after emergence. Lower instar larvae were reared in the laboratory and were identified after emergence using adult keys. Larval indices were calculated using WHO methods. Of the 280 houses surveyed mosquito breeding was encountered in 38 houses. Three *Aedes* species viz., *Ae. aegypti*, *Ae. albopictus* and *Ae. vittatus* were detected. *Ae. aegypti* and *Ae. albopictus* were breeding in 30.5% and 43.9% of the outdoor habitats and 56.0% and 16.0% of the indoor habitats respectively. The overall Container Index for (CI), Breteau Index (BI) and House Index (HI) for both species together were 56.07, 23.07 and 14.61 respectively. Two established urban Zika vectors viz., *Ae. aegypti* and *Ae. albopictus* were prevalent in the city with very high container indices. For the first time in the world, indoor flower vases used for money plant has been observed as an important breeding habitat of *Aedes* mosquitoes. Rapid elimination of the breeding habitats with community support is recommended to reduce the larval indices.

Keywords: Zika, *Aedes aegypti*, *Aedes albopictus*, Container Index, House index, Breteau index

1. Introduction

The history of Zika dates back to 1947, when a new virus was detected from a Rhesus monkey in Uganda, Africa, which was later named as Zika virus after the name of the forest in which the virus was isolated. The first incidence of the virus in humans was reported in 1952 from Nigeria^[1]. Although there were occasional outbreaks after the first outbreak in different parts of Africa and Asia, the disease was not considered a serious public health problem owing to its benign nature^[2]. However, the re-emerged Zika, starting with Yap Island, Micronesia in 2007 which spread to French Polynesia and several South American countries, appeared more virulent causing microcephaly in infants and Guillain Barre Syndrome in adults. This led World Health Organisation to declare Zika as a Public Health Emergency of International Concern (PHEC) on 1 February 2016, on the advice of an Emergency Committee of the International Health Regulations and of other experts^[3].

The first report of the re-emerged Zika in the WHO South-Eastern Region (WHO-SEAR) was in 2012 from Indonesia^[4]. In India serological evidence for the prevalence of Zika virus was available as far back as in 1952 with 33 samples out of 196 samples collected from six states turning positive. However, post re-emergence, Zika appeared in India for the first time during 2016-17. There were four cases reported from Gujarat and Tamil Nadu during that period^[5]. Subsequently, in 2018, there were two major outbreaks in Rajasthan and Madhya Pradesh with 153 and 130 confirmed cases respectively^[5].

On 8th July 2021 media reported a case of Zika in Thiruvananthapuram, the capital city of Kerala state. The patient was a 24 year old pregnant woman admitted in a private hospital in the city on 28th June 2021. She delivered a healthy baby on 7th July 2021, a day before the confirmation of Zika. In the subsequent days more cases were reported from different parts of the city. In reply to the starred question No. 275 by the member of Parliament Shri Hibi Eden

(available in public domain), the minister of health and family welfare, Government of India stated that there were 65 cases of Zika in Kerala as on 2nd August 2021. 61 cases were reported from Thiruvananthapuram city and another four cases from three cities outside the city. These four cases had histories of travel to Thiruvananthapuram.

Against this background we had designed a study to investigate the prevalence and pattern of breeding of potential vectors of Zika in the city. The study was carried out from 22 July 2021 to 27 July 2021.

2. Materials and Methods

2.1. Study area: The study was carried out in Thiruvananthapuram, the capital city of the South Indian state Kerala. The city has an area of 214 KM² and a population of 957, 730 (2011 Census).

2.2. Larval survey: Larval surveys were conducted in seven localities in the city, viz., Nanthancode, Kannanmoola, Karamana, Chakkai, Medical college, Thycaud and Nalanchira, from where Zika cases were reported. 35-40 houses were surveyed in each locality. The number of houses surveyed varied according to the size of the premises. Overall 260 premises were surveyed. Intensive searches were conducted indoor and outdoor for larval habitats, especially containers and tanks. Only those containers/ tanks with water were considered as breeding habitats. From small containers, entire water with larvae were emptied in to plastic containers. From large tanks and barrels, five samples each were collected using 300 ml dippers.

2.3. Identification: Fourth instar larvae were identified with larval keys [6]. Early instar larvae were reared in the laboratory and the adults were identified using adult keys [7].

2.4. Data analysis: Container index, House index and Breteau index were calculated as recommended by World Health Organisation [8].

3. Results and Discussion

3.1. Habitat diversity: Eight types of breeding habitats viz., barrels/drums, plastic tanks, cement tanks, coconut shells, discarded tyres, flower pots and minor plastic containers were encountered outdoors. Plastic tanks (28.0%), flower pots (24.4%) and minor plastic containers (23.2%) were the major breeding habitats, which together formed 75.6% of the total habitats (Table-1). The indoor breeding habitats encountered were flower vases/ pots used for keeping money plants or lucky bamboos, drip trays of refrigerators and coolers, and leaf axil. Flower pots/ vases (60%) was the topmost habitat (Table -2).

3.2. Mosquito breeding: Three *Aedes* species viz., *Ae. aegypti*, *Ae. albopictus* and *Ae. vittatus* were found breeding both indoor and outdoor. Of the 82 outdoor habitats *Ae. aegypti* bred alone in 10 habitats and in combination with *Ae. albopictus* in 15 habitats. *Ae. albopictus* was found breeding alone in 21 habitats and *Ae. vittatus* in one habitat. Four habitats had breeding of non-Aedine mosquitoes. There were 25 indoor habitats, of which 10 had *Aedes aegypti* breeding. Co-breeding of *Ae. aegypti* and *Ae. albopictus* was found in four habitats. *Ae. vittatus* breeding was restricted to a single habitat. While 25 (30.5%) outdoor habitats had breeding of *Ae. aegypti*, 36 (43.9%) habitats had *Ae. albopictus*. Among 25 indoor habitats 14 (56%) had *Ae. aegypti* and 4 (16%) had *Ae. albopictus* breeding. Overall percentage breeding of *Aedes aegypti*, *Ae. albopictus* and *Ae. vittatus* were 36.4, 37.3 and 1.87 respectively.

Table 1: Breeding pattern of *Aedes* mosquitoes in outdoor habitats in Thiruvananthapuram city.

Breeding Habitats	Total habitats surveyed (%)	Positive Habitats				
		<i>Ae. aegypti</i>	<i>Ae. albopictus</i>	<i>Ae. aegypti</i> + <i>Ae. albopictus</i>	<i>Ae. vittatus</i>	Non- <i>Aedes</i> species
Barrels/ drums	6 (7.3)		4			
Plastic tanks	23 (28.0)	3		6	1	2
Cement tanks	3 (3.7)		2	1		
Coconut shells	5 (6.1)		3			
Discarded tyres	6 (7.3)	3	1			
Flower pots	20 (24.4)	1	10	4		
Minor plastic containers	19 (23.2)	3	1	4		2
Total	82	10	21	15	1	4

Table 2: Breeding pattern of *Aedes* mosquitoes in indoor habitats in Thiruvananthapuram city

Breeding Habitats	Total habitats surveyed	Positive Habitats				
		<i>Ae. aegypti</i>	<i>Ae. albopictus</i>	<i>Ae. aegypti</i> + <i>Ae. albopictus</i>	<i>Ae. vittatus</i>	Non- <i>Aedes</i> species
Flower vases /pots	15 (60.0)	6		3	1	
Drip trays of refrigerators/ coolers	9 (36.0)	3		1		
Leaf axils	1 (4.0)	1				
Total	25	10		4	1	0

3.3. Larval indices: Mosquito breeding was detected in 38 houses out of 260 houses surveyed. Number of positive habitats for *Ae. aegypti* and *Ae. albopictus* together was 60 out of 107 habitats surveyed. The overall Container Index

(CI), Breteau Index (BI) and House Index (HI) for both species together were 56.07, 23.07 and 14.61 respectively ((Figure-1).

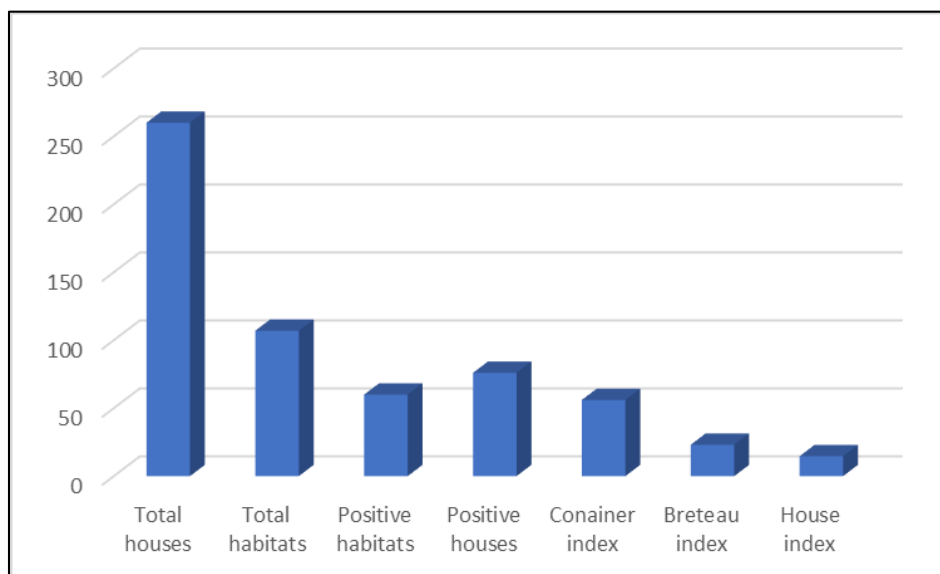


Fig 1: Breeding status of *Ae. aegypti* and *Ae. albopictus* in Thiruvananthapuram

Zika virus has two different life cycles, urban cycle and sylvian cycle. Major vectors in the urban cycles in Asia are *Ae. aegypti* and *Ae. albopictus*, with the former playing the dominant role [9]. Both species were prevalent in the study area. *Ae. aegypti* was the predominant indoor species occupying 56% of the breeding habitats surveyed. In the outdoor habitats, both species were prevalent with *Ae. albopictus* (43.9%) exhibiting moderate edge over *Ae. aegypti* (30.5%). Another interesting observation was the co-breeding of these two species both outdoor (18.3%) and indoor (16.0%).

Immediately after the report of the first case of Zika in Thiruvananthapuram city, an intensive drive for the elimination of *Aedes* breeding was launched in the city under the aegis of the Directorate of health Services, Government of Kerala. Our study started after a gap of exactly two weeks. Hence, the quantity of breeding habitats and the extent of *Aedes* breeding did not represent the real picture which would have existed prior to 8th June 2021, the day when the first case was reported. Nevertheless, there were epidemiologically significant number of breeding habitats as well as *Aedes* breeding supported by those habitats as revealed by the high larval indices (CI =56.07, BI =23.07 and HI=14.61). This has exposed the lacunae in the habitat elimination drive. Ward level planning led by the elected representatives of the municipal corporation and forming sub-ward level teams for house to house search for breeding habitats and their elimination are likely to reduce the indices rapidly and effectively. Except for cement tanks, all other positive breeding habitats observed in the study area are easily disposable. Since minor plastic containers formed a significant contributor to breeding habitats, anti-plastic drive would reap collateral benefits. Cement tanks could either be demolished or larvivorous fishes can be introduced.

Another interesting observation was vector breeding in flower pots/ flower vases indoors. Refrigerators and coolers have been widely reported as important contributors for the proliferation of *Ae. aegypti* from many parts of India [10, 11]. Flower pots/vases were used for keeping either money plant (*Epipremnum aureum*) or Lucky bamboo (*Dracaena sanderiana*). While growing money plants is believed to improve financial status of the family, lucky bamboos are

used in the Feng shui, a traditional Chinese practice, again for improving the quality of life. Though outdoor flower vases with money plants were reported to harbour *Ae. aegypti* and *Ae. albopictus* in Dhaka city, Bangladesh, their indoor prevalence has not been reported so far [12]. International trade in lucky bamboo was reported as means for the dispersal of the invasive mosquito *Aedes albopictus* on several occasions [13, 14]. However, their role as breeding habitats in the context of mosquito-borne diseases have not been reported from anywhere in the world.

Kerala, being a state with very high population density and intense inter-city travelling the possibility of spread of the disease to other cities is very high. As stated in the introduction, four cases originated from the city were reported from two other cities in the state. Rapid reconnaissance and elimination of vector breeding would reduce larval indices as reported from other Zika outbreak areas in India [15].

4. Conclusion

Although the first outbreak of Zika in India was reported during 2016-17, its emergence in Kerala was in July 2021. Though stray cases were reported from Tamil Nadu earlier, this was the major outbreak in South India, with 65 cases. Though Zika has not been associated with mortality, it should not be ignored as a trivial disease owing its ability to cause microcephaly in foetuses during pregnancy and Guillain Barre syndrome in adults. The present study showed the prevalence of two established vectors viz., *Aedes aegypti* and *Aedes albopictus* in Thiruvananthapuram city. They were found breeding in outdoor as well as indoor habitats. While *Aedes aegypti* was the predominant breeder indoors and *Aedes albopictus* was dominant outdoors. With well organised source reduction strategies involving the community could prevent future outbreaks in the city and elsewhere in Kerala.

5. Acknowledgements

The first two authors acknowledge the facilities provided by the principal, Mahatma Gandhi College, Thiruvananthapuram-695004, Kerala, India. The third author thanks the principal, Government College, Madappally, Vadakara-673102, Kerala, India.

6. References

1. MacNamara FN. Zika Virus. A report on three cases of human infection during an epidemic of jaundice in Nigeria. Transactions of Royal Society of Tropical Medicine and Hygiene 1954;48(2):139-145.
2. Abushouka AI, Negidac A, Ahmed H. An updated review of Zika virus. Journal of Clinical Virology 2016;84:53-58.
3. Heymann DL, Hodgson A, Sall A, Freedman DO, Staples JE, Althabe F *et al.* Zika virus and microcephaly: why is this situation a PHEIC? Lancet 2016;387:719-721.
4. Kwong JC, Druce JD, Leder K. Zika virus infection acquired during brief travel to Indonesia. Am J Trop Med Hyg 2013;89:516-517.
5. Biswas A, Kodan P, Gupta N, Soneja M, Baruah K, Sharma KK *et al.* Zika outbreak in in India in 2018. Journal of Travel Medicine 2020;27(4):1-3.
6. Tyagi BK, Muniratnam A, Venkatesh A. A catalogue of Indian Mosquitoes. International Journal of Mosquito Research 2015;2(2):50-97.
7. Barraud PJ. The fauna of British India including Ceylon and Burma. Diptera Volume V: Culicidae. Tribes Megarhinini and Culicini. Taylor and Francis 1934.
8. World Health Organisation . Entomological surveillance of *Aedes* spp in the context of Zika virus: Interim guidance for entomologists. WHO 2016.
9. Boyer S, Calvez E, Chouin-Carneiro T, Diallo D, Failloux AB. An overview of mosquito vectors of Zika virus. Microbes and Infection 2018;20:646-660.
10. Sharma RS, Kaul SM, Sokhay J. Seasonal fluctuations of Dengue vector, *Aedes aegypti* (Diptera: Culicidae) in Delhi, India. Southeast Asian Journal of Public Health 2005; 36(1): 186-190.
11. Srinivasan R, Mariappan T and Jambulingam P. Defrost water collection trays of refrigerators – A potential breeding habitat of *Aedes aegypti* in dengue and chikungunya infested areas of Southern India. Dengue Bulletin 2007;31:174-75.
12. Bashar K, Shamsuzzaman M, Chowdhury MAK. Container breeding mosquitoes in Dhaka city, Bangladesh. Bangladesh Journal of Life Sciences 2006;18(1):69-78.
13. Madon M, Mulla MS, Shaw MW, Kluh S, Hazelrigg JE. Introduction of *Aedes albopictus* (Skuse) in Southern California and potential for its establishment. Journal of Vector Ecology 2002;27:149-154.
14. Hofhuis A, Reimerink J, Reusken C, Scholte EJ, de Boer A, Takken W *et al.* Hidden passenger of lucky bamboo: Do imported *Aedes albopictus* mosquitoes cause dengue virus in the Netherlands ? Vector-Borne and Zoonotic Diseases 2009;9(2):217-220.
15. Singh R, Gupta V, Malhotra B, Singh Sujeet, Ravindran P, Meena D *et al.* Cluster containment strategy: addressing Zika virus outbreak in Rajasthan, India. BMJ Global Health. 2019;4:e001383. doi:10.1136/bmjgh-2018-001383. Available from <https://gh.bmj.com/content/4/5/e001383.full>



Optical Materials

Volume 117, July 2021, 111124

Research Article

An experimental investigation on structural, mechanical and physical properties of Strontium–Silicon Borate glass system through Bismuth–Aluminum substitution

Shams A.M. Issa^{a,b}, Hesham M.H. Zakaly^{b,c}  , Ali Badawi^{d,j}  , Reda Elsaman^b, H.O. Tekin^{e,f}  , A.A. Showahy^b, P.S. Anjana^g, Devika R. Nath^{g,h}, N. Gopakumar^h, Yasser B. Saddeek^{b,i}

[Show more](#)  Share  Cite<https://doi.org/10.1016/j.optmat.2021.111124> [Get rights and content](#) 

Highlights

- This study aimed to fabricate a high-density Strontium–Silicon Borate glass sample.
- Physical, structural and mechanical properties were determined.
- Gamma-ray attenuation properties were experimentally measured.
- Experimental Radiation Protection Efficiency (RPE) was determined.
- Al–Bi4 glass sample was reported with superior material properties.

Abstract

This study aimed to fabricate a high-density glass sample with superior physical, structural and mechanical properties that can be used in medical and industrial radiation facilities. For the chief purpose of originating a translucent radiation shielding with remarkable mechanical properties, a glass system of a heavy metal oxide alumino-borosilicate glass of composition $(5-x)\text{Al}_2\text{O}_3-50\text{SrO}-25\text{B}_2\text{O}_3-20\text{SiO}_2-x\text{Bi}_2\text{O}_3$ ($0 \leq x \leq 5$ wt%) was fabricated by traditional melt-quenching technique. XRD curves presented the disappearance of regular sharp lines, affirming the glassy nature of the glass system. Additionally, the determination of experimentally elastic moduli of the translucent glasses showed their good rigidity, along with good elastic constants. The comprehensive analysis of experimentally determined γ -radiation

Growth and Characterisation of Copper Complex of 2, 4, 6-Trioxypyrimidine: A Novel Luminescent and Active Pharmaceutical Material in Metal Organic Framework

Published: 14 September 2020

Volume 31, pages 426–436, (2021) Cite this article



Journal of Inorganic and Organometallic Polymers and Materials

[Aims and scope](#)

[Submit manuscript](#)

[V. T. Vineeth](#), [R. Divya](#), [B. R. Bijini](#), [M. Deepa](#), [B. Suresh Kumar](#) & [K. Rajendra Babu](#) 

 216 Accesses  1 Citation [Explore all metrics](#) →

Abstract

Emerald coloured crystal of copper complex of barbituric acid (CuB) ($C_8H_{10}CuN_4O_9$) is grown by conventional gel method. The crystal structure is orthorhombic with space group Fdd_2 and has unit cell dimensions $a = 11.6951(7) \text{ \AA}$, $b = 30.1113(19) \text{ \AA}$, $c = 7.1767(7) \text{ \AA}$ and $\alpha = \beta = \gamma = 90^\circ$. Analysis of the crystal by Hall–Williamson plot revealed the strain free nature of the grown crystals. Identification of the functional groups by FTIR and the study of thermal behaviour of the crystal by TGA/DTA were done. The optical band gap is determined as 1.57 eV from UV–visible absorption studies. The photoluminescence study provides information about the structural quality and purity of the crystal. Antibacterial studies of the sample revealed its medicinal applications. The high hardness value of the crystal is identified by Vickers micro hardness test.

 This is a preview of subscription content, [log in via an institution](#)  to check access.

Access this article

Log in via an institution

Buy article PDF 39,95 €

Price includes VAT (India)

Instant access to the full article PDF.



Synthesis and crystal structure of a heterobimetallic cadmium–sodium complex of 1,3,5-triazine-2,4,6-trione, [CdNa₂(C₃H₂N₃O₃)₄(H₂O)₈]

R. Divya,^a B. R. Bijini,^a V. S. Dhanya,^a K. Rajendra Babu^a and M. Sithambaresan^{b*}



^aPG Department and Research Centre in Physics, M.G. College, University of Kerala, Thiruvananthapuram 695004, India, and ^bDepartment of Chemistry, Faculty of Science, Eastern University, Sri Lanka, Chenkalady, Sri Lanka

*Correspondence e-mail: msithambaresan@gmail.com

Edited by J. Reibenspies, Texas A & M University, USA (Received 5 July 2021; accepted 8 August 2021; online 17 August 2021)

Heterobimetallic crystals of a cadmium–sodium complex of 1,3,5-triazine-2,4,6-trione, namely, μ -aqua-1:2 κ^2 O:O-heptaaqua-1 κ^3 O,2 κ^2 O,3 κ^2 O-bis(μ -4,6-dioxo-1,4,5,6-tetrahydro-1,3,5-triazin-2-olato)-1:2 κ^2 O²:N¹;2:3 κ^2 N¹:O²-bis(4,6-dioxo-1,4,5,6-tetrahydro-1,3,5-triazin-2-olato)-1 κ O²,3 κ O²-2-cadmium-1,3-disodium, [CdNa₂(C₃H₂N₃O₃)₄(H₂O)₈], were grown by the single gel diffusion technique. The asymmetric unit of the title compound comprises four 1,3,5-triazine-2,4,6-trione ligands, two sodium atoms and one cadmium atom. Of the four ligands, two are monodentately coordinated to two Na atoms. The third ligand is coordinated bidentately to one Na and the Cd atom and the fourth is also coordinated bidentately to the Cd atom and the other Na atom. All the metal atoms are six-coordinate with a distorted octahedral geometry. The water molecules bridge the Na atoms, constructing coordination polymer chains along the *a* axis and hence are linked by two Cd and one Na coordinations through the cyanuric acid ligands present in the coordination polymer chains, generating a two-dimensional coordination polymer in the (110) plane. The polymer formation is further assisted by means of many intermolecular and intramolecular N–H \cdots O, O–H \cdots O and O–H \cdots N hydrogen bonds between the water molecules and the ligands.

Keywords: crystal structure; heterobimetallic cadmium–sodium complex; gel growth; 1,3,5-triazine-2,4,6-trione; two-dimensional coordination polymer.

CCDC reference: 1576691

[Similar articles](#)

[Reuse permissions](#)

[PowerPoint slides](#)

1. Chemical context

Chelation is considered as the preferred method for the reduction of toxic effects of heavy metals, in which the metals are removed in the form of stable complex chelates. Cadmium, one of the most toxic heavy metals, can accumulate in the human body, leading to renal dysfunction, lung cancer, etc. In

Comparative study of antibacterial activity of zinc oxide and copper oxide nanoparticles synthesized by green method

Cite as: AIP Conference Proceedings **2369**, 020195 (2021); <https://doi.org/10.1063/5.0060909>
Published Online: 13 September 2021

P. S. Vindhya and V. T. Kavitha



View Online



Export Citation

ARTICLES YOU MAY BE INTERESTED IN

[Dielectric properties of zinc oxide nanoparticles using annona muricata leaf](#)

AIP Conference Proceedings **2082**, 080005 (2019); <https://doi.org/10.1063/1.5093888>

[Investigation of structural, optical and antibacterial properties of zinc sulphide quantum dots prepared by sol-gel method](#)

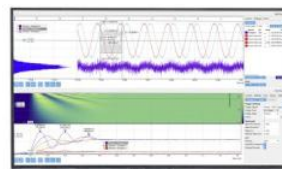
AIP Conference Proceedings **2369**, 020177 (2021); <https://doi.org/10.1063/5.0060815>

[Microwave assisted synthesis of graphene oxide - MnO₂ nanocomposites for electrochemical supercapacitors](#)

AIP Conference Proceedings **1953**, 030136 (2018); <https://doi.org/10.1063/1.5032471>

Challenge us.

What are your needs for periodic signal detection?



Zurich Instruments



Comparative Study of Antibacterial Activity of Zinc Oxide and Copper Oxide Nanoparticles Synthesized by Green Method

P S Vindhya, V T Kavitha^{a)}

Post Graduate and Research Department of Physics, Mahatma Gandhi College, Thiruvananthapuram-695004, Kerala, India.

a)Corresponding author: kavithavasant@gmail.com

Abstract. In this present work, we report the antibacterial activity of Zinc Oxide (ZnO) and Copper Oxide (CuO) nanoparticles synthesized by environment friendly, cost effective, less complex, safe and stable method using *Annona Muricata* leaf extract as reducing and stabilizing agent without adding any surfactants. Synthesized metal oxide nanoparticles were characterized by X-Ray Diffraction, Fourier Transform Infrared Spectroscopy and Scanning Electron Microscope. X-Ray Diffraction results revealed that the biosynthesized ZnO and CuO nanoparticles were crystalline in nature with higher purity. The bacterial effect of ZnO and CuO nanoparticles were tested on both gram positive and gram negative bacteria. The results indicate gram positive bacteria shows greater sensitivity to ZnO nanoparticles whereas gram negative bacteria are more sensitive to CuO nanoparticles.

Key words: Zinc Oxide and Copper Oxide nanoparticles, *Annona Muricata* leaf, Antibacterial activity

INTRODUCTION

Metal oxide nanoparticles play vital role in scientific, industry and medicinal field. Depends up on concentration, size, shape and morphology of nanoparticles enable several applications in the field of sensors, microelectronic circuits, piezoelectric devices, and catalysis [1]. ZnO and CuO nanoparticles have got more attention due to their various applications and physiochemical properties. Recently, nanotechnology becomes important in biomedical and pharmaceutical areas by the reemergence of infectious diseases and the appearance of antibiotic resistant strains of bacteria especially gram negative microorganisms [2]. Current investigation mainly focused on the growth of resistant microbial pathogens to presently used synthetic antibiotics. Biosynthesis of nanoparticles using plant extract is an interesting area as it is a cost effective, environment friendly, use of non-toxic chemicals and it provides advancement over chemical and physical methods [3]. Metal and metal oxide nanoparticles have attracted a special attention due to high surface to volume ration and small size. It enables to initiate interaction with microbial membranes. Several bacterial species causes variety of diseases in humans [4]. Sometimes prescribed antibiotic is not capable of killing/controlling the growth of multidrug resistant bacteria. Effective antibiotic treatment is required to cure microbes that cause infection. So it is necessity to recognize and build up nano based drugs to control bacterial infections [5]. Properties of the nanoparticles were changed by size, shape and morphology, by modifying the nanoparticles at atomic level unique property can be achieved [6]. The bacteria such as *Bacillus* and *E.coli* seemed to be sensitive to size and concentration of ZnO and CuO nanoparticles in the growth medium [7].

In this paper, we report synthesis of ZnO and CuO nanoparticles using *Annona Muricata* leaf extract. The obtained powders were characterized by XRD, FTIR and FE-SEM techniques. The antibacterial activity of metallic ZnO and CuO nanoparticles has been studied against gram negative *Escherichia coli* and gram positive *Bacillus*.

EXPERIMENTAL DETAILS

The fresh leaves of *Annona muricata* leaf were collected and are cleaned by tap water followed by double distilled water to remove dust particles. $Zn(NO_3)_2 \cdot 6H_2O$ and $Cu(NO_3)_2 \cdot 9H_2O$ (99.99%, purity, sigma Aldrich) as precursors. For the preparation of leaf extract 25g of fresh leaf was cut into fine pieces and boiled into 250 ml of double distilled water. Then extract was cooled and filtered through Whatman No.42 filter paper. For the synthesis of ZnO nanoparticles known molarity of Zinc nitrate solution mixed with leaf extract and stirred. After 3 hour stirring the solution was filtered using Whatman filter paper. A white color precipitate is obtained. The filtered powder is dried under Infrared radiation and hot air oven at a $100^\circ C$ to yield pure ZnO nano powder and is collected for further characterization. Synthesis of CuO nanoparticles, leaves extract was mixed with 5g of copper nitrate solution. Suddenly green colored solution was formed. As stirring time proceeds the reaction mixture changes color from green to dark and then finally black colored powder was formed. This powder was collected in silica crucible and heated at $500^\circ C$ for 2hrs using muffle furnace. The obtained black colored material was carefully collected, grinded then packed for further characterization.

The phase purity and crystalline nature were determined from the X-ray diffraction (XRD) patterns recorded using D8 Advance Bruker X ray diffractometer equipped with a $CuK\alpha$ radiation source; the samples were scanned over the 2θ range from 300 to 800. Functional group present in the FTIR was recorded by using Thermo Nicolet Avatar 370 in the range of $4000-400\text{ cm}^{-1}$. The surface morphology was analyzed using high resolution field emission scanning electron microscopy carried out on Hitachi SEM S4300.

Antibacterial Assay

Agar well diffusion method is widely used to evaluate antimicrobial activity of the compound. Autoclaved 15-20 mL of Mueller-Hinton agar was poured on glass petri plates and allowed to solidify. Standardized inoculum of the test organism was uniformly spread on the surface of these plates using sterile cotton swab. Four wells with a diameter of 8 mm (20 mm apart from one another) were punched aseptically with a sterile cork borer in each plate. Compound solution (40 and 80 μL) at desired concentration from 10mg/mL stock was added to three of the wells and one well with Gentamycin (80 μg /well) as positive and compound solvent as negative control. Then, the agar plates were incubated under $37^\circ C$ for 24 hrs. After incubation, clear zone was observed. Inhibition of the bacterial growth was measured in mm.

RESULTS AND DISCUSSION

Powder X-Ray Diffraction

Fig.1 (a) illustrates the XRD pattern of synthesized ZnO nanoparticles. The diffraction peaks labeled at 31.77° , 34.43° , 38.83° , 47.35° , 56.53° , 62.8° , 67.8° , 68.82° , 72.18° , 76.92° correspond to the (110), (100), (002), (101), (102), (110), (103), (112), (201), (004), (202) planes, confirming the formation of hexagonal wurtzite zinc oxide phases (JCPDS 36-1451) [8]. Fig.1 (b). shows a series of diffraction peaks having 2θ at 32.24° , 35.54° , 38.71° , 48.72° , 53.54° , 58.26° , 61.52° and 65.81° which were assigned to $(\bar{1}10)$, (002), (111), $(\bar{2}02)$, (020), (202), $(\bar{1}1\bar{3})$, and $(\bar{3}11)$ planes respectively confirming the formation of monoclinic structure of CuO nanoparticles with ICDD Card No 45-0937 [6]. XRD patterns shows strong and narrow diffraction peaks indicates the synthesized nanoparticles are pure and crystalline in nature. No extra diffraction peaks of other phases are detected, indicating the phase purity of nanoparticles. In the hexagonal structure of ZnO oxygen atoms are arranged in the hexagonal close packed type and Zinc atoms occupying half the tetragonal sides. In CuO nanoparticles copper atom is coordinated with oxygen atoms. Crystalline size was estimated by using Debye-scherrer's formula,

$$D = \frac{k\lambda}{\beta \cos\theta}$$

Where D is the crystalline size, λ is the wavelength of X-ray used, K is the shape factor, β is the full line width at the half maximum (FWHM), and θ is the Bragg angle.

The obtained Crystalline size was 24 nm and 21 nm for ZnO and CuO nanoparticles.

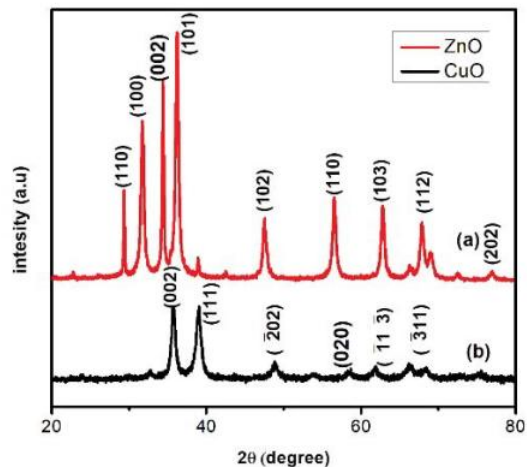


FIGURE 1. XRD Pattern of (a) ZnO; (b) CuO Nano Powder

FT-IR Spectroscopy

The presence of vibration peaks of ZnO and CuO nanopowder was examined by FTIR spectroscopy shown in fig.2. (a) & (b). The broad peak corresponds to 3424 cm^{-1} and 3416 cm^{-1} is due to OH stretching of the hydroxyl group or different carboxylic acids. The peak at 1632 cm^{-1} is attributed to the bending vibrations of absorbed H_2O molecules. The band at 1383 cm^{-1} is corresponding to bending vibrations of $-\text{OH}$ in phenols or symmetric stretching vibration of $-\text{COOH}$ functional group. The spectrum also shows a peak at 875 cm^{-1} which correspond to $-\text{OH}$ stretching of intermolecular H-bond, C=O and C-C stretching of alkanes. Absorption at 415 cm^{-1} is the stretching frequency of Zn-O bonds confirms the presence of M-O vibrational band [9]. The band at 525 cm^{-1} confirms the stretching vibration of Monoclinic CuO nanoparticles [10].

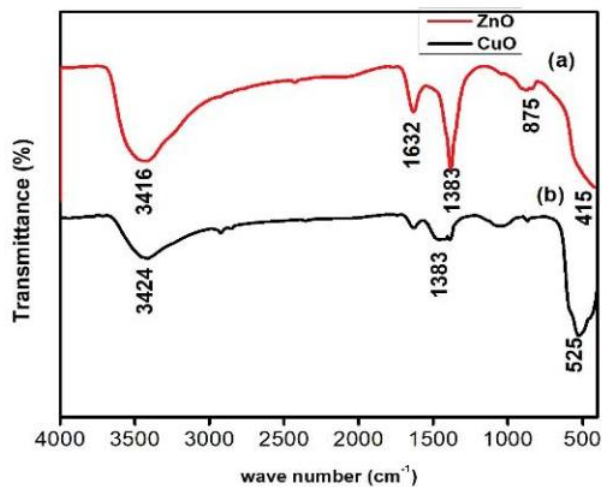


FIGURE 2. FT-IR spectrum of (a) ZnO; (b) CuO sample

FE-SEM ANALYSIS

FE-SEM image of obtained ZnO & CuO nanoparticles shown in Fig.3 (a) & (b). Image depicts formation of crystalline phase having spherical shape with agglomerated particles [11]. Micrograph shows morphology consist of

voids and pores of various sizes and shapes that are inter linked to one another due to large amounts of hot gases that escape out from the reaction mixture during synthesis procedure.

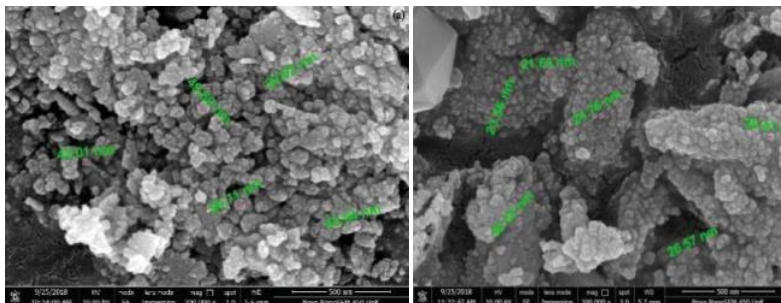


FIGURE 3. FE-SEM image of (a) ZnO;(b) CuO nanopowder

ANTIBACTERIAL ACTIVITY

There are several possible mechanisms to explain the effect of bacterial surface on nanoparticles. Antibacterial activity of nanoparticle takes place due to denaturation of DNA, proteins, enzymes, oxidation and reduction of reactive oxygen species, it produce hydroxyl free radicals and peroxide formed under UV-irradiation. In suspension nanoparticles were trapped into the bacterial surface resulting absorption of nanoparticles on the bacterial surface, which lead to inactivation of bacteria in with photocatalytic oxidation reaction [12-13]. The antibacterial activity of nanoparticles depends on the size and capping agent, smaller the size, better the bacterial activity.

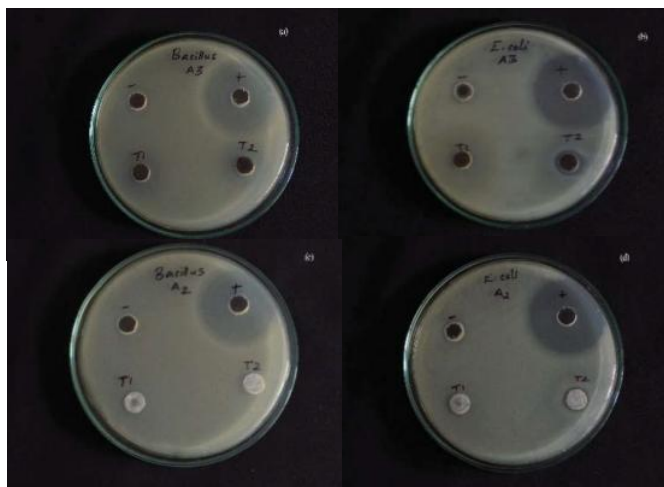


FIGURE 4. Antibacterial activity of (a,b) ZnO; (c,d) CuO

Fig.4 (a) & (b) shows the investigation for antibacterial activity of ZnO nanoparticles against gram positive (*Bacillus*) and gram negative (*Escherichia coli*) bacteria. The ZnO nanoparticles show highly significant antibacterial activity on all four bacterial strains in agar well diffusion method. The diameter of the zone of inhibition is in millimeters. The zone of inhibition was found to be highest for *Escherichia coli* (34mm) when compared to *Bacillus* (32mm). Fig. 4 (c) & (d) shows the investigation for antibacterial activity of CuO nanoparticles against gram positive *Bacillus*(26mm) and gram negative *E. coli* (30mm) bacteria. The zone of inhibition around the entire well of petriplates clearly indicates antibacterial potential of biosynthesized CuO nanoparticles. In this study, effect of CuO nanoparticles on gram negative bacteria was observed higher than gram

positive bacteria it may be due to difference in bacterial membrane structures. Hence CuO nanoparticles synthesized using *Annaona Muricata* extract is found to be good antibacterial agent against gram negative bacteria.

CONCLUSION

We have fabricated environment friendly, efficient, safe and cost-effective procedure for the green synthesis of ZnO and CuO nanoparticles using leaf extract without use of any toxic and hazardous materials. The synthesized nanoparticles were characterized by XRD, FT-IR and FESEM. The spherical-like morphology of ZnO and CuO NPs was confirmed by FESEM. The presence of hexagonal wurtzite phase of ZnO NPs with average size of 24 nm and monoclinic phase of CuO NPs with average size of 21 nm was confirmed by XRD. The observed vibration peaks in the FT-IR analysis indicated the presence of metal–oxygen species. The bacterial effect was tested for both gram positive and gram negative bacteria. ZnO and CuO nanoparticles are appeared to be new tool for treatment of infections and antibiotics.

ACKNOWLEDGMENTS

Authors would like to thank University of Kerala for financial support under university Junior Research Fellowship. We were also thanks to STIC (Cochin), SICC (University of Kerala), Athmic Biotech for antibacterial studies and Mahatma Gandhi College, Thiruvananthapuram for the analysis carried out.

REFERENCES

1. Wesam Salem, Deborah R. Leitner, Franz G. Zingl, Gebhart Schratte, Ruth Prassl, Walter Goessler, Joachim Reidl, Stefan Schild, [International Journal of Medical Microbiology](#) 305, 85–95 (2015).
2. Deepali Sharma, Myalowenkosi I. Sabela, Suvaradhan Kanchi, Phumlane S. Mdluli, Gulshan Singh, Thor A. Stenström, Krishna Bisetty, [Journal of Photochemistry & Photobiology, B: Biology](#) 162 199–207 (2016).
3. P. S. Vindhya, T. Jeyasingh, and V. T. Kavitha, [AIP Conference Proceedings](#) 2082, 080005 1-5 (2019).
4. Amna Sirelkhatim, Shahrom Mahmud, Azman Seeni, Noor Haida Mohamad Kaus, Ling Chuo Ann, Siti Khadijah Mohd Bakhori, Habsah Hasan, Dasmawati Mohamad, [Nano-Micro Lett.](#) 7 219–242 (2015).
5. Ameer Azam, Arham S Ahmed, Mohammad Oves, Mohammad S Khan, Sami S Habib, Adnan Memic, [International Journal of Nanomedicine](#) 7 6003–6009 (2012).
6. P. S. Vindhya, T. Jeyasingh, V. T. Kavitha, [AIP Conference Proceedings](#) 2162, 020021 -5 (2019).
7. Abdelali Merah, Abdenabi Abidi, Hana Merad, Nouredine Gherraf, Mostepha Iezid, Abdelghani Djahoudi, [ASN](#) 6 63-72 (2019).
8. S. Sheik Mydeen, R. Raj Kumar, M. Kottaisamy, V.S. Vasantha, [Journal of Saudi Chemical Society](#) 24, 393–406 (2020).
9. Di Liu, Lu Liu, Lei Yao, Xiaoyu Peng, Yang Li, Tingting Jiang, Hongyu Kuang, [Journal of Drug Delivery Science and Technology](#) 55 (2020) 101364.
10. Saranya Sukumar, Agneeswaran Rudrasenan, and Deepa Padmanabhan Nambiar, [ACS Omega](#) 2020, 5, 1040–1051.
11. Waseem Ahmad, Divya Kalra, [Journal of King Saud University – Science](#) 32 (2020) 2358–2364
12. K. Lingaraju, H. Raja Naika, K. Manjunath, R. B. Basavaraj, H. Nagabhushana, G. Nagaraju, D. Suresh, [Appl Nanosci](#) 6 703–710 (2016).
13. Rania Dadi, Rabah Azouani, Mamadou Traore, Christine Mielcarek, Andrei Kanaev, [Materials Science & Engineering C](#) 104 109968-109977 (2019).



Research paper

Emergence of fifth-order optical nonlinearity in 2-(2-Quinolyl)-1,3-indandione with strong third-order nonlinear effect under low power CW laser excitation

I.P. Primsa^a, M.C. Sreenath^b, V.M. Anandakumar^{a,c}  , I. Hubert Joe^d[Show more](#)  Share  Cite<https://doi.org/10.1016/j.cplett.2021.138434> [Get rights and content](#) 

Highlights

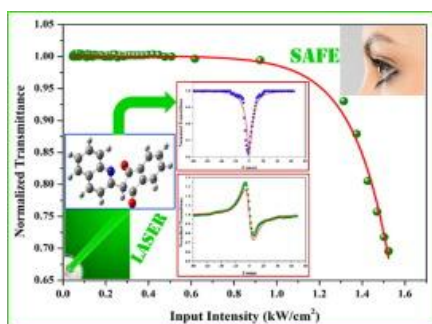
- Z-Scan method is used to characterize the third-order nonlinear optical properties.
- Fifth-order nonlinearity is observed along with third-order nonlinear optical properties.
- Different curve fitting methods were used for the calculation of third-order nonlinear optical coefficients.
- Optical limiting property is studied and optical limiting threshold value is calculated.

Abstract

The present work reports the presence of fifth-order optical nonlinearity in 2-(2-Quinolyl)-1,3-indandione, an organic dye, at low intensity level. Photophysical, structural and vibrational properties were studied by theoretical and experimental methods. Z-scan study of the dye revealed that the compound has a self-defocusing behaviour at continuous Nd:YAG 532 nm laser excitation and exhibited reverse saturable absorption. The positive fifth-order nonlinear refractive index (n_4) is of the order of $10^{-10} \text{ cm}^4/\text{W}^2$. The nonlinearities present in the compound has both thermal and electronic origin. This study reveals that the material is a potential candidate as an optical limiter at low

power.

Graphical abstract



[Download : Download high-res image \(136KB\)](#)

[Download : Download full-size image](#)

Introduction

The field of nonlinear optics has grown exceptionally since the invention of lasers. At high intensity levels, polarization can be expanded to nonlinear regime and have greater scope for applications in photonics and optoelectronics [1]. Insulators, semiconductors, organic and inorganic materials, crystals etc. are investigated for nonlinear optical (NLO) properties. Among these, organic materials have attracted much attention in recent years for their large nonlinearities in hyper polarizabilities and susceptibilities. The chemical flexibility resulting from their delocalized π -electron systems, their wide absorption bands and low threshold can be exploited for optical data storage, optical switching and optical limiting applications. The nonlinear susceptibility of a material is a macroscopic effect caused by the hyper polarizability and provides a framework for describing nonlinear optical phenomena. The intensity of transmitted light is considerably modified because of the inherent absorptive and refractive properties of the material. So it is important to determine the nonlinear optical coefficients of materials to overcome the difficulty in finding suitable media for practical devices [2], [3], [4], [5], [6]. One of the methods to measure third-order nonlinear properties such as nonlinear refractive index (n_2), nonlinear absorption coefficient (β) and real and imaginary part of $\chi^{(3)}$ is the Z-scan technique. Z-scan is based on spatial beam distortion and Gaussian TEM₀₀ beam is used for the absolute measurements. The simplicity and the sensitivity of this method makes it a valuable tool compared to other measurement techniques like nonlinear interferometry, degenerate four wave mixing, nearly degenerate three-wave mixing, ellipse rotation etc. [7], [8]. It is an efficient technique for filtering out new nonlinear materials as the data analysis is fast and simple [9]. The mechanisms responsible for nonlinear absorption and nonlinear refraction are immediately known from the Z-scan trace. Various processes such as saturation of absorption (SA), reverse saturable absorption (RSA) and multiphoton absorption (MPA) can occur which leads to nonlinear absorption in a material. SA behaviour is used in passive mode locking/Q-switching of lasers. Molecules possessing excited state absorption exhibits RSA. This property is found to be useful in pulse smoothening/shortening, spatial light modulation and power limiting. Multiphoton absorption is used in microscopy and photodynamic therapy. In continuous wave regime, thermal lensing also plays a major role in the nonlinear properties of a material [10], [11], [12], [13].

The present work reports investigations on the nonlinear properties of 2-(2-Quinoly)-1,3-indandione, an organic dye. 2-(2-Quinoly)-1,3-indandione is a synthetic yellow colour dye made up of a mixture of sodium disulfonates, monosulfonates, and trisulfonates and used for colouring foods, drugs, drinks and hair products [14]. Quinoline and its derivatives are used in DSSCs due to their strong electron accepting behavior emerging from the nitrogen atom [15] and

Synthesis and Characterization of Ag Added Nanostructured TiO₂ using Sol-gel Technique

Nimmy A V¹, V Biju² and Ananda Kumar V M³

¹Department of Physics, Mahatma Gandhi College, Thiruvananthapuram, Kerala, 695004, India

²Department of Physics, University of Kerala, Kariavattom, Thiruvananthapuram, Kerala 695581, India

³Department of Physics, VTMNSS College, Dhanuvachapuram, Thiruvananthapuram, Kerala, 695503, India

¹nimmyav@gmail.com

²bijunano@gmail.com

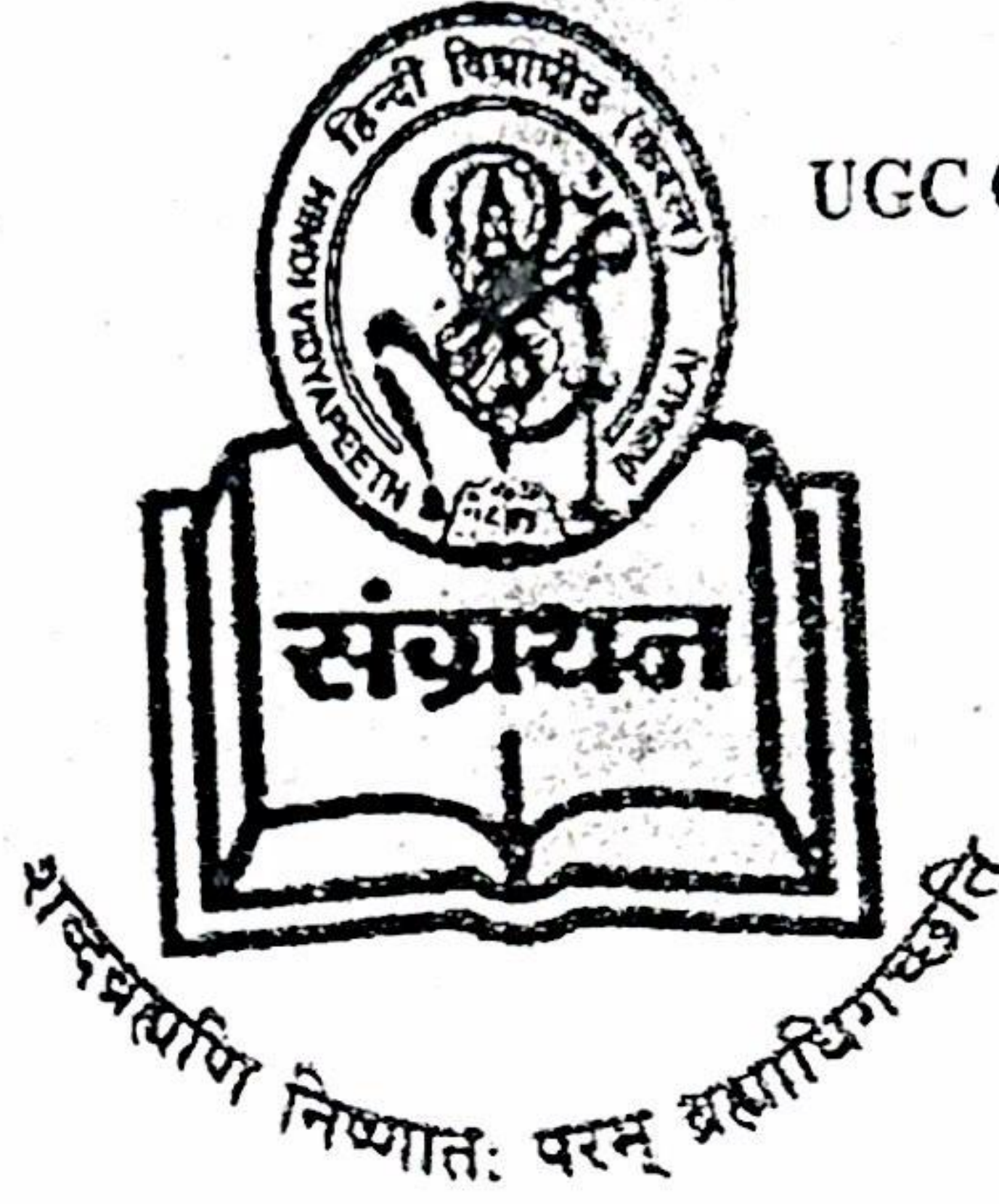
³anand@vtmnssclege.ac.in

Abstract— Metal doped TiO₂ has considerable applications in visible light enhanced photocatalysis for hydrogen production, waste water treatment and self-cleaning surfaces. The initial phase to achieve visible light activated metal doped TiO₂ is to synthesize them in a suitable method and to analyse the effect of metal ions on the nanosized TiO₂ crystal lattice. Herein, we report the synthesis of pure and silver doped nanostructured TiO₂ at three different molar concentrations by sol-gel method using titanium tetraisopropoxide [Ti(OC₃H₇)₄] (TTIP) and silver nitrate (AgNO₃) as precursors. The thermal decomposition of the xerogel was studied using TGA-DTA. FT-IR spectrum of the xerogel of the pure sample and the annealed samples were recorded. The crystal structure, average crystallite size and the amount of phase contents were determined using the powder XRD. The results show that the synthesized nanostructured TiO₂ containing both anatase and brookite phases. In addition to this, the effects of silver addition in the titania matrix were studied using Diffuse Reflectance Spectroscopy.

Keywords— Sol-Gel Technique, Ag added TiO₂ nanoparticles, Anatase and Brookite Titania, Phase percentage calculation, Band gap

I. INTRODUCTION

Titania (TiO₂) is a very good UV sensitized photocatalytic material because of its wide bandgap and it also shows high visible light transparency[1]–[3]. Hence, one has to develop visible light enhanced and popularized photocatalytic materials for emerging applications by engineering the bandgap of these transition metal oxides. One of the way is to select the suitable dopants to create discrete energy levels in their wide bandgap region their crystal lattice[3], [4]. It is very difficult to find out suitable dopants incorporate and their concentration of addition which will affect the properties of the parent material in a suitable way for a particular synthesis route. Noble metal doped or deposited TiO₂ has given promising results for visible light activated photocatalytic activity. This is due to the fact that conduction electrons of TiO₂ are transferred to the added metal particles in the TiO₂ surface since the Fermi levels of most of the noble metals are lower than that of TiO₂[5]. The deposition of noble metals such as Au, Ag and Pt enhances the photocatalytic activity of TiO₂ by acting as electron traps on the surface and thereby delaying electron-hole recombination[6]–[8]. Among the noble metals, Silver ions have attracted immense interest, because of the improvement of photoactivity of semiconductor photocatalysts and its antibacterial activity[9]. Silver doped titanium is used for coating the medical devices, food preparation surfaces, and sanitary wares. The sol-gel method is a suitable and a convenient chemical method for the preparation of doped Titanium dioxide (TiO₂). In the present study, we report the synthesis of silver incorporated nanophase TiO₂



ISSN 2278 - 6880
UGC Care - List Sr. No.305 (177)

यू.जी.सी. से अनुमोदित हिन्दी मासिक पत्रिका

हिन्दी विद्यापीठ,
टी.सी. 44/2670, जगती,
तिरुवनन्तपुरम- 695014
केरल।



संस्थापक संपादक :
स्व. पी. जी. वासुदेव

मुख्य संपादक :
डॉ. वी. वी. विश्वम
Mob: 9446662694
sangrathan2012@gmail.com

संपादक:
डॉ. एन. एस. विनयचन्द्रन
Mob: 9447657301
msvinayachandran61@gmail.com

Web Edition : www.sangrathan.com

वर्ष : ३३

अंक : 11

नवंबर : 2021

मूल्य : २० रुपये मात्र

आजीवन सदस्यता शुल्क : २,००० रुपये मात्र

वार्षिक चन्दा : दो सौ रुपये मात्र



माधविकुट्टी

केरल में कमला सुरय्या (माधविकुट्टी) जैसी चर्चित कोई अन्य महिला कहानीकार नहीं होगी। आराधना पात्र बनकर, अनुकरण को नृति बनकर, साथ ही साथ अपने पात्रों को चौंकाकर वे केरल के लोगों के, पाठकों के मन में पूरी गहराई से समाई गई हैं। 'माधविकुट्टी', 'कमला दास', 'आनी', 'कमला सुरय्या' ऐसे ऐसे नामों से हम उन्हें पुकारते हैं लेकिन उनके उन्नाद, नये नये सुझाव, लेखन, बातें सब केरल के लोगों को एकदम नये थे। वे सब देखकर कुछ लोग डर गए, उन पर पत्थर फेंके, थुंके, आश्चर्य चकित हुए। फिर भी वे केरल के लिए, देश के लिए तथा दुनिया के लिए हमारी अपनी है। माधविकुट्टी नाम से उन्होंने मलयाळम में रचना की थी और कमला दास नाम से अंग्रेजी में कविताएँ लिखकर विश्व साहित्य में

नारीत्व के कहानीकार माधविकुट्टी



डॉ. गायत्री एन.

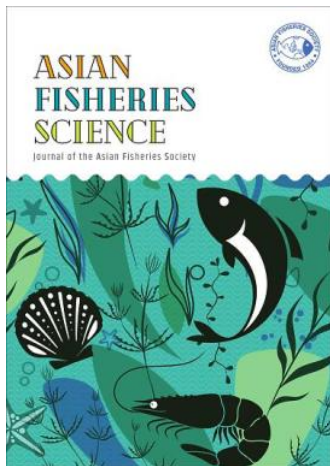
भी अपना अलग अस्तित्व साबित किया था।

माधविकुट्टी की संपूर्ण कहानियों में नारी-जीवन की ही प्रमुखता है। प्यार करनेवाली और प्यार पाने की इच्छा एक नारी-जीवन की वैविध्यपूर्ण, अनुभवों की पुनः सृष्टि हैं ये कहानियाँ। वे स्वयं अपने को एक स्त्री स्वभाववाली लेखिका मानती हैं। उनकी कविताओं में भी यही हम देखते हैं। 'आशान वेल्ड प्रैस' के लिए कमला दास के काव्य-संग्रहों का नाम निर्देशित करते हुए फ्लिन्टर्स यूनिवर्सिटी ऑफ़ सौथ आस्ट्रेलिया (Flinters University of South Australia) के डॉ.एस.सी. हारेक्स लिखते हैं : भूतकाल की दबोच से मिली गुलामी से मुक्ति चाहनेवाली भारतीय नारी का अन्तःसंघर्ष ही कमला दास की कविताओं में मुखरित है। कठोर रुढ़ियों और आचारों को ललकारकर काम-

वासना और पुरुष सत्ता का उल्लंघन करके नयी मिथक की सृष्टि ही उनकी कविताओं की खासियत है।

एक स्त्री के रूप में अपने कर्तव्यों को निभाने के साथ साथ एक कलाकार के रूप में अपने प्यार संबन्धी मान्यताओं का बनाय रखन की लड़ाई में भी वे सक्रिय भातूम पड़ती हैं। इनकी कहानियों में व्यक्त जीवन स्त्री को प्रधानता देनेवाली है। मात्र एक कवयित्री बनना नें नहीं चाहती "मैं आराधना एवं प्यार का पात्र एक नारी बनना चाहती हूँ" उनके पात्र का यह मोह माधविकुट्टी का अपना भातूम पड़ता है।

सामाजिक और सांस्कृतिक रूप से पुरुष मेधावी एक समाज में, अपना अलग व्यक्तित्व स्थापित करने की इच्छा ही "मुझे अपनी आवाज़ में बोलना है, मुझे अपनी आवाज़ में बोलना है" ऐसा कवयित्री से बतलवाया था।



Histopathology of *Anilocra leptosoma* Bleeker, 1857 (Isopoda, Cymothoidae) Infestation on Its New Host *Nematalosa nasus* (Bloch, 1795) From India

AMRUTHA SHYLA SURESH¹, BALAMURALI RAGHAVAN PILLAI SREEKUMARAN NAIR^{1,*}, ARYA UNNI¹, BINUMON THANKACHAN MANGALATHETTU²

¹Post Graduate Department of Zoology and Research Centre, Mahatma Gandhi College, Pattom PO., Trivandrum 695004, Kerala, India

²Department of Zoology, University of Kerala, Karyavattom, Trivandrum 695581, Kerala, India

©Asian Fisheries Society

ISSN: 0116-6514

E-ISSN: 2073-3720

<https://doi.org/10.33997/j.afs.2021.34.1.010>

*E-mail: drbala@mgcollegetvm.ac.in | Received: 07/09/2020; Accepted: 21/03/2021

Abstract

Cymothoid isopods are parasitic crustaceans that cause serious impact on marine fish and might lead to fish mortality and consequently, economic losses. Histopathological alterations caused by *Anilocra* spp. have not been studied well. This study aims to report the histopathological changes caused by Cymothoid, *Anilocra leptosoma* Bleeker, 1857 in the skin of Bloch's gizzard shad, *Nematalosa nasus* (Bloch, 1795). Histopathological examination of processed skin tissues showed changes caused by *A. leptosoma*, such as hyperplasia and erosions of the epidermis associated dermal oedema and muscle degeneration. The host response also included an aggregation of subepithelial dense sheets of hemosiderin-laden macrophages within the dense mixed inflammatory cells. The cymothoid, *A. leptosoma* are serious parasites of marine fish that can cause severe economic loss in the commercially important fish species. The present study represents the first record of the parasitic cymothoid, *A. leptosoma* on *N. nasus* from India.

Keywords: parasitic cymothoid, epithelial hyperplasia, inflammation, hemosiderin-laden macrophage

Introduction

Parasitic isopods belonging to the family Cymothoidae Leach, 1814 are extremely serious fish parasites that adversely affect the health of aquatic animals with considerable economic losses (Aneesh et al., 2017). Fifty valid species of the genus *Anilocra* Leach, 1818 have been reported (Bruce, 1987). Only two valid species are known from India, *Anilocra dimidiata* Bleeker, 1857 (Rameshkumar et al., 2011), and *Anilocra leptosoma* Bleeker, 1857 (Aneesh et al., 2017). Species of *Anilocra* are known to prefer the external surfaces of marine fish hosts that inhabit subtropical, tropical, and temperate waters (Smit et al., 2014). Blood feeding and parasitic association cause a variety of pathological effects on their host fish. The impaired swimming ability of the fish tends to reduce their capacity to escape from the predator, and hence there is a greater risk of being eaten (Ostlund-Nilsson et al., 2005). The parasites are associated with many commercially important fish species worldwide and cause significant economic losses to fisheries either by killing, stunting, or damaging these fishes (Elgendy

et al., 2018).

The Bloch's gizzard shad (*Nematalosa nasus* Bloch, 1795) is an anadromous fish that inhabits a wide range of marine environments (Mukherjee et al., 2016). There are several reports on *N. nasus* parasitised by isopods belonging to the genera, *Agarna* Schioedte and Meinert, 1884; *Cymothoa* Fabricius, 1793; and *Nerocila* Leach, 1818 (Trilles et al., 2011). Although there are reports on *Anilocra* infestation of fish from India, there is no record of the parasite from *N. nasus* and only one previous report of the parasite on *N. nasus* from Australia (Bruce, 1987).

The effect of the isopod parasite on host fish shows considerable variation (Cuyas et al., 2004). In India, few studies have reported the effect of parasitic isopods on host fishes (Rand, 1986; Jalajakumar, 1988; Lailabeevi, 1996). These studies have indicated that the harmful effects of parasites varied from tissue damage at their site of attachment to mortality of the hosts. A review of literature revealed that there exist only two previous reports on the effects of isopod

genus *Anilocra* on host fishes. In this study, an attempt was made to elucidate the pathological changes in *N. nasus* due to infestation by the cymothoid, *A. leptosoma*.

Materials and Methods

A total of 120 fish samples of Bloch's gizzard shad, *N. nasus* were collected from Neendakara (Lat. 8°56'19" N, Long. 76°32'25" E), South-West coast of India. The fish were examined thoroughly for the isopod parasites. The mode of attachment of isopods to the host skin and the gross changes made by them were observed and photographed. The specimens of *A. leptosoma* were examined and identified according to the taxonomic keys of Bruce, 1987 and Aneesh et al. (2017) using stereo dissecting microscope (SDM) (Stemi 508, Carl Zeiss, Germany). Photomicrographs were taken using SDM and taxonomic drawings were made using CorelDraw software.

Ten specimens each for uninfested and infested host fish skin was excised and fixed in 10% neutral buffered formalin for histopathological analysis (Ananda Raja and Jithendran, 2015). The tissues were washed with distilled water for cleaning and dehydrated in a series of ethyl alcohol (50, 70, 90 and 100 %) cleared in xylene, embedded in paraffin wax and sections were made at 4 µm using a microtome (HistoCore BIOCUT, Leica, Germany). Tissue sections on the glass slides were hydrated in a series of ethyl alcohol (100 %, 80 % and 70 %) and stained with haematoxylin and eosin, cleared in xylene and mounted using DPX mountant (Carleton, 1980). The sections were examined and photomicrographed using transmission light microscope (TLM) and Optikam B5 Digital Camera (Optika, Italy).

Ethical approval

The animals used in this study did not require ethical approval.

Results

Anilocra leptosoma were attached posterodorsally to the head of *N. nasus* (Fig. 1a) and some of them recovered from the base of the dorsal fin, facing the cephalon towards the host mouth. Out of 120 fish examined, 13 were found to be infested each with a single ovigerous female. Discrete alterations such as skin depression and darkening were observed at the attachment site of the parasite (Fig. 1b).

The parasitic isopod, *A. leptosoma* (Figs. 1c-e) collected from the body surface of the host was identified by the key taxonomic characteristics: Pleotelson ovate, lateral margins converging smoothly to caudomedial point, and pleonite 1 lateral margin posteriorly produced (Figs. 1f-g).

Histopathology of normal skin from the head region of the uninfested fish showing compactly arranged cells and normal tissue architecture (Fig. 2a). Sections of muscle showed normal morphology and no specific lesion in the uninfested fish skin (Fig. 2b).

The histopathology of skin tissues infested with *A. leptosoma* was undergoing degenerative changes. At the point of parasite attachment, there was depression (Fig. 3a) and epidermal erosion (Fig. 3b) along with hyperplasia (Fig. 3b). The underlying epidermis and dermis were infiltrated with inflammatory cells (Fig. 3b), oedema (Figs. 3a, b, c,) and tissue undergoing necrosis (Figs. 3c, d). In addition, in the inflammatory cells large numbers of eosinophilic cells were seen (Fig. 3d inset).

The host response to *A. leptosoma* infestation also included an intense increase in subepithelial dense sheets of hemosiderin-laden clusters of macrophages (melanomacrophages) (Fig. 3b inset) within the dense mixed inflammatory infiltrate (Figs. 3b, c). These melanomacrophages (MMs) were enlarged and closely packed aggregates of melanomacrophage centres (MMCs). In skin tissues, most of the MMs appeared in yellowish-brown colour, but in some regions, they were darkly pigmented (Figs. 3b, c)

Discussion

Histopathological examination of the infected skin revealed significant changes in all layers. In the present study, the parasite was seen to be specifically attached to the fish's head region. According to Fogelman (2009) the body surface is the preferred attachment site for this parasite. *Anilocra* species are usually found just beneath either the eye or attached posterodorsally to the eye of their hosts. In the present study the parasite was attached mainly a little above the postero-dorsal region of the eye after the operculum. The selection of the site of attachment may depend on the host's morphology, body movement or habitat (Rameshkumar and Ravichandran, 2013a).

The depression observed in the skin of the infested fish may be due to erosion of the body surface due to the attachment of the parasite for a long period. According to Mladineo et al. (2020) pressure is exerted by the isopod at the attachment site in turbulent sea conditions and the tissue reactions seen is caused by the feeding activities, in addition, there is skin darkening associated with parasite infestation as reported by Rojas et al. (2018) in rainbow trout, *Oncorhynchus mykiss* (Walbaum, 1972) due to copepod infestation. This darkening may be due to the increased concentration of melanin-based pigmentation, which also forms a defence mechanism to resist the ectoparasite (Kittilsen et al., 2009).

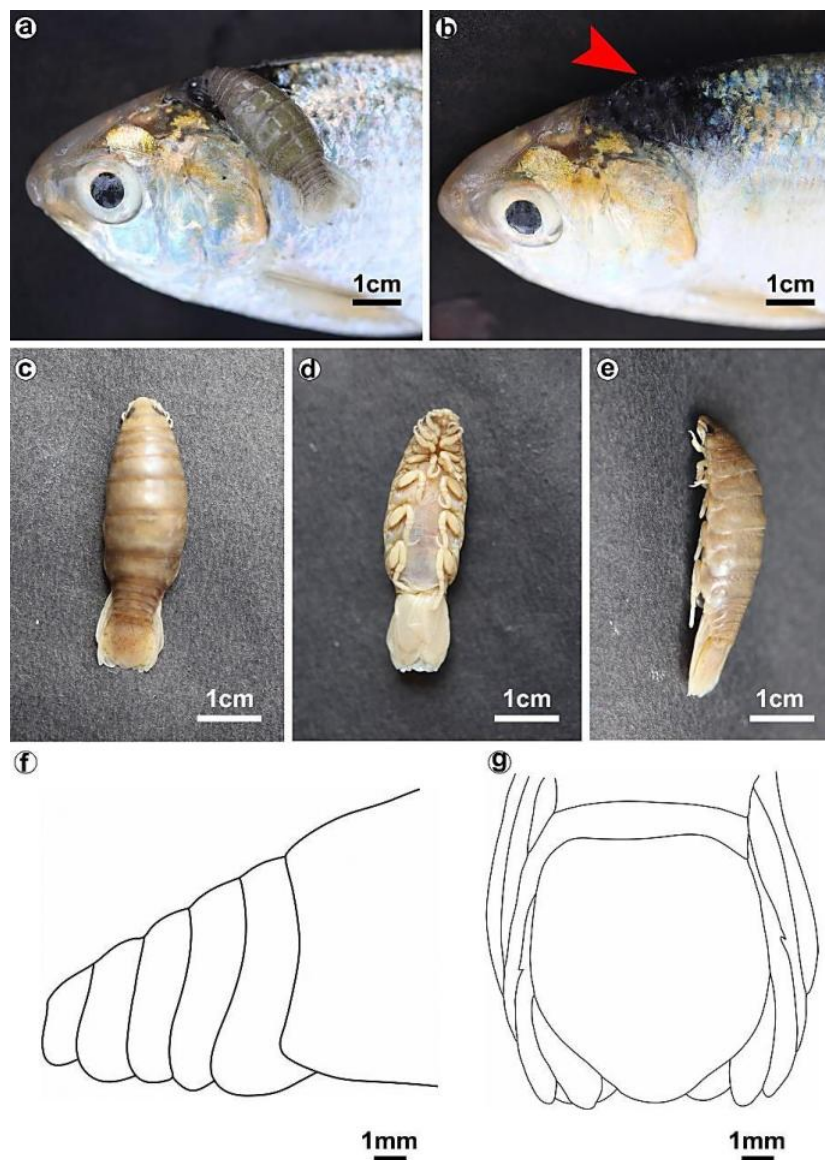


Fig. 1. (a) Parasite *Anilocra leptosoma* attached to the head of *Nematalosa nasus*; (b) The site of parasite attachment (red arrow) showing dark colour and depression in the skin. The parasite *Anilocra leptosoma* ovigerous female (4 cm): (c) dorsal view, (d) ventral view, (e) lateral view, (f) Pleon, (g) Pleotelson.

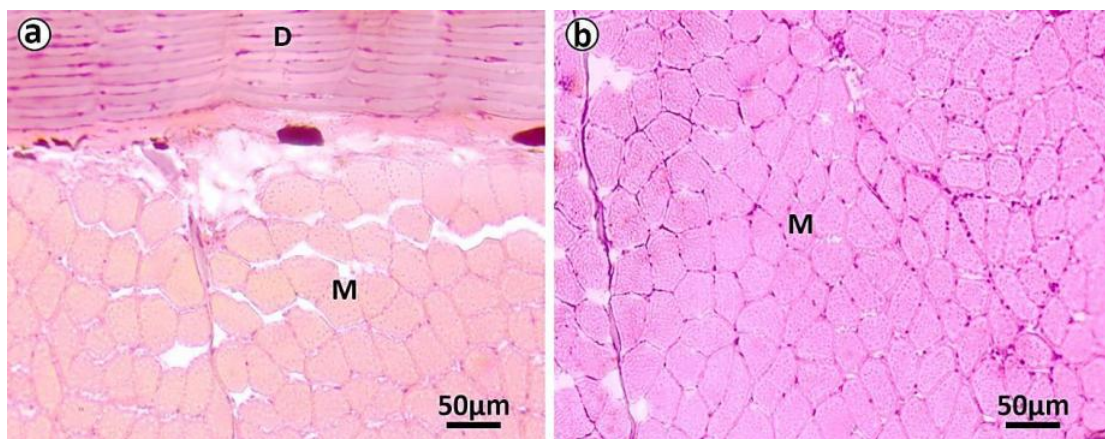


Fig. 2. Transverse sections of normal skin of *Nematalosa nasus*. (a) Compactly arranged cells in the skin layers; (b) Normal muscle tissue shows compactly arranged muscle fibres.

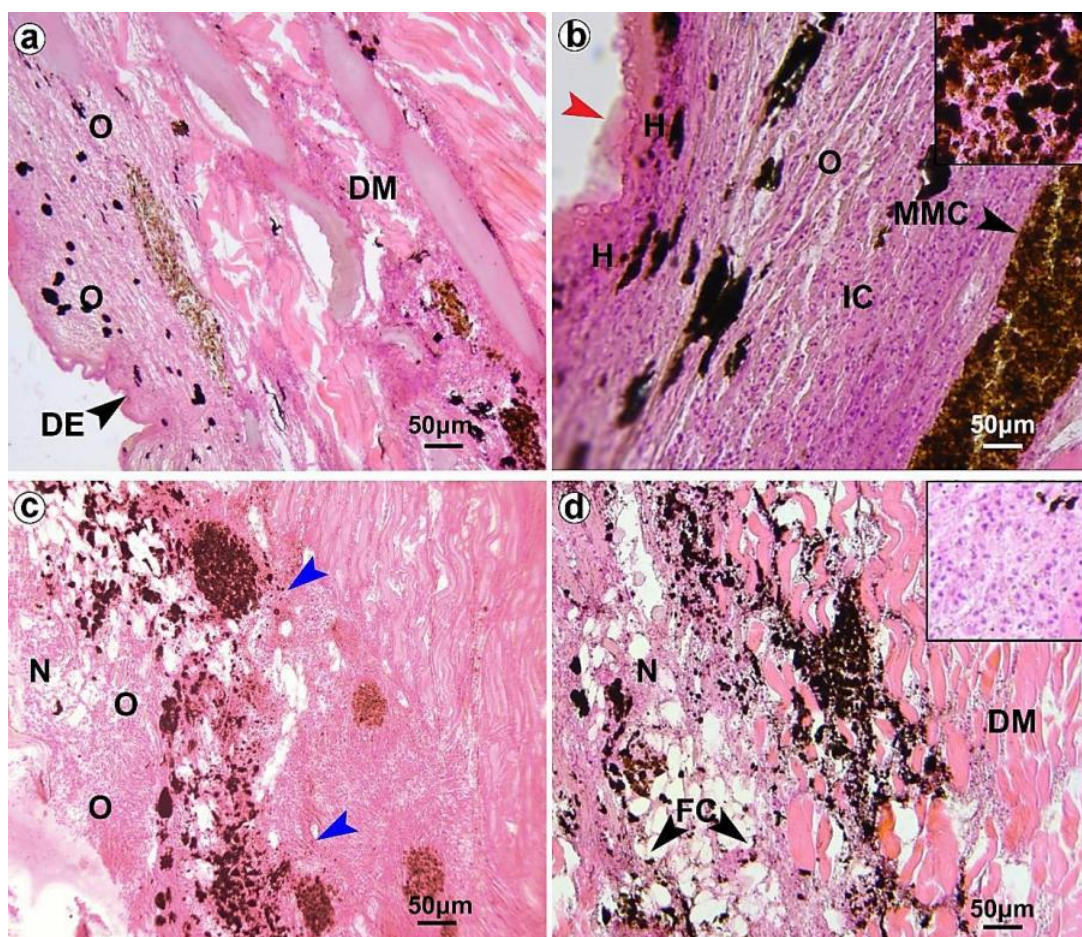


Fig. 3. Histopathological sections of head of *Nematalosa nasus* infested by *Anilocra leptosoma*. (a) Depression (DE) at the site of parasite attachment, with muscle degeneration (DM) and oedema (O) below the site of parasite attachment; (b) Epidermal erosion (red arrow), hyperplasia (H) in the epidermal layer, and severe degenerative changes in the dermal layers. Proliferation of melanomacrophage centre (MMC) and infiltration of inflammatory cells (IC). Melanomacrophages (inset); (c) Oedema (O) and muscle tissue undergoing necrosis (N). Severe proliferation of melanomacrophage centres within the mixed inflammatory infiltrate (blue arrows); (d) Infiltration of eosinophils and lymphocytes (inset), muscle degeneration (DM) and presence of fat cells (FC).

Histopathology of skin of *N. nasus* infested with *A. leptosoma* showed several variations than the normal tissue architecture. In the present study, the epidermis at the site of pereopod attachment was irregular and eroded. Purivirojkul (2012) also reported erosion of the epidermis and dermis at the attachment site of the isopod, *Nerocila depressa*. According to Rameshkumar and Ravichandran (2013b) the isopods use claw-like prehensile pereopods for attachment to the host skin and the insertion using the appendages, causing severe erosion in the dermis and the underlying muscular tissues at the site of attachment similar to the damages caused by *Catoessa boscii* in the buccal cavity of *Carangoides malabaricus* (Bloch & Schneider, 1801). The degenerative changes seen in the underlying tissue at the point of parasite attachment could also be due to the parasite feeding activity as reported by Ravichandran et al. (2007). He reported the necrotic lesions in *Parastromateus niger* due to the infestation of isopod, *Joryma tartoor*.

An increase in subepithelial dense sheets of

hemosiderin-laden macrophages within the dense mixed inflammatory infiltrate was observed in *N. nasus* infected with *A. leptosoma*. Based on the type of injury made by the parasites and their depth of penetration, the cellular response to infestation may change. Dezfuli et al. (2011) reported an increase in granular leukocytes as an inflammatory response when the parasites adhering to the tissue, whereas the immune cells and MMCs increase due to deeper penetration of the pereopods into the tissues. The inflammatory infiltration of white blood cells is a common feature of the isopod infesting fish (Ravichandran et al., 2007) which serves as a defence mechanism against the parasite infestation (Rand, 1986). According to Roberts (1975) MMCs are seen involved in the innate and adaptive immune response. Large numbers of MMCs were noticed in all layers of the skin tissues of infested fish. An increase in MMCs due to similar infestations in fishes were also reported by Ziegenfuss and Wolke (1991) and Ananda Raja et al. (2020). These macrophage aggregations distort skin architecture and may develop necrotic regions (Guarner and Brandt, 2011). The excessive

accumulation of the haemosiderin pigment in organs (haemosiderosis) represents a typical pathological process (Wolke et al., 1985). Haemosiderin is normally seen associated with lipofuscin granules (Agius and Agbede, 1984). In some regions of the skin layers, MMs were darkly pigmented. Agius and Roberts (2003) suggested that increased haemosiderin, lipofuscin and melanin pigments deepen the dark colouration of MMs.

Status of MMCs in parasite infested fish helps to monitor the health of wild fish populations (Wolke et al., 1985). MMCs are formed as a chronic inflammatory response to serious tissue damages. MMCs numbers also increase in the supportive tissues due to the extensive skin damages (Roberts, 2001). In the present study, the tissue damage was visible by the naked eye as a depression at the attached site of the parasite. The parasite does not penetrate into the host but the damage was seen in the underlying tissue with degeneration of the muscle fibres, along with infiltration of eosinophilic granulocytes. This indicates that the parasite was almost permanently attached to this location throughout its life (Overstreet, 2017). Williams Jr and Bunkley-Williams (2019) indicated this as a successful adaptation of isopod parasites in locations around the cephalic region of the host without making deep penetrations.

Conclusion

The present study revealed the deleterious effect of a cymothoid, *Anilocra leptosoma* on the marine fish, *Nematalosa nasus* through histopathological analysis. The parasite induced severe inflammatory responses, hyperplastic and degenerative changes in the skin and underlying muscles, thus can harmfully affect the physiological status of the host. A heavy infestation can affect the commercial value of fish. The report is a new host record from India and provides information on the histopathology of fish infestation by *A. leptosoma*.

Acknowledgements

The authors acknowledge Dr. B. Santhosh, Principal Scientist, Central Marine Fisheries Institute, Vizhinjam, Thiruvananthapuram for supporting research work. We acknowledge Dr. Aneesh P.T., UGC-DS Kothari Post-Doctoral Fellow, Dept. of Aquatic Biology & Fisheries, University of Kerala for the constant support. We thank University of Kerala for providing Research Grant (AcE VI/117/ZOO/15059/2017).

References

Agius, C., Agbede S.A. 1984. Electron microscopical studies on the genesis of lipofuscin, melanin and haemosiderin in the haemopoietic tissues of fish. *Journal of Fish Biology* 24:471–488. <https://doi.org/10.1111/j.1095-8649.1984.tb04818.x>

Agius, C., Roberts, R.J. 2003. Melano-macrophage centres and their

role in fish pathology. *Journal of Fish Diseases* 26:499–509. <https://doi.org/10.1046/j.1365-2761.2003.00485.x>

Ananda Raja, R., Jithendran, K.P. 2015. Aquaculture disease diagnosis and health management. In: *Advances in marine and brackishwater aquaculture*, Perumal S., Pachiappan P., Thirunavukkarasu, A.R. (Eds.), Springer, New Delhi, pp.247–255. https://doi.org/10.1007/978-81-322-2271-2_23

Ananda Raja, R., Patil, P.K., Avunje, S., Aravind, R.P., Alavandi, S.V., Vijayan, K.K. 2020. Biosafety, withdrawal and efficacy of anti-parasitic drug emamectin benzoate in Asian Seabass (*Lates calcarifer*). *Aquaculture* 525:735335 <https://doi.org/10.1016/j.aquaculture.2020.735335>

Aneesh, P.T., Helna, A.K., Trilles, J.P. 2017. Occurrence and redescription of *Anilocra leptosoma* Bleeker, 1857 (Crustacea: isopoda: Cymothoidae) parasitizing the clupeid fish *Tenualosa toli* (Valenciennes) from the Arabian Sea, India. *Marine Biodiversity* 49: 443–450. <https://doi.org/10.1007/s12526-017-0828-7>

Bruce, N.L. 1987. Australian *pleopodias* Richardson, 1910, and *Anilocra* Leach, 1818 (Isopoda: Cymothoidae), crustacean parasites of marine fishes. *Records of the Australian Museum* 39:85–130. <https://doi.org/10.3853/j.0067-1975.39.1987.166>

Carleton, H.M. 1980. *Histological technique*. Oxford University Press, New York. 520 pp.

Cuyas, C., Castro, J.J., Santana Ortega, A.T., Carbonnel, E. 2004. Insular stock identification of *Serranus atricauda* (Pisces: Serranidae) through the presence of *Ceratothoa steindachneri* (Isopoda: Cymothoidae) and *Pentacapsula cutancea* (Myoxoa: Pentacapsulidae) in the Canary Islands. *Scientia Marina* 68:159–163. <https://doi.org/10.3989/scimar.2004.68n1159>

Dezfuli, B.S., Giari, L., Squerzanti, S., Lui, A., Lorenzoni, M., Sakalli, S., Shinn, A.P. 2011. Histological damage and inflammatory response elicited by *Monobothrium wagneri* (Cestoda) in the intestine of *Tinca tinca* (Cyprinidae). *Parasites & Vectors* 4:225. <https://doi.org/10.1186/1756-3305-4-225>

Elgendy, M.Y., Hassan, A.M., Zaher, M.F.A., Abbas, H.H., El-Din Soliman, W.S., Bayoumy, E.M. 2018. *Nerocila bivittata* massive infestations in *Tilapia zillii* with emphasis on hematological and histopathological changes. *Asian Journal of Scientific Research* 11:134–144. <https://doi.org/10.3923/ajsr.2018.134.144>

Fogelman, R.M., Kuris, A., Grutter, A.S. 2009. Parasitic castration of a vertebrate: Effect of the cymothoid *Anilocra apogonae* on the five-lined cardinal fish. *International Journal for Parasitology* 39:577–583. <https://doi.org/10.1016/j.ijpara.2008.10.013>

Guarner, J., Brandt, M.E. 2011. Histopathologic diagnosis of fungal infections in the 21st century. *Clinical Microbiology Reviews* 24:247–280. <https://doi.org/10.1128/CMR.00053-10>

Jalajakumar, V.S. 1988. Parasite distribution and histopathological studies on certain commercially important fishes of Cochin area. PhD Thesis. Cochin University of Science and Technology, India. 65–74 pp.

Kittilsen, S., Schjolden, J., Beitnes-Johansen, I., Shaw, J.C., Pottinger, T.G., Sorensen, C., Braastad, B.O., Bakken, M., Overli, O. 2009. Melanin-based skin spots reflect stress responsiveness in salmonid fish. *Hormones and Behavior* 56:292–298. <https://doi.org/10.1016/j.yhbeh.2009.06.006>

Lailabeevi, M. 1996. Studies on the isopod fish parasites of Kerala and environs. PhD Thesis. University of Kerala, India. 112–174 pp.

Mladineo, I., Hrabar, J., Vidjak, O., Bocina, I., Colak, S., Katharios, P., Cascarano, M.C., Keklikoglou, K., Volpatti D., Beraldo, P. 2020. Host-Parasite interaction between parasitic Cymothoid *Ceratothoa oestroides* and its host, farmed European Sea Bass (*Dicentrarchus labrax*). *Pathogens* 9:230. <https://doi.org/10.3390>

- Mukherjee, M., Suresh, V.R., Manna, R.K., Panda, D., Sharma, A.P., Pati, M.K. 2016. Dietary preference and feeding ecology of Bloch's gizzard shad, *Nematalosa nasus*. *Journal of Ichthyology* 56:373–382. <https://doi.org/10.1134/S0032945216030097>
- Ostlund-Nilsson, S., Curtis, L., Nilsson, G.E., Grutter, A.S. 2005. Parasitic isopod *Anilocra apogonae*, a drag for the cardinal fish *Cheilodipterus quinquelineatus*. *Marine Ecology Progress Series* 28:209–216. <https://doi.org/10.3354/meps287209>
- Overstreet, R.M., Hawkins, W.E. 2017. Diseases and mortalities of fishes and other animals in the Gulf of Mexico. Habitats and biota of the Gulf of Mexico: Before the Deepwater Horizon oil spill. Springer, New York. pp.1589–1738. https://doi.org/10.1007/978-1-4939-3456-0_6
- Purivirojkul, W. 2012. Histological change of aquatic animals by parasitic infection. In: *Histopathology-Reviews and recent advances*, Martinez, E.P. (Ed.), IntechOpen, U.K., pp. 170–171. <https://doi.org/10.5772/52769>
- Rameshkumar, G., Ravichandran, S. 2013a. Problems caused by isopod parasites in commercial fishes. *Journal of Parasitic Diseases* 38:138–141. <https://doi.org/10.1007/s12639-012-0210-4>
- Rameshkumar, G., Ravichandran, S. 2013b. Effect of the parasitic isopod, *Catoessa boscii* (Isopoda, Cymothoidae), a buccal cavity parasite of the marine fish, *Carangoides malabaricus*. *Asian Pacific Journal of Tropical Biomedicine* 3:118–122. [https://doi.org/10.1016/S2221-1691\(13\)60035-0](https://doi.org/10.1016/S2221-1691(13)60035-0)
- Rameshkumar, G., Ravichandran, S., Trilles, J.P. 2011. Cymothoidae (Crustacea, Isopoda) from Indian fishes. *Acta Parasitologica* 56:78–91. <https://doi.org/10.2478/s11686-011-0002-5>
- Rand, T.G. 1986. The histopathology of infection of *Paranthias furcifer* (L.) (Osteichthyes; Serranidae) by *Nerocila accuminata* (Schioedte and Meinert) (Crustacea) (Isopoda-Cymothoidae). *Journal of Fish Diseases* 9:143–146. <https://doi.org/10.1111/j.1365-2761.1986.tb00995.x>
- Ravichandran, S., Ajithkumar, T.T., Ronaldross, P., Muthulingam, M. 2007. Histopathology of the infestation of parasitic isopod *Joryma tartoor* of the host fish *Parastromates niger*. *Journal of Parasitology Research* 2:68–71. <https://doi.org/10.3923/jp.2007.68.71>
- Roberts, R.J. 2001. *Fish pathology*. 3rd Edition. W.B. Saunders, London. 125 pp. <https://doi.org/10.1046/j.1365-2761.2002.00335.x>
- Roberts, R.J. 1975. Melanin-containing cells of teleost fish and their relation to disease. In: *The pathology of fishes*, Ribelin, W.E., Migaki, G. (Eds.), University of Wisconsin Press, Madison, pp. 399–428.
- Rojas, V., Sanchez, D., Gallardo, J.A., Mercado, L. 2018. Histopathological changes induced by *Caligus rogercresseyi* in rainbow trout (*Oncorhynchus mykiss*). *Latin American Journal of Aquatic Research* 46:843–848. <https://doi.org/10.3856/vol46-issue4-fulltext-23>
- Smit, N.J., Bruce, N.L., Hadfield, K.A. 2014. Global diversity of fish parasitic isopod crustaceans of the family Cymothoidae. *International Journal of Parasitology* 3:188–197. <https://doi.org/10.1016/j.ijppaw.2014.03.004>
- Trilles, J.P., Ravichandran, S., Rameshkumar, G. 2011. A checklist of the Cymothoidae (Crustacea, Isopoda) recorded from Indian fishes. *Acta Parasitologica* 56:446–459. <https://doi.org/10.2478/s11686-011-0077-z>
- Williams, E.H. Jr., Williams, L.B. 2019. Life cycle and life history strategies of parasitic crustacea. *Parasitic Crustacea* 3:179–266. https://doi.org/10.1007/978-3-030-17385-2_5
- Wolke, R.E., Murchelano, R.A., Dickstein, C., George, C.J. 1985. Preliminary evaluation of the use of macrophage aggregates (MA) as fish health monitors. *Bulletin of Environmental Contamination and Toxicology* 35:222–227. <https://doi.org/10.1007/BF01636502>
- Ziegenfuss, M.C., Wolke, R.E. 1991. The use of fluorescent microspheres in the study of piscine macrophage aggregate kinetics. *Developmental Comparative Immunology* 15:71–165. [https://doi.org/10.1016/0145-305X\(91\)90007-L](https://doi.org/10.1016/0145-305X(91)90007-L)



INTERNATIONAL JOURNAL OF ADVANCE RESEARCH, IDEAS AND INNOVATIONS IN TECHNOLOGY

ISSN: 2454-132X

Impact Factor: 6.078

(Volume 7, Issue 3 - V7I3-1603)

Available online at: <https://www.ijariit.com>

Preliminary phytochemical screening and Invitro antioxidant activities of “*Antidesma alexitera* L.” leaf extract

Noreen Grace George

noreenrgracegeorge2@gmail.com

Jawaharlal Nehru Tropical Botanic
Garden and Research Institute,
Palode, Kerala

Dr. S. R. Suja

drsujasremep@gmail.com

Jawaharlal Nehru Tropical Botanic
Garden and Research Institute,
Palode, Kerala

Meera T. S.

meeratarasuresh96@gmail.com

Jawaharlal Nehru Tropical Botanic
Garden and Research Institute,
Palode, Kerala

B. S. BijuKumar

bijukumarbsd@gmail.com

Mahatma Gandhi College,
Trivandrum, Kerala

R. Prakash Kumar

rprak62@gmail.com

Jawaharlal Nehru Tropical Botanic
Garden and Research Institute,
Palode, Kerala

ABSTRACT

There is no plant in the world that is non- medicinal, or which cannot be used as medicine is used as medicine. Folk or traditional systems of medicines always played an imperative role in the global healthcare system. *Antidesma alexiteria*.L (Thalimaram), belongs to the Phyllanthaceae family. *Antidesma* species has been used in many traditional medicines to treat diarrhea, skin complaints, hemorrhages, and abdominal disorders. The present study focuses on the preliminary Phytochemical screening and evaluation of the antioxidant potential of *Antidesma alexiteria*.L .For qualitative analysis ,standard tests were used to identify phytochemicals present in the extract and confirmed the presence of carbohydrates, coumarins, glycosides, saponins, phenols and phytosterols. Leaf extracts were also subjected for total phenolic content(TPC), total tannin content (TTC) and total flavonoid content(TFC). In quantitative estimation, TPC content of each extract was 24.13, 32.65 & 3.89 mg of GA/g extract, TFC was 230.38, 493.85 &217.15 mg of Ru/g extract and total tannin were 613, 503 &39.67 mg of CTN/g extract respectively. Antioxidant properties of the three extracts were evaluated using DPPH assay, Nitric oxide scavenging activity and total antioxidant activity. Ascorbic acid was used as standard. In DPPH free radical scavenging assay IC50 value of alcoholic, hydroalcoholic and aqueous root extracts was found to be 650.7,534.1 and 7704.18µg/mL respectively. For Nitric Oxide Radical Scavenging assay IC50 value of alcoholic, hydroalcoholic and aqueous root extracts was found to be 928.9, 354.6 and 380.24µg/mL respectively. The Total antioxidant activity of the plant extracts was calculated from the calibration curve of ascorbic acid, and the results showed 49.76, 44.97 and84.14 mg of AA/g activity for ethanolic, hydroethanolic and aqueous extracts respectively

Keywords— *Antidesma alexiteria*. L, antioxidant potentials, leaf extracts, phytochemical constituents

1. INTRODUCTION

Traditional folk/herbal medicinal practitioners have described the therapeutic benefits of many indigenous plant species, the natural plant extracts are the source of herbal medicine. *Antidesma alexitera*. L is an example for such plants.

Antidesma alexitera.L belongs to the Phyllanthaceae family; it was previously classified under Euphorbiaceae family. This species is indigenous to South India and Sri Lanka commonly known as “ thalimaram” in Kerala and “Heen embilla/Hinembilla” in Sri Lanka. *Antidesma alexiteria*.L is dioecious trees or shrubs with a simple indumentum and its fruits drupaceous, edible, and red to black. [9]

A.alexiteria.L fruit has potential antioxidants which stabilizes oxidation in edible oils[2] and can be used as natural food colour[1]. Its leaves are used as an antidote for snake bites: by the tribal in Tirunelveli Hills, Western Ghats.[7] and young leaves are boiled

with potherbs in case of syphilis in India[3]. The bark fibre is used to make cord and root bark is said to be a cure for dysentery [4]. Based on traditional knowledge local communities use its leaves as herbal shampoo.

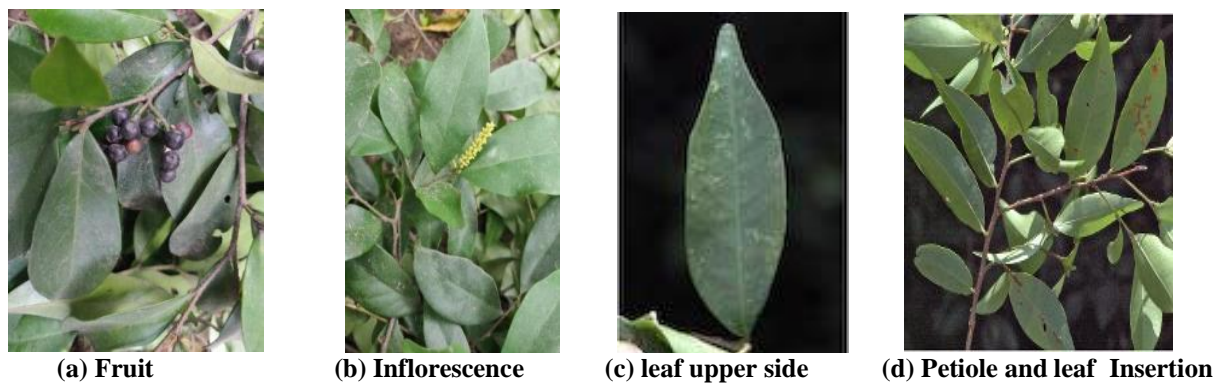


Fig 1: *Antidesma alexiteria.L* (leaf, fruit & inflorescence)

In Southeast Asian folk medicine different *Antidesma* species were used to treat diarrhoea, skin complaints, haemorrhages, and abdominal disorders, for which tannin components could possibly be an active principle. Two important hydrolysable tannins “carpusin” and a novel dimer “antidesmin A” [8,5] were reported from Euphorbiaceae plants. The anti-cholesteric activity of *Antidesma pentandruin Merran* is due to the presence of triterpene (lupeolactone) [8]. For the first time *Antidesma alexitera.L.*” was selected to evaluate its antioxidant potential and screening of phytochemicals present in it.

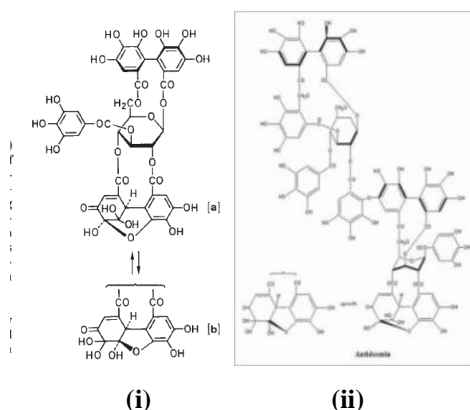


Fig 2: Tannin (i) novel dimer “antidesmin” structure (ii) carpusin structure [8,5]

2. MATERIAL AND METHODS

2.1 Plant Material

Leaves of *A.alexiteria.L* were collected from Trivandrum district of Kerala, India. A voucher specimen (38314,38315) has been deposited at the herbarium of the Institute. The leaves were washed, and shade dried then ground to coarse powder with a mechanical grinder. Preparation of Plant Extract: 100g of the leaf powder was cold extracted (using magnetic stirrer) with 100% ethanol for 3hrs. The extract was filtered using whatman no.1 filter paper and the residue was replenished with fresh solvent for next round of extraction. The extraction step was totally carried out for 3 times to maximize the extract yield. The collected filtrates were pooled together and concentrated in a rotary vacuum evaporator at 40 °C to obtain ethanolic extract. The extraction was repeated sequentially with 50% ethanol in water and 100% water and the collected filtrates were concentrated in a rotary vacuum evaporator at 40°C to obtain 50% hydroalcoholic and aqueous extracts respectively. The condensed extract was used for preliminary phytochemical screening and to test its antioxidant activities.

2.2 Preliminary Phytochemical analysis

Comparative preliminary phytochemical study on crude and various fractions of *A.alexiteria.L* were carried out using standard procedures [14,16,15] in order to detect the presence of phytoconstituents such as alkaloids, phenols, flavonoids, Phyto steroids, saponins, glycosides and carbohydrates.(Table 1)

2.3 Quantitative phytochemical analysis

(a) **Estimation of Total phenolic content (TPC):** This was estimated by spectrophotometry according to Singleton and Rossi, 1965 [17], method. 0.5 ml of extract was transferred into tubes containing 2.5ml 10% Folin-Ciocalteu’s reagent. After 10 min, 2ml of sodium carbonate solution was added to the sample and it was allowed to stand at room temperature for 30 min. Absorbance was read at 743nm, the concentration of polyphenols in the sample was derived from a standard curve of Gallic acid. The TPC was expressed as Gallic acid equivalents (GAE) in mg/g of dry extract.

(b) **Estimation of Total Flavonoids (TFC):** it is determined according to the Aluminium chloride colorimetric method of Chang *et al*,2003 [18] with slight modification. Plant extract (1mg/ml) in methanol was mixed with 0.1 mL of 10% Aluminium chloride hexahydrate, 0.1ml of 1M potassium acetate and 2.8ml of deionized water. After 30 min incubation at room temperature, the absorbance of the reaction mixture was determined spectrophotometrically at 415nm. Rutin was taken as a standard (con range

12.5 to 400µg/ml), the total flavonoid content was calculated from the standard curve and expressed as Rutin equivalents in mg/g of dry extracts

- (c) **Total condensed Tannin:** Condensed tannins were colorimetrically estimated by vanillin hydrochloride method [19]. The condensed tannins content was calculated from the calibration curve of standard catechin ranging between 20-100µg/ml. Tubes containing 1ml each of standard/ plant extract in methanol were incubated at 30 °C in a water bath and this 5ml of working reagent was added to an interval of 1 min to one set of the tubes and 5ml of 4% HCL was added to the other set at intervals of 1.0 min. Kept the samples in the water bath for 20min and the absorbance was read at 500nm. The absorbance of the blank was subtracted from that of the sample containing vanillin reagent.

2.4 Antioxidant assay

- (a) **Nitric oxide scavenging assay [13]:** Sodium nitroprusside (10mM) was mixed with 1ml of different plant extract concentration in phosphate buffer pH 7.4. The mixture was incubated at 25 °C for 150 min. To 500µl of the incubated solution, 500µl of Griess reagent was added, absorbance was measured at 546nm and percentage of incubation was calculated. Ascorbic acid was used as a standard.
- (b) **DPPH Radical Scavenging assay [11]:** Methanolic solution of 2ml DPPH in 10ml was added to different con of plant extracts & allowed to react at room temperature for 30 min in the dark. Absorbance was taken at 517nm, methanol was used as blank and 200µl of methanol was added to DPPH in positive control tube. Ascorbic acid was used as standard. The percentage of radical scavenging of samples was calculated.
- (c) **Total Antioxidant activity:** This was analysed by phosphomolybdenum method [12]. 200µl of extract in respective solvent was mixed with 2ml of reagent solution (0.6M sulphuric acid, 28mM sodium phosphate & 4mM ammonium molybdate). The reaction mixture was incubated at 95 °C for 90 min. Absorbance of the sample was measured at 635nm. The total antioxidant capacity of the plant was calculated from the calibration curve of ascorbic acid and expressed as µg ascorbic acid equivalents /g of dry extracts

Statistical Analysis: The results obtained were expressed as mean(+/-) standard deviation and presented as graphs and tables.

3. RESULTS AND DISCUSSION

3.1 Preliminary phytochemical analysis

Table 1: Qualitative Phytochemical analysis results

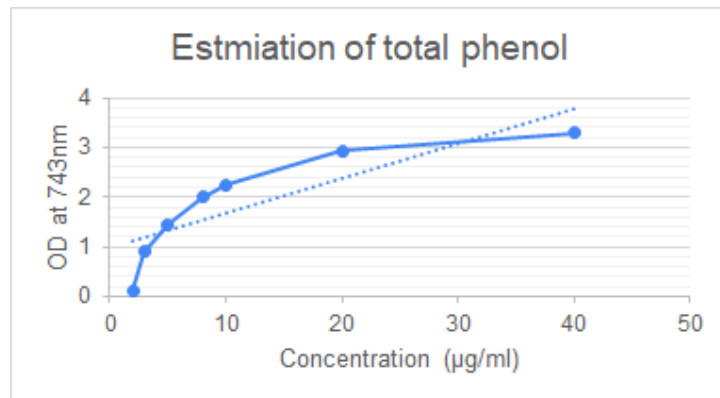
No	Phytochemicals	Test	Ethanollic extract(AAE)	Hydroethanollic extract(AAH)	Aqueous extract(AAA)
1	ALKALOIDS	Wagner’s test	-	-	-
		Hager’s test	-	-	-
		Dragendroff’s test	-	-	-
2	FLAVONOIDS	Shinoda’s test	-	-	+
3	CARBOHYDRATE	Fehling's test	+ (reddish orange ppt)	+ (reddish orange ppt)	+ (reddish orange ppt)
		Benedict test	+ (red ppt)	+ (red ppt)	-
4	COUMARINS		+	+	+
5	GLYCOSIDES	Bontrager’s test	-	-	-
		Legal’s test	+	+	-
		Keller Kiliani test	+	+	+
6	SAPONINS	Foam test	-	+	+
7	PHYTOSTEROL & TERPENOIDS	Salkowski test	-	+ (golden yellow-terpenes)	+ (red-sterols)
8	PROTEINS & AMINO ACIDS	Millon’s Test	-	-	-
		Biuret's test	-	-	-
		Ninhydrin test	-	-	-
9	PHENOLIC COMPOUNDS & TANNIN	Ferric Chloride test	+	+	+
		Lead Acetate test	-	+	+
10	GUM & MUCILAGE		-	-	-
11	FIXED OILS & FATS	Spot test	-	-	-
		Saponification test	-	-	-

+present – absent

The preliminary phytochemical analysis of ethanolic ,hydroethanolic ,and aqueous extracts of *Antidesma alexitera* leaves shows the presence or absence of various phytochemical constituents. The presence of phenolic compounds, carbohydrates, glycosides and coumarin was found in ethanolic, hydroethanolic and aqueous extract. Saponins, phytosterols and terpenoids were found in

hydroethanolic and aqueous extract. Only in aqueous extract showed positive results for flavonoids. So, when compared to ethanolic extract hydroethanolic and aqueous extract have more phytochemical compounds.

3.2 Quantitative Phytochemical Analysis
Determination of total phenolic content

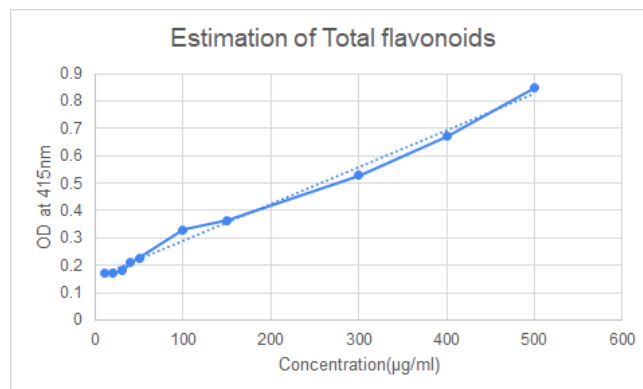


Graph 1: Total phenol estimation, OD at 743nm against the concentration.

Table 2: The total phenolic content calculated from Graph 1

Concentration of test	Total phenolic content(µg/ml)
Ethanolic extract- AAE (0.5ml)	24.13
Hydroethanolic extract- AAH (0.5ml)	32.65
Aqueous extract- AAA (0.5ml)	3.89

Estimation of total flavonoids

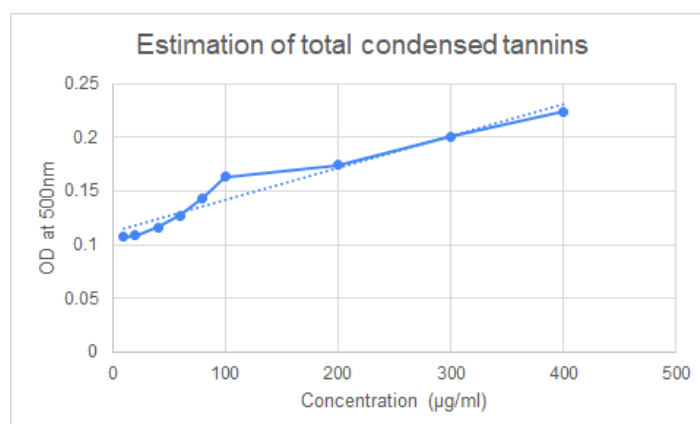


Graph 2: Total flavonoid estimation, OD at 415nm against the concentration

Table 3: The total flavonoids content calculated from Graph 2

Concentration of test	Total flavonoids (µg/ml)
Ethanolic extract- AAE (0.5ml)	230.38
Hydroethanolic extract- AAH (0.5ml)	493.85
Aqueous extract- AAA (0.5ml)	217.15

Estimation of Total Condensed Tannins



Graph 3: Total condensed tannin, OD at 500nm against the concentration.

Table 4: The total condensed tannin calculated from Graph 3

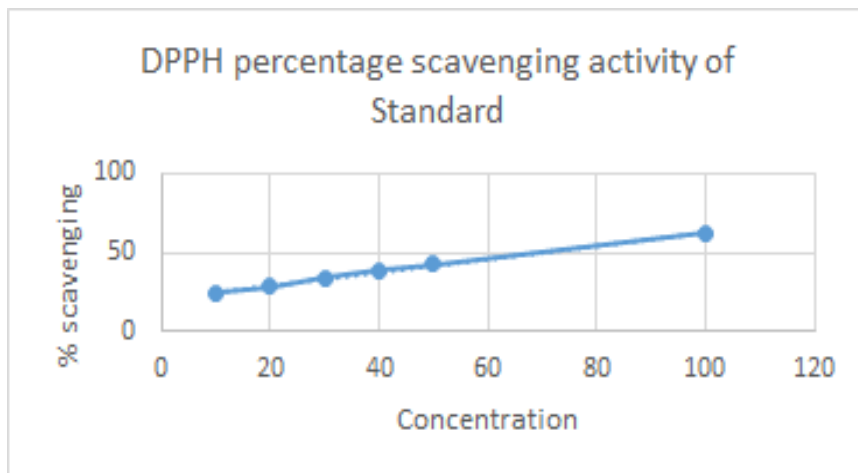
Concentration of test	Total Condensed Tannins (µg/ml)
Ethanolic extract- AAE (0.5ml)	613
Hydroethanolic extract-AAH (0.5ml)	503
Aqueous extract-AAA (0.5ml)	39.67

3.3 Antioxidant Assay

DPPH radical scavenging activity

Table 5: DPPH radical scavenging assay,

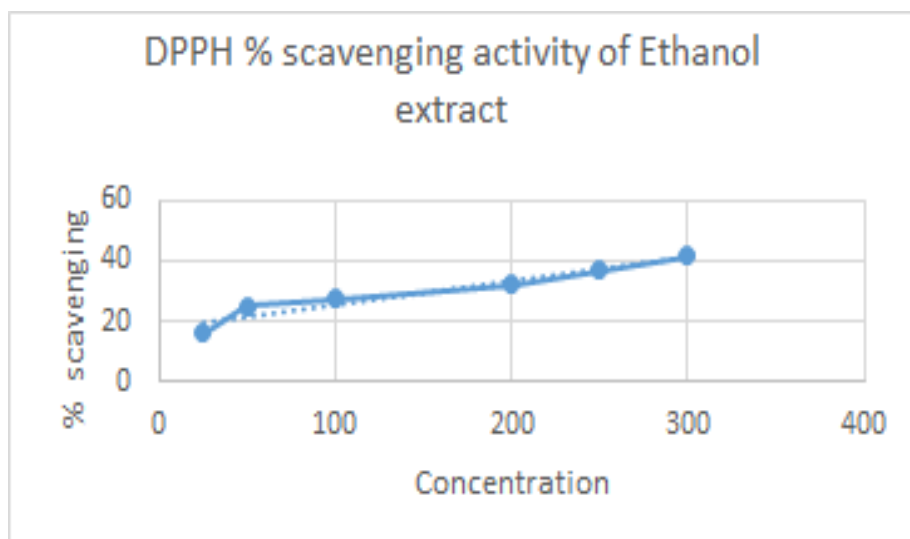
Concentration of standard (µg/ml)(Ascorbic acid)	%scavenging activity	IC50
20	24.84	391.60
40	38.63	
60	43.78	
80	50.20	
100	62.15	

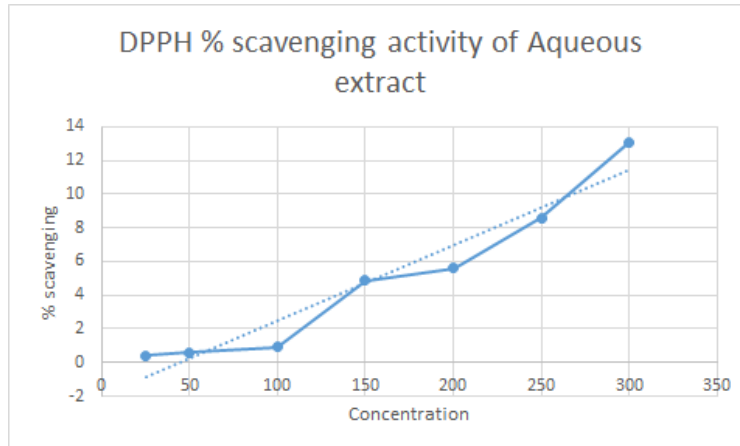
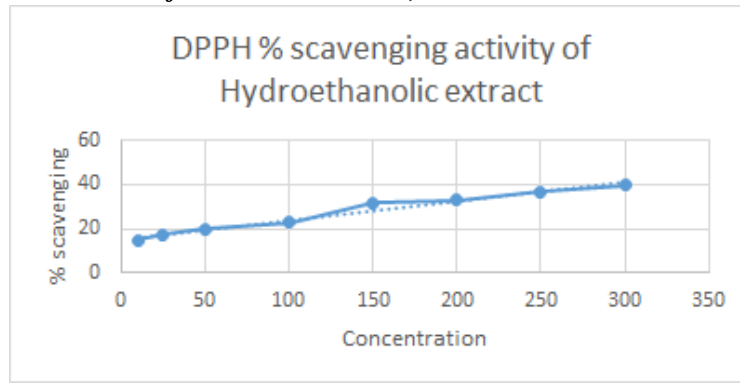


Graph 4: DPPH scavenging activity of standard

Table 6: Percentage scavenging activity of ethanolic hydroethanolic and aqueous extract at various concentrations

Concentration of extracts(µg/ml)	Ethanolic extract percentage scavenging activity - AAE	Hydroethanolic extract Percentage scavenging activity- AAH	Aqueous extract percentage scavenging activity- AAA
25	16.29	14.87	0.40
50	25.13	17.28	0.61
100	27.20	19.81	0.94
150	31.29	22.93	4.86
200	31.56	31.51	5.61
250	38.85	36.83	8.60
300	41.69	39.87	13.09





Graph 5: DPPH scavenging activity of ethanolic, hydroethanolic and aqueous extract

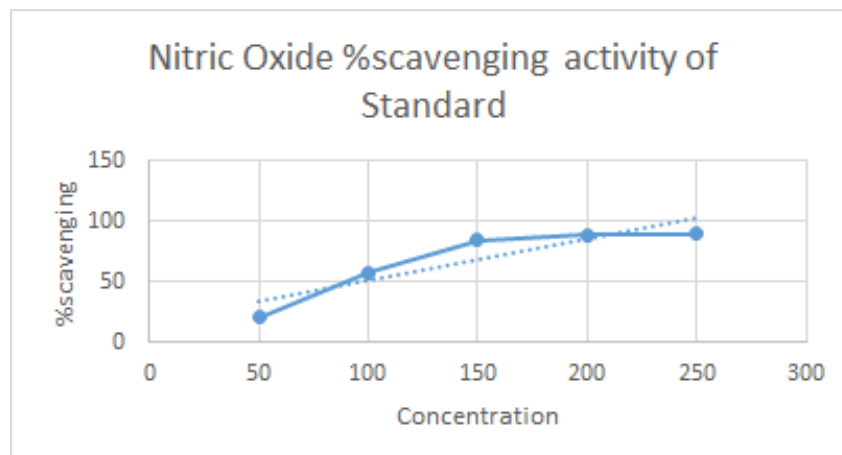
Table 7: IC₅₀ value of ethanolic, hydroethanolic, aqueous and standard as follows

Sample/Standard	IC ₅₀
Ethanolic extract- AAE	650.65
Hydroethanolic extract-AAH	534.05
Aqueous extract- AAA	7704.18
Standard	391.60

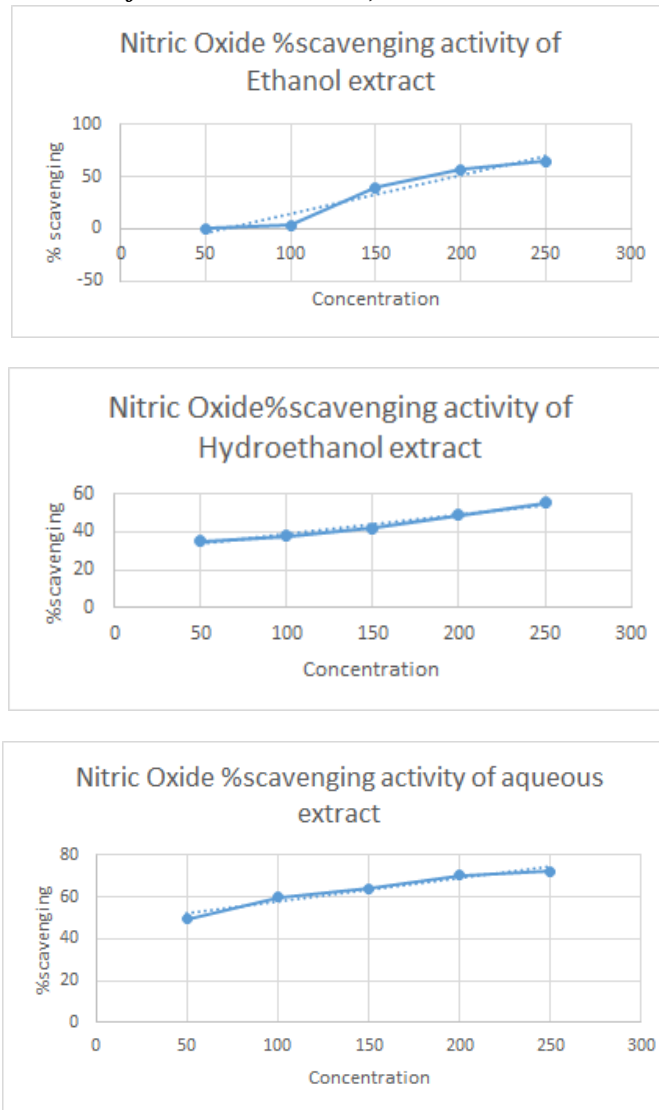
Nitric Oxide radical scavenging activity

Table 8: Nitric oxide radical scavenging activity of ascorbic acid (standard) and % scavenging activity

Concentration of standard (µg/ml) (Ascorbic acid)	Percentage scavenging activity	IC ₅₀ of Standard
50	20.63	82.21
100	58.08	
150	84.63	
200	89.14	
250	19.73	



Graph 6: nitric oxide percentage scavenging activity of standard ascorbic acid

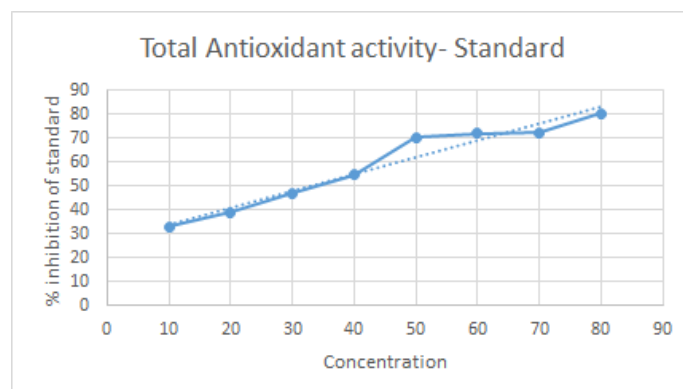


Graph 7: nitric oxide percentage scavenging activity of ethanolic, hydroethanolic and aqueous extract

Table 9: Nitric oxide percentage scavenging activity of ethanolic hydroethanolic and aqueous extract at various concentrations along with its IC₅₀ value is as follows

Concentration of extracts (µg/ml)	Ethanolic extract percentage scavenging activity- AAE	IC ₅₀ of Ethanolic extract	Hydroethanolic extract Percentage scavenging activity- AAH	IC ₅₀ of Hydroethanolic extract	Aqueous extract percentage scavenging activity- AAA	IC ₅₀ of Aqueous extract
50	0.12134	928.95	35.2996	354.64	49.3396	380.24
100	2.95875		37.7123		59.8539	
150	39.4437		41.8471		64.047	
200	56.5382		48.698		70.1162	
250	64.4531		55.2828		72.2312	

Total antioxidant activity



Graph 8: the total antioxidant activity of standard

Table 10: total antioxidant activity of the standard

Concentration of standard (µg/ml) (Ascorbic acid)	Mean absorbance (635 nm)
10	0.220
20	0.2922
30	0.3745
40	0.4234
50	0.8860
Control	0.0823

Table 10: total antioxidant activity of three extracts

Concentration of test (µg/ml)	Total antioxidant activity
Ethanolic extract- AAE (200µg/ml)	49.76
Hydroethanolic extract- AAH(200µg/ml)	44.98
Aqueous extract- AAA (200µg/ml)	84.14

The results of the study revealed that hydroethanolic and aqueous extract possess more phytochemical compounds than ethanolic extract. In quantitative estimation, total phenolic content of each extract was 24.13, 32.65 & 3.89 mg of GA/g extract, total flavonoid was 230.38, 493.85 & 217.15 mg of Ru/g extract and total tannin were 613, 503 & 39.67 mg of CTN/g extract respectively. Natural extracts with proven antioxidant activity are typically composed with their phenolic moiety, for instance flavonoids, coumarins and tocopherols and these are present in all the extracts. Organic acids, carotenoids and tannins may also be present and act as antioxidants or have a synergistic impact with phenolic compounds

The DPPH assay is based on the ability of DPPH, a stable free radical, to decolorize in the presence of antioxidants. The DPPH radical contains an odd electron, which is responsible for the absorbance at 517 nm and also for visible deep purple colour. When DPPH accepts an electron donated by an antioxidant compound, the DPPH is decolorized which can be quantitatively measured from the changes in absorbance. In DPPH free radical scavenging assay IC₅₀ value of alcoholic, hydroalcoholic and aqueous root extracts was found to be 650.7, 534.1, 7704.18µg/mL respectively.

For Nitric Oxide Radical Scavenging assay IC₅₀ value of alcoholic, hydroalcoholic and aqueous root extracts was found to be 928.95, 354.64, 380.24 µg/mL respectively. The total antioxidant activity of the plant extracts was calculated from the calibration curve of ascorbic acid, the results showed the antioxidant activity of ethanolic, hydroethanolic and aqueous extracts were 49.76, 44.97 and 84.14 mg of AA/g extract respectively.

This study was able to prove the antioxidant potential of *Antidesma alexitera* leaves, further studies must be done to find out its medicinal potential. These extracts should undergo purification and isolation process to find out its phytochemicals because for all the assay and tests crude ethanolic, hydroethanolic and aqueous extracts were used. Due to human error percentage scavenging assays results vary by small digits.

4. CONCLUSION

Based on the results obtained in the present study, it is concluded that hydroethanolic extract of *Antidesma alexitera* leaf, possess large amounts of flavonoid, phenolics and tannin content. In qualitative analysis, the phytochemical compounds such as carbohydrates, coumarins, glycosides, saponins, phenols and phytosterols were screened using standard methods, and the results showed the hydroethanolic and aqueous extract possess more phytochemical constituents when compared with ethanolic extract. In quantitative estimation, total phenolic content of each extract 24.13, 32.65 & 3.89 mg of GA/g extract, total flavonoid was 230.38, 493.85 & 217.15 mg of Ru/g extract and total tannins were 613, 503 & 39.67 mg of CTN/g extract respectively. So hydroethanolic extract of *Antidesma alexitera* leaf has a high amount of flavonoid, phenolic and tannin content, when compared with other extracts. The presence of the identified phytochemical components makes the leaves pharmacologically active, which exhibits high antioxidant and free radical scavenging activities. Antioxidant assays such as, DPPH radical scavenging activity and total antioxidant activities of ethanolic hydroethanolic and aqueous extracts of *Antidesma alexiteria.L* were compared with the standard ascorbic acid curve. Hydroethanolic extract of *Antidesma alexiteria.L* leaves has got profound antioxidant potential when compared with the ethanolic and aqueous extracts. *Antidesma alexiteria.L* is a good candidate as it is a significant source of natural antioxidant, which might be helpful in preventing the progress of various oxidative stress related diseases. Thus, the present study concluded that, natural products from medicinal plants, either as pure compounds or as standardized extracts, provide unlimited opportunities for new drug leads because of their unmatched availability of chemical diversity and further studies on *Antidesma alexiteria.L* is warranted.

5. ACKNOWLEDGEMENT

The authors thank Director, Jawaharlal Nehru Tropical Botanic Garden Research Institute, Palode for the facilities .

Author's contribution

NG and MTS performed the experimental work as per the guidance of SRS and BBS in designing the protocol. NG and MTS completed the report and project paper and SRS, and BBS and RPK reviewed the manuscript.

REFERENCES

- [1] Narayana, S. D. T. U., Wedamulla, N. E., Wijesinghe, W. A. J. P., Raja Karuna, R. A. M. A. T., & Wijerama, H. J. K. S. S. (2019). Extraction of Anthocyanin from Hinembilla (*Antidesma alexiteria*) Fruit as a Natural Food Colorant.
- [2] Nanayakkara, S. U. G., Wedamulla, N. E., Wijesinghe, W. A. J. P., Rajakaruna, R. A. M. A. T., & Wijerama, H. J. K. S. S. (2019). Effect of Hinembilla (*Antidesma alexiteria*) Extract on Oxidative Stability of Selected Edible Oils.
- [3] Lindley, J. (1853). *The Vegetable Kingdom, Or, The Structure, Classification, and Uses of Plants, Illustrated Upon the Natural System*. Bradbury & Evans.
- [4] Gould, G. M. (1894). *An illustrated dictionary of medicine, biology and allied sciences*. P. Blakiston, Son & Company.
- [5] Mahomoodally, M. F., Korumtollee, H. N., & Chady, Z. Z. B. K. (2015). Ethnopharmacological uses of *Antidesma madagascariense* Lam. (Euphorbiaceae). *Journal of intercultural ethnopharmacology*, 4(1), 86.
- [6] Belmi, R. M., Giron, J., & Tansengco, M. L. (2014). *Antidesma bunius* (Bignay) fruit extract as an organic pesticide against *Epilachna* spp. *Journal of Asian Scientific Research*, 4(7), 320.
- [7] Dey, A., & De, J. N. (2012). Traditional use of plants against snakebite in Indian subcontinent: a review of the recent literature. *African Journal of Traditional, Complementary and Alternative Medicines*, 9(1), 153-174.
- [8] Namba, O., Yoshida, T., Lu, C. F., Yang, L. L., Yen, K. Y., & Okuda, T. (1991). Antidesmin A: A New Dimeric Ellagitannin from *Antidesma pentandrum*. *Planta Medica*, 57(S 2), A125-A126.
- [9] Hoffmann, P. (1999). The genus *Antidesma* (Euphorbiaceae) in Madagascar and the Comoro Islands. *Kew Bulletin*, 877-885.
- [10] Quattrocchi, U. (2012). *CRC world dictionary of medicinal and poisonous plants: common names, scientific names, eponyms, synonyms, and etymology (5 Volume Set)*. CRC press.
- [11] Kedare, S. B., & Singh, R. P. (2011). Genesis and development of DPPH method of antioxidant assay. *Journal of food science and technology*, 48(4), 412-422.
- [12] Prieto, P., Pineda, M., & Aguilar, M. (1999). Spectrophotometric quantitation of antioxidant capacity through the formation of a phosphomolybdenum complex: specific application to the determination of vitamin E. *Analytical biochemistry*, 269(2), 337-341.
- [13] Mondal, S. K., Chakraborty, G., Gupta, M., & Mazumder, U. K. (2006). In vitro antioxidant activity of *Diospyros malabarica* Kostel bark.
- [14] Shirwaikar, A., Rajendran, K., & Barik, R. (2006). Effect of aqueous bark extract of *Garugapinnata* Roxb. in streptozotocin-nicotinamide induced type-II diabetes mellitus. *Journal of ethnopharmacology*, 107(2), 285-290.
- [15] Raaman, N. (2006). *Phytochemical techniques*. New India Publishing.
- [16] Harborne, A. J. (1998). *Phytochemical methods a guide to modern techniques of plant analysis*. Springer science & business media.
- [17] Singleton, V. L., & Rossi, J. A. (1965). Colorimetry of total phenolics with phosphomolybdic-phosphotungstic acid reagents. *American journal of Enology and Viticulture*, 16(3), 144-158.
- [18] Kim, D. O., Jeong, S. W., & Lee, C. Y. (2003). Antioxidant capacity of phenolic phytochemicals from various cultivars of plums. *Food chemistry*, 81(3), 321-326.
- [19] Hagerman, A. E., Robbins, C. T., Weerasuriya, Y., Wilson, T. C., & McArthur, C. (1992). Tannin chemistry in relation to digestion. *Rangeland Ecology & Management/Journal of Range Management Archives*, 45(1), 57-62.
- [20] Fabricant, D. S., & Farnsworth, N. R. (2001). The value of plants used in traditional medicine for drug discovery. *Environmental health perspectives*, 109(suppl 1), 69-75.
- [21] Elgorashi, E. E., Taylor, J. L., Maes, A., De Kimpe, N., Van Staden, J., & Verschaeve, L. (2002). The use of plants in traditional medicine: potential genotoxic risks. *South African Journal of Botany*, 68(3), 408-410.

**INSOLVENCY AND BANKRUPTCY CODE, 2016 & GROWTH OF WILFUL
DEFAULTERS IN INDIA: A RE-LOOK**

Maya Babu.BP¹ and Dr. S. Jayadev²

¹Research Scholar,

²Assistant Professor & Research Supervisor,
P.G. Department of Commerce & Research Centre, Mahatma Gandhi College,
Thiruvananthapuram-695004, Kerala, India

ABSTRACT

New Economic policy or LPG policy of Government of India (in 1991) considered as the ever biggest and innovative economic reforms in the economic history of India. This policy open up a new and most modern global business arena for the Indian economy. Likewise, the Insolvency and Bankruptcy Code, 2016 Act also gained overwhelming appreciation and familiarity in India. This law consolidates and amends the law relating to insolvency resolution process in India. The risk of insolvency and bankruptcy not only borne by the debtor (businessman i.e. insolvent) but also the bank (financial creditor) and suppliers (operational creditors). One of the most dangerous problem faced by the Indian banking sector is the raising of Non-Performing Assets (NPAs) and wilful defaulters of loan. This paper mainly concentrate on role of IBC, 2016 Act in solving the issue of bulging the number of wilful defaulters in Public Sector Banks in India.

Keywords: Insolvency and Bankruptcy Code (IBC), Indian banking sector, Non-Performing Assets (NPAs), Wilful defaulters.

INTRODUCTION

Since independence, India has been following several traditional laws and regulations on insolvency and debt recovery. Some of them were presidency towns insolvency act 1909, provincial insolvency Act 1920, Part VI and Part VII of companies act 1956, Sick Industrial Companies Act (SICA Act) 1985. But after emergence of Liberalization, Privatization and Globalization (LPG) Policy of Government of India (in 1991), these traditional laws and common practices found as insufficient. New financial reform transformed India's traditional business outlook into new global manner. This also paved the way for global entry of most modern technologies and business collaborations with foreign companies. Indian economy started to apply strict international standards of prudential regulations on their business and compete with global rivalries. For the existence of business, corporates took huge amount of loans from banks and borrow raw materials and other needed elements for the business from suppliers. But after a period, some ventures suffered loss which resulted winding up of companies leading to insolvency procedures. Years back insolvency and bankruptcy was a shameful process but now-a-days this is common thing in India. The risk of insolvency and bankruptcy not only borne by the debtor (businessman i.e. insolvent) but also the bank (financial creditor) and suppliers (operational creditors). One of the most dangerous problem faced by the Indian banking sector is the raising of Non-Performing Assets (NPAs). Thus, in India, several laws like Recovery of debts due to Banks & Financial institutions Act (RDDBFI Act) 1993, *Securitization and Reconstruction of Financial Assets and Enforcement of Securities Interest (SARFAESI) Act* 2002, Limited Liability Partnership (LLP) Act 2008, Chapter XIX and XX of Companies Act 2013 are introduced to protect the insolvent i.e. businessman, financial creditors and operational creditors in India. In this dynamic business world, time is a precious thing which cannot be substitute with anything. All are required time bound services from each adjudicating authority. These multiple laws and lengthy procedures on insolvency and bankruptcy created many confusions and complications to the individual investors, institutional investors, partnership firms, banks, companies and other business ventures in India. When compared to any other sectors, the contribution from these categories towards the GDP is immense. Thus, the adversities found in this category totally affect the economic growth of a nation as well. In order to promote